

Network Pharmacology-Based Investigation of the Anti-diabetic Potential of L-arginine-Encapsulated Lipid-Nanoparticles Synthesized from *Trigonella foenum-graecum*



BY

Urooj Ali

Registration Number: 02272113004

Session: 2021-2023

**Department of Biotechnology
Faculty of Biological Sciences
Quaid-I-Azam University
Islamabad, Pakistan
2022**

Network Pharmacology-Based Investigation of the Anti-diabetic Potential of L-arginine-Encapsulated Lipid-Nanoparticles Synthesized from *Trigonella foenum-graecum*



BY

Urooj Ali

Supervisor

Dr. Bilal Haider Abbasi

A thesis submitted in the partial fulfillment of the requirements for the degree of

**MASTER OF PHILOSOPHY
IN
BIOTECHNOLOGY**

**Department of Biotechnology
Faculty of Biological Sciences
Quaid-I-Azam University
Islamabad, Pakistan
2022**

APPROVAL PAGE

DECLARATION

I, Urooj Ali, daughter of Mrs. Tasneem Iqbal and Mr. Riffat Ali, bearing Registration Number 02272113004, and pursuing an MPhil in Biotechnology within the Department of Biotechnology at the Faculty of Biological Sciences, Quaid-i-Azam University Islamabad, Pakistan, affirm that the data cited in the thesis titled "Network Pharmacology-Based Investigation of the Anti-diabetic Potential of L-arginine-Encapsulated Lipid-Nanoparticles Synthesized from *Trigonella foenum-graecum*" is a product of my genuine endeavors. This work was conducted under the guidance and supervision of Dr. Bilal Haider Abbasi, and it has yet to be submitted or disseminated in any other form.

I am well acquainted with the principles of 'copyright' and 'plagiarism,' and I am fully aware of their implications. The thesis accurately represents original research ideas and analyses, and a comprehensive plagiarism assessment utilizing the Turnitin Software reported a minor instance of 15% similarity. It is noteworthy, however, that I am fully committed to original and authentic scholarly work. Should any evidence of plagiarism beyond the specified percentage come to light at any stage, I acknowledge the university's prerogative to nullify or withdraw my degree, even after its conferral. An appended plagiarism report, attached at the end of this thesis, further substantiates the originality of my work.

Signature: _____

Urooj Ali

Dated: _____

بِسْمِ اللّٰهِ الرَّحْمٰنِ الرَّحِیْمِ

MY EVERY EFFORT IS WHOLE-HEARTEDLY DEDICATED TO



Mr. Muhammad
Ali



Prof. Dr.
Muhammad Iqbal



Mrs. Sharifan
Bibi (Late)



Mr. Riffat Ali
Khan



Mrs. Tasneem
Iqbal



Mrs. Sidra Akram



Miss Arfa'A Ali
Khan



Miss Rafia Ali
Khan

*These beautiful souls, my family,
Who has shaped me into the person
I am today!*

&



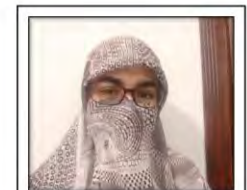
Syeda Izma
Makhdoom



Mr. M. Mustajab
Khan



Miss Eesha
Zafar



Miss Afiya
Shafaqat

*A special mention to these amazing people
Without whom
I would have been lost!*

TABLE OF CONTENTS

ACKNOWLEDGMENTS	xi
LIST OF FIGURES	xiii
LIST OF TABLES	xvii
LIST OF ABBREVIATIONS	xviii
ABSTRACT.....	xx
CHAPTER 01: INTRODUCTION AND LITERATURE REVIEW.....	2
1.1 Diabetes: Overview and Current Management.....	2
1.1.1 Type 1 Diabetes Mellitus	3
1.1.2 Type 2 Diabetes Mellitus	3
1.1.3 Gestational Diabetes	4
1.2 Global Prevalence and Burden of Diabetes	4
1.2.1 Impact of Diabetes on World Health	5
1.2.2 Impact of Diabetes on Pakistan.....	5
1.2.3 Predictions and Targets for the Future.....	6
1.2.4 The Current Anti-Diabetic Therapies and Their Limitations	7
1.3 <i>Trigonella foenum-graecum</i> (Fenugreek): Bioactive Compounds and Anti-Diabetic Properties.....	9
1.3.1 <i>Trigonella foenum-graecum</i> and its Bioactive Compounds	10
1.3.2 The Anti-Diabetic Potential of <i>Trigonella foenum-graecum</i>	10
1.3.3 Mechanisms Underlying Fenugreek's Anti-Diabetic Effects.....	11
1.4 L-Arginine: A Potential Anti-Diabetic Agent.....	13
1.4.1 The Role of L-Arginine in Diabetes Management	13
1.4.2 Proposed Mechanisms of Action	13
1.5 Lipid Nanocarriers for Drug Delivery.....	15

1.5.1	Enhanced Solubility and Stability.....	18
1.5.2	Focused Drug Administration.....	18
1.5.3	Preservation from Degradation.....	18
1.5.4	Findings on Lipid Nanocarriers in Diabetic Therapy.....	19
1.5.5	Critical Evaluation of Safety and Efficacy of Lipid Nanocarriers.....	20
1.6	<i>Network Pharmacology in Diabetes Research</i>	22
1.6.1	The Applications of Network Pharmacology in Diabetes Research.....	22
1.6.2	Network Pharmacology Studies in Diabetes Treatment.....	23
1.7	<i>Purpose of the Thesis Research: Integration of L-Arginine and Lipid Nanocarriers</i>	30
1.8	<i>Research Rationale</i>	31
1.9	<i>Scope and Limitations of the Study</i>	33
1.10	<i>Research Objectives</i>	35
CHAPTER 02: MATERIAL AND METHODS		37
2.1	<i>Plant Selection</i>	37
2.1.1	Rationale for <i>Trigonella foenum-graecum</i> Selection.....	37
2.1.2	Exploration of Fenugreek's Therapeutic Potential.....	37
2.2	<i>Seed Collection</i>	37
2.3	<i>Network Pharmacology for Active Compound Identification</i>	38
2.3.1	Therapeutic Potential of the Plant.....	38
2.3.2	Active Compound Screening.....	38
2.3.3	Identification of T2DM Gene Targets & Collective Targets.....	39
2.3.4	Network Visualization of Target Genes and Active Compounds.....	39
2.3.5	Protein-Protein Network Analysis.....	40
2.4	<i>Molecular Docking of Target Proteins and Active Compounds</i>	41

2.5	<i>Absorption, Distribution, Metabolism, Excretion, and Toxicity (ADMET) Analysis</i>	42
2.5.1	Oral Bioavailability and Drug-Likeness Criteria.....	43
2.5.2	Optimal Solubility and Penetration.....	43
2.5.3	Molecular Weight and Pharmacophores.....	43
2.5.4	Lipinski's Rule of Five and Toxicity Considerations.....	43
2.5.5	Online Tools for Comprehensive Analysis.....	44
2.6	<i>Seed Extract Preparation</i>	44
2.7	<i>Seed Oil Preparation</i>	44
2.7.1	Apparatus Setup.....	45
2.7.2	Solvent Addition.....	45
2.7.3	Extraction Process.....	45
2.7.4	Post-Extraction Steps.....	45
2.8	<i>Phytochemical Screening</i>	46
2.8.1	Wagner's Test for Alkaloid Identification.....	46
2.8.2	Foam Test for Saponin Differentiation.....	46
2.8.3	Ferric Chloride Test for Phenol Detection.....	47
2.8.4	Braymer's Test for Tannin Recognition.....	47
2.8.5	Salkowski's Test for Terpenoid Demonstration.....	47
2.8.6	Bontrager's Test for Quinone Assessment.....	47
2.8.7	Keller Killian's Test for Cardiac Glycoside Screening.....	47
2.8.8	Glycosides Test for Phytochemical Identification.....	48
2.8.9	Alkaline Reagent Test for Flavonoid Detection.....	48
2.8.10	Precipitate Test for Phlobatannin Screening.....	48
2.9	<i>Evaluation of Total Flavonoid Content</i>	48

2.10	<i>Evaluation of Total Phenolic Content</i>	49
2.11	<i>Synthesis of Lipid Nanoparticles</i>	51
2.12	<i>Encapsulation of L-Arginine in Lipid Nanoparticles</i>	51
2.13	<i>Characterization of the Synthesized Nanoparticles</i>	52
2.13.1	UV-Visible Spectrophotometry	52
2.13.2	Scanning Electron Microscopy (SEM).....	52
2.13.3	Fourier Transform Infrared Spectroscopy (FTIR)	53
2.13.4	Energy-Dispersive X-Ray Spectroscopy (EDX)	53
2.13.5	Particle Size Distribution Analyzer	53
2.13.6	Zeta (ζ) Potential Analysis.....	53
2.13.7	X-Ray Diffraction (XRD) Analysis	54
2.14	<i>Assessing the Biological Potential of the Encapsulated Nanoparticles</i>	55
2.14.1	Anti-Oxidant Activity	55
2.14.2	Anti-Inflammatory Activity	55
2.14.3	Anti-Diabetic Assay.....	56
2.14.4	Hemolytic Activity.....	57
2.14.5	Anti-bacterial Activity	57
CHAPTER 03: RESULTS AND ANALYSIS		60
3.1	<i>Seed Collection</i>	60
3.2	<i>Network Pharmacology Analysis</i>	60
3.2.1	Therapeutical Potential of the Plant.....	61
3.2.2	Active Compound Screening	63
3.2.3	Identification of Gene/Protein Targets.....	69
3.2.4	Network Visualization of Common Genes	72
3.2.5	Protein-Protein Network Analysis	72

3.3	<i>Molecular Docking Analysis</i>	80
3.4	<i>ADMET Profiles of the Target Compounds</i>	84
3.5	<i>Seed Extract Preparation</i>	93
3.6	<i>Seed Oil Preparation</i>	93
3.7	<i>Phytochemical Screening</i>	93
3.7.1	Wagner's Test.....	93
3.7.2	Foam Test.....	94
3.7.3	Ferric Chloride Test	94
3.7.4	Braymer's Test	94
3.7.5	Salkowski's Test.....	94
3.7.6	Bontrager's Test	95
3.7.7	Keller-Killian's Test.....	95
3.7.8	Glycosides Test.....	95
3.7.9	Alkaline Reagent Test.....	95
3.7.10	Precipitate Test.....	95
3.8	<i>Evaluation of Total Flavonoid Content</i>	95
3.9	<i>Evaluation of Total Phenolic Content</i>	96
3.10	<i>Synthesis of Lipid Nanoparticles</i>	96
3.11	<i>Encapsulation of L-Arginine in Lipid Nanoparticles</i>	97
3.12	<i>Characterization of Encapsulated Nanoparticles</i>	97
3.12.1	UV-VIS Spectrophotometry	97
3.12.2	Scanning Electron Microscopy	98
3.12.3	FTIR Analysis.....	99
3.12.4	EDX Analysis	100
3.12.5	Particle Size Distribution Analyzer	100

3.12.6	ζ-potential Analysis.....	101
3.12.7	XRD Analysis.....	102
3.13	<i>Biopotential Analysis of the Encapsulated Nanoparticles.....</i>	103
3.13.1	Anti-Oxidant Activity.....	103
3.13.2	Anti-Inflammatory Potential.....	104
3.13.3	Anti-Diabetic Activity.....	106
3.13.4	Hemolytic Activity.....	108
3.13.5	Anti-Bacterial Activity.....	109
CHAPTER 04: DISCUSSION AND CONCLUSION		112
4.1	<i>Concluding Remarks.....</i>	117
4.2	<i>Future Prospects of this Study.....</i>	118
4.2.1	Optimization of Nanoparticles.....	118
4.2.2	Cell-line and <i>In vivo</i> Assays.....	118
4.2.3	Formulation Development.....	119
4.2.4	Clinical Trials.....	119
CHAPTER 05: REFERENCES.....		121

ACKNOWLEDGMENTS

All praise is due to **Almighty Allah**, the omnipotent, the most compassionate, and His **Prophet Muhammad** (P.B.U.H.), the most perfect among all born on the earth's surface, who is a forever source of guidance and knowledge for humanity.

First, I am grateful to my supervisor, Professor **Dr. Bilal Haider Abbasi**, Pakistan, for his uttermost guidance, motivation, and skilled boosting attitude during my research work. Besides the academic supervision, Dr. Bilal acted as a father figure to me. He taught me how to stay strong and face every problem head-on! He taught me to understand everyone else's situations and keep going but not at the expense of someone else's efforts. I am forever grateful to you, Sir. I sincerely acknowledge **Dr. Javaria Qazi**, Chairperson, Department of Biotechnology, Quaid-i-Azam University. I am truly inspired by women who are leaders in today's world full of patriarchy and social dilemmas. Women who stand tall and within the boundaries of their religion and culture are rare, and Dr. Javaria is one of them. During my short stay at QAU, I learned many things from her.

I learned to be *saabir*, first of all. I learned to be courageous and perseverant, and most importantly, I learned to be helpful to others, no matter what. Also, I would like to specially acknowledge **Dr. Muhammad Naveed**, Head of the Department of Biotechnology, University of Central Punjab, for he has taught me to live, learn, unlearn, and relearn infinitely. He is another father figure who taught me that the sky is the limit and that you can reach the stars only if you do not give up! Lastly, I would like to acknowledge **Syeda Izma Makhdoom**, for I would only write this with her. She has been my rock throughout this process. She helped me with my practical tasks; she sacrificed many things, especially her time and sleep, to reach university daily and set up my experiments. ALLAH. has mentioned many times that I have sent you for your companions. Izma embodies this fact. Anyone would be lucky to have her as a friend. She is like an angel sent from above, and I will be forever grateful for her untiring efforts and contribution to this research thesis.

In my BS thesis, I acknowledged all my friends because I am what I am because of every one of them. I made new friends in these two years, and not acknowledging them

will be unfair. I will start by expressing my cordial thanks to all my friends that were there during my BS.

Additionally, I would like to acknowledge **Miss Afiya Shafaqat**, for I would not have survived Islamabad without her. She used to take care of me like a baby. Moreover, she holds the same respect and love in my heart as Izma. I still miss our long conversations, our laughs, our walks, and especially the cricket games. Afiya, you are a gem of a person, and I am so grateful to have known you!

I will continue to express my sincere gratitude to my class fellows and great friends; **Mr. Mustajab Khan, Mr. Usama Khan, Mr. Uzair Javed, Mr. Ahsan Saeed, Mr. Tahir Hayat, Mr. Razeen Ahmad, Mr. Hassan Ayaz, Miss Naveera Khan, Miss Tehreem Mehmood, Miss Bushra Khan, Miss Rida tul Haya, Miss Hamna Sajjad, Miss Ume-Aimen Hameed, and Miss Atiqa Tariq**. The pages will not be enough if I start writing about your contribution to my life. However, thank you, people, for making this journey beautiful. I am honored to have been your friend!

I acknowledge my seniors, especially **Dr. Zubia Shahid, Dr. Anbareen Gul, Miss Saman Zahoor, our beloved Annie Aapi, and Mr. Hasnat Tariq** for all the love, support, guidance, and memories! Also, I acknowledge my fellows at the Molecular Biotechnology and Bioinformatics Lab, back in the University of Central Punjab, for being one of my core supports forever. Amidst the pages of my journey, all my teachers stand as the ink that gives meaning to my story, the colors illuminating my path, and the melody that resonates in every chapter of my growth. Their wisdom, patience, and unwavering belief have sculpted not only my mind but also my heart. To them, I owe not just knowledge but the very essence of whom I am becoming.

Lastly, I would not be here without my family. My parents, kids, cousins, uncles, and aunts, thank you for bearing me and tolerating my tantrums. I try to be better every day for you, and InShaALLAH, with your duas and support, I will keep on succeeding. You are my roots, strength, and constant reminder of the love that fuels my journey. May our bond grow stronger, and may my achievements be a testament to your boundless faith.

With Lots of Love and Infinite Gratitude,

Urooj Ali

LIST OF FIGURES

Figure 1.1: A snapshot of the global distribution of Diabetes in 2021 (IDF, 2021).....	5
Figure 1.2: Current drug classes against diabetes and their therapeutic efficacy. Adapted from the works of Tahrani et al. (2016) and Chaudhury et al. (2017).....	7
Figure 1.3: Anti-diabetic effects of L-arginine derived from <i>T. foenum-graecum</i>	14
Figure 1.4: Potential therapeutic pathway targets in anti-diabetic research; A. The insulin signaling pathway; B. Protein targets of diabetes and its comorbidities; C. Diabetes pathway and therapeutic targets adapted from Kanehisa Laboratories (2023).....	31
Figure 2.1: TFC content of <i>Trigonella foenum-graecum</i>	49
Figure 2.2: TPC content of <i>Trigonella foenum-graecum</i>	50
Figure 3.1: Seeds collection from the local shop ‘Kashmiri Dawa Khana’ of Wazirabad. A. Seed Texture; B. Map of Kashmiri Dawa Khana.	60
Figure 3.2: Information about <i>Trigonella foenum-graecum</i> . A. Geographical distribution; B. Gene ontology targets; C. Disease targets; D. Target processes and pathways.	61
Figure 3.3: Therapeutic activity of fenugreek. A. Diseases targeted by <i>Trigonella foenum-graecum</i> ; Our target disease is highlighted in the red circle; B. Activity profiles of fenugreek’s active compounds. The green box highlights L-arginine’s activity profile, the yellow box highlights Daidzein’s activity profile and the purple boxes highlights the common gene targets of these compounds.	63
Figure 3.4: Fenugreek’s active compounds and their therapeutic profiling. A. Molecular weight distribution graph of the compounds; B. TPSA vs XlogP distribution chart of the active compounds; C. Hydrogen bond donors vs acceptors graph; D. Rule-of-5 violation graph.	69
Figure 3.5: Venn diagram showcasing the common gene/protein targets of T2DM and the active compounds.....	70
Figure 3.6: Cytoscape network of gene/protein targets of the active compounds. Genes in pink are targeted by Daidzein, genes in green are targeted by L-arginine, while those in yellow are targeted by both.....	73
Figure 3.7: STRING networks of the gene targets. A. Network of L-arginine targets; B. Network of Daidzein targets; C. Network of the three common gene targets.....	79

Figure 3.8: 2D interaction profiles of different poses of L-arginine, Daidzein, and Metformin (Control) with CYP1A2 protein. The ligands are present in the centre whereas the protein's surrounding amino acids are present around them. The amino acids shown in yellow are involved in direct molecular interaction with the ligands. The numbers represent the docking pose for each interaction.	80
Figure 3.9: 2D interaction profiles of different poses of L-arginine, Daidzein, and Metformin (Control) with CYP2C19 protein. The ligands are present in the centre whereas the protein's surrounding amino acids are present around them. The amino acids shown in yellow are involved in direct molecular interaction with the ligands. The numbers represent the docking pose for each interaction.	81
Figure 3.10: 2D interaction profiles of different poses of L-arginine, Daidzein, and Metformin (Control) with NFKB1 protein. The ligands are present in the centre whereas the protein's surrounding amino acids are present around them. The amino acids shown in yellow are involved in direct molecular interaction with the ligands. The numbers represent the docking pose for each interaction.	83
Figure 3.11: ADMET profiles of the target compounds. A-B. ADMET profiles of L-arginine provided by SwissADME (A) and ADMETLab 2.0 (B); C-D. ADMET profiles of Daidzein provided by SwissADME (A) and ADMETLab 2.0 (B); E. The BOILED-Egg analysis of both compounds.....	92
Figure 3.12: Processing of <i>T. foenum-graecum</i> ; A. Seed extract; B. Oil Extract.....	93
Figure 3.13: UV-visible spectroscopy for synthesized lipid nanoparticles showing maximum peak at 415 nm using oil extract of fenugreek seeds as precursor with methanolic seed extract at 1:1.....	96
Figure 3.14: UV visible spectroscopy for synthesized L-arginine encapsulated lipid nanoparticles showing maximum absorbance at 521 nm.	97
Figure 3.15: SEM micrograph of L-arginine encapsulated lipid nanoparticles synthesized by using seed and oil extract of fenugreek showing an average size of 100.2 nm at 10,000X and 1 micrometer known distance.	98
Figure 3.16: FTIR analysis of L-arginine encapsulated lipid nanoparticles.....	99

Figure 3.17: EDX analysis showing graphical representation of the elements present in L-arginine encapsulated lipid nanoparticles.	100
Figure 3.18: Size calculation of arginine-encapsulated lipid nanoparticles using PSD.	101
Figure 3.19: The ζ -potential of the arginine-encapsulated lipid nanoparticles.....	102
Figure 3.20: XRD graph of arginine-encapsulated lipid nanoparticles indicating their amorphous to semi-crystalline nature.	102
Figure 3.21: Experimental overview of anti-oxidant activity; A. Control; B. Seed Extract; C. Seed Oil, and D. Nanoparticles; all, at concentrations of 100 g/mL, 200 g/mL, 300 g/mL, 400 g/mL, and 500 g/mL.	103
Figure 3.22: Percentage of free radical scavenging by the control, seed extract, oil extract, and L-arginine-encapsulated lipid nanoparticles at various concentrations.	104
Figure 3.23: Experimental overview of anti-inflammatory activity; A. Control; B. Seed Extract; C. Seed Oil, and D. Nanoparticles; all, at concentrations of 150 g/mL, 250 g/mL, 350 g/mL, 450 g/mL, and 550 g/mL.....	105
Figure 3.24: Percentage inhibition of albumin denaturation by the control, seed extract, oil extract, and L-arginine-encapsulated lipid nanoparticles at various concentrations.	106
Figure 3.25: Experimental overview of anti-diabetic activity; A. Control; B. Seed Extract; C. Seed Oil, and D. Nanoparticles; all, at concentrations of 200 g/mL, 400 g/mL, 600 g/mL, 800 g/mL, and 1000 g/mL.	107
Figure 3.26: A graphic representation of the anti-diabetic effect demonstrates the percentage inhibition of the α -amylase assay by the control, seed extract, oil extract, and L-arginine-encapsulated lipid nanoparticles at various concentrations.....	107
Figure 3.27: Experimental overview of hemolytic activity; A. Control; B. Seed Extract; C. Seed Oil, and D. Nanoparticles; all, at 150 g/mL, 200 g/mL, 250 g/mL, 300 g/mL, and 350 g/mL.....	108
Figure 3.28: A graphic representation of the hemolysis effect showing RBCs destruction by the control, seed extract, oil extract, and L-arginine-encapsulated lipid nanoparticles at various concentrations.	109

Figure 3.29: Inhibition zones of synthesized L-arginine encapsulated lipid nanoparticles and control antibacterial disc cefoxitin against specific bacteria (A) *Vibrio cholera* (B) *Bacillus anthracis*. 110

LIST OF TABLES

Table 1.1: <i>Comparison of different nanoparticles and their anti-diabetic efficacy.</i>	16
Table 1.2: <i>L-arginine drug delivery approaches to treat Diabetes.</i>	17
Table 1.3: <i>Network pharmacology studies in natural products for diabetes mellitus treatment: mechanisms, targets, and active compounds.</i>	24
Table 2.1: <i>Core protein targets selected for molecular docking.</i>	41
Table 3.1: <i>A detailed insight into the disease targets of Trigonella foenum-graecum.</i> ...	62
Table 3.2: <i>Identification of active compounds present in Trigonella foenum-graecum, provided by the CMAUP database. The target compounds are highlighted in Yellow.</i> ...	64
Table 3.3: <i>Potential gene targets of L-arginine.</i>	70
Table 3.4: <i>Potential gene targets of Daidzein.</i>	71
Table 3.5: <i>Details of the Gene/Protein Targets of the Active Compounds.</i>	73
Table 3.6: <i>Molecular docking energy scores (indicated as S) of target compounds with the three common proteins.</i>	82
Table 3.7: <i>ADMET profiles of the target compounds of Trigonella foenum-graecum. The green sphere indicates favorable results, whereas spheres in red indicate non-favorable outcomes.</i>	84
Table 3.8: <i>Phytochemical screening of seed and oil extracts in fenugreek.</i>	94
Table 3.9: <i>Elemental Composition of L-arginine encapsulated lipid nanoparticles</i>	100

LIST OF ABBREVIATIONS

CYP1A2	Cytochrome P450 Family 1 Subfamily A Member 2
CYP2C19	Cytochrome P450 Family 2 Subfamily C Member 19
NFKβ	Nuclear Factor Kappa β
DM	Diabetes Mellitus
IDDM	Insulin Dependent Diabetes Mellitus
T2DM	Type 2 Diabetes Mellitus
NIDDM	Non-Insulin-Dependent Diabetes Mellitus
MOE	Molecular Operating Environment
ADMET	Absorption, Distribution, Metabolism, Excretion, and Toxicity
TPC	Total Phenolic Content
TFC	Total Flavonoid Content
SEM	Scanning Electron Microscope
XRD	X-Ray Diffraction
FTIR	Fourier-Transform Infrared Radiation
PSD	Particle Size Distribution
GDM	Gestational Diabetes Mellitus
IDF	International Diabetes Federation
WHO	World Health Organization
DPP-4	Dipeptidyl-Peptidase-4
SGL-2	Sodium Glucose Cotransporter 2
GLP-1	Glucagon-like Peptide-1
IRS-1	Insulin Receptor Substrate-1
NO	Nitric Oxide
ROS	Reactive Oxygen Species
SLN	Solid Lipid Nanoparticles
NLC	Nanostructured Lipid Carriers
MLN	Methocel-Lipid Hybrid Nanocarrier
RA	Receptor Agonist

FDA	Food and Drug Administration
PPARG	Peroxisome Proliferator-activated Receptor Gamma
NAFLD	Nonalcoholic Fatty Liver Disease
CCF	<i>Coptis</i> Categorized Formula
HIF1A	Hypoxia-Inducible Factor 1 Alpha
NFE2L2	Nuclear Factor, Erythroid 2 Like 2
NOS3	Nitric Oxide Synthase 3
NR3C1	Nuclear Receptor Subfamily 3 Group C Member 1
PIK3CA	Phosphatidylinositol-4,5-Bisphosphate 3-Kinase Catalytic Subunit Alpha
SIRT1	Sirtuin 1 / Silent Information Regulator 1
AKT1	AKT Serine/Threonine Kinase 1
MAPK1	Mitogen-Activated Protein Kinase 1
IL-6	Interleukin 6
GAPDH	Glyceraldehyde-3-Phosphate Dehydrogenase
NP	Nanoparticles
CMAUP	Collective Molecular Activities of Useful Plants
PDB	Protein Data Bank
OB	Oral Bioavailability
DL	Drug-Likeness
W/O/W	Water-Oil-Water
DPPH	2,2-Diphenyl-1-Picrylhydrazyl Radical

ABSTRACT

Diabetes, a globally prevalent chronic condition, necessitates effective therapeutic approaches. This research investigated the roles of L-arginine and *Trigonella foenum-graecum* (Fenugreek) in diabetes management while evaluating lipid nanocarriers synthesized from fenugreek seed oil for drug delivery. Network pharmacology's implications in diabetes research were also explored. Compounds Daidzein and L-arginine emerged as potential anti-diabetic agents, with L-arginine selected as the lead compound. Docking analysis revealed L-arginine's strong interactions with three Diabetes-target genes (CYP1A2, CYP2C19, AND NFKB) involving multiple hydrogen bonds and excellent binding energies. Total Flavonoid Content (TFC) and Total Phenolic Content (TPC) assessments revealed higher concentrations in seed extracts than in oil extracts. UV-Vis spectroscopy identified distinctive absorbance peaks for simple and L-arginine encapsulated lipid nanoparticles at 415 and 521 nm, respectively. Scanning electron microscopy (SEM) affirmed the nanoparticles' average size of 100.2 nm. In contrast, the Zeta-potential analysis indicated a neutral charge of -9.37 mV, while X-ray diffraction (XRD) confirmed the nanoparticles' amorphous nature. Synthesized nanoparticles demonstrated remarkable antioxidative efficacy with 84.44% inhibition and an IC₅₀ value of 40.5, surpassing control (62.84%: IC₅₀-231.27), fenugreek seed extract (59.73%: 208.98), and oil extract (61.03%: 196.6). L-arginine encapsulated lipid nanoparticles exhibited substantial inhibition of albumin denaturation (81.10%) and alpha-amylase (89.30%), outperforming metformin (78.43% at 1000 µg/mL). Notably, hemolysis percentage stood out favorably at 10.54%, in contrast, to control (91.70%), fenugreek seed extract (39.17%), and fenugreek oil extract (46.08%). In conclusion, this study offers an understanding of potential anti-diabetic agents and innovative drug delivery mechanisms. These quantified results hold promise for advancing therapeutic interventions in diabetes management, bridging crucial knowledge gaps, and guiding future research directions.

CHAPTER ONE

INTRODUCTION & LITERATURE REVIEW

INTRODUCTION AND LITERATURE REVIEW

Diabetes is a highly prevalent and complex chronic condition that has a significant impact on a large number of individuals globally. Diabetes research is important in advancing efficacious therapeutic approaches, given its prominent contribution to morbidity and mortality rates. This study examines the potential of L-arginine and *Trigonella foenum-graecum* (Fenugreek) as agents for managing Diabetes, as well as to assess the effectiveness of lipid nanocarriers for delivering drugs in treating Diabetes. We will also explore the nascent domain of network pharmacology and its ramifications in Diabetes investigation. This chapter aims to establish a solid foundation for future inquiries in this field through a rigorous analysis of current research and thoroughly identifying areas that must be adequately addressed in the literature. By conducting a thorough examination, our objective is to make a scholarly and applied contribution to the field of Diabetes research and facilitate the development of enhanced therapeutic interventions for individuals grappling with this complex condition.

1.1 Diabetes: Overview and Current Management

Diabetes is a complex metabolic disorder that substantially impacts the overall well-being of individuals worldwide. The condition is distinguished by chronic hyperglycemia, which arises from impairments in either insulin secretion, insulin action, or both (Feldman et al., 2019). The categorization of Diabetes into discrete types holds significant significance as it allows healthcare practitioners to customize treatment approaches with efficacy. Gaining a comprehensive understanding of the fundamental mechanisms and distinct attributes associated with each type enables the implementation of focused interventions, resulting in enhanced patient outcomes. Diabetes mellitus can be categorized into various types according to its etiology, pathophysiology, and age of onset. The primary classifications encompass Type 1 diabetes, Type 2 diabetes, and gestational Diabetes (Kuzuya et al., 2002).

1.1.1 Type 1 Diabetes Mellitus

Type 1 diabetes, referred to as insulin-dependent diabetes mellitus (IDDM) or juvenile-onset Diabetes, is classified as an autoimmune disorder (Cooke and Plotnick, 2008). In this category, the immune system exhibits an erroneous response by targeting and eliminating the beta cells responsible for insulin production within the pancreas. Consequently, the pancreas exhibits diminished or negligible insulin production, resulting in an insufficiency of this pivotal hormone (DiMeglio et al., 2018). It commonly manifests during the early stages of childhood or adolescence. However, it can emerge at any point in an individual's lifespan. Individuals diagnosed with Type 1 diabetes necessitate regular administration of insulin injections or utilization of an insulin pump to regulate their blood glucose levels effectively (Pickup, 2018). As per the reports of Centers for Disease Control and Prevention (2022), this particular type of Diabetes constitutes approximately 5-10% of the total number of diabetes cases.

1.1.2 Type 2 Diabetes Mellitus

Type 2 diabetes mellitus (T2DM), non-insulin-dependent diabetes mellitus (NIDDM), or adult-onset Diabetes is the prevailing manifestation of diabetes mellitus. The condition arises when the body develops resistance to the physiological effects of insulin or experiences insufficient insulin production to fulfill the body's metabolic demands adequately (Galicia-Garcia et al., 2020). Several risk factors have been identified for developing Type 2 diabetes, including a lack of physical activity, being overweight or obese, engaging in unhealthy dietary practices, having a family history of Diabetes, and belonging to certain ethnic groups (Fletcher et al., 2002; Bi et al., 2012; Bellou et al., 2018). In contrast to Type 1 diabetes, Type 2 diabetes frequently lends itself to initial management through lifestyle modifications, encompassing consistent engagement in physical activity, a nutritious dietary pattern, and effective weight control (Galaviz et al., 2018; Powers et al., 2020). Nevertheless, as the disease advances, it may become necessary to administer oral medications or insulin therapy to manage blood glucose levels effectively.

1.1.3 Gestational Diabetes

Gestational diabetes mellitus (GDM) is a transient manifestation of Diabetes that arises during pregnancy. Gestational Diabetes arises due to the hormonal fluctuations and insulin resistance characteristic of pregnancy, resulting in heightened glucose levels in the bloodstream (Mukhtar et al., 2020). It typically manifests between the 24th and 28th week of pregnancy and tends to resolve following delivery (Law & Zhang, 2017). Nevertheless, it is worth noting that women with a previous medical record of GDM face an elevated likelihood of developing Type 2 diabetes later, as reported by England et al. (2009) and Dennison et al. (2019). Effectively managing gestational Diabetes is imperative to promote a favorable outcome during pregnancy and mitigate potential adverse consequences for maternal and fetal health (Cheung, 2009).

1.2 Global Prevalence and Burden of Diabetes

The rising incidence of Diabetes worldwide seriously affects public health and healthcare delivery worldwide. About 10.5% of the adult population (20-79 years) globally has Diabetes, and roughly half of them are ignorant of their illness, according to the International Diabetes Federation (2021). Since 1980, the percentage of adults with Diabetes has almost quadrupled, from 4.7% to 8.5%. According to IDF (2021), the anticipated worldwide age-standardized prevalence of Diabetes in 2021 was 537 million people. It equates to more than 6.0% of the global population being diabetic. In the Western Pacific (10.4%) and South Asia (9.9%), the incidence is greatest, followed by the Middle East and North Africa (11.3%) and the rest of the world, as shown in Figure 1.1. In comparison, the prevalence is 4.1% in sub-Saharan Africa and 7.4% in Latin America and the Caribbean (IDF, 2021).

Prevalence by Age Group reveals a clear correlation between being older and having a greater risk of developing type 2 diabetes. Over 20% of those between 65 and 95 have Diabetes, with the greatest incidence in those aged 75–79 (24.4%) (Laiterapong & Huang, 2018). The prevalence is less than 1% among those under 20, highlighting the effect of aging populations on the global burden of Diabetes (American Diabetes Association, 2022). Approximately 96% of all cases of Diabetes worldwide are attributable to type 2

diabetes (IDF, 2021). The leading risk factor for developing type 2 diabetes is a high body mass index (BMI), accounting for 52.2% of the worldwide DALYs attributable to this disease (Zhang et al., 2022). To successfully battle the diabetes pandemic, it is essential to tackle obesity and promote healthy lifestyles.



Figure 1.1: A snapshot of the global distribution of Diabetes in 2021 (IDF, 2021).

1.2.1 Impact of Diabetes on World Health

According to World Health Organization (2023), blindness, renal failure, heart disease, stroke, and lower limb amputation are some of the many serious health problems that may result from Diabetes. It accounted for 6.7 million deaths worldwide in 2021 alone (IDF et al., 2021). It makes Diabetes the ninth biggest cause of mortality globally (WHO, 2023). According to the IDF (2021), the worldwide cost of Diabetes was around \$966 billion in 2021, a 316% increase since 2006. Bommer et al. (2018) estimate that by 2030, the economic effect of Diabetes will climb to over \$2.1 trillion.

1.2.2 Impact of Diabetes on Pakistan

An alarming number of Pakistani people are developing Diabetes, making it a rising public health problem. Hassan (2022) estimated that 7 million people in Pakistan had

Diabetes in 2015. Family history, obesity, and other socioeconomic variables increase an individual's likelihood of developing Diabetes. Pakistan had the 18th highest prevalence of Diabetes out of 21 nations in 2017, with almost 7.5 million people aged 20-79 with Diabetes (Azeem et al., 2022). Diabetes had a weighted overall prevalence of 26.3%, with 19.2% already diagnosed and 7.1% receiving one. Urban regions had a 28.3% higher prevalence of Diabetes than rural areas (25.3%) (Basit et al., 2018).

Over 19 million Pakistani people are thought to be living with Diabetes in 2019, with an alarming 8.5 million of them still undiagnosed (Azeem et al., 2022). About 33 million Pakistani individuals, or about 26.7% of the adult population, had Diabetes in 2022, according to IDF (2021) and Jamshaid (2023). According to Azeem et al. (2022), the prevalence increased dramatically from 17.1% in 2019 to 26.7% in 2022. Type 2 diabetes mellitus affects 90% of the 463 million persons who have Diabetes globally (Saeedi et al., 2019). It was reported to be more common in Pakistan than in China or India till 2020 (Aamir et al., 2019). However, Sherrell (2022) reports that China has reported the greatest number of diabetes cases recently. Nonetheless, it is still believed that due to underreporting, the incidence of Diabetes in Pakistan is probably greater. Proper diagnosis, reporting, and treatment may greatly increase the likelihood of problems. (Khan, 2022)

1.2.3 Predictions and Targets for the Future

According to Gregory (2023), the prevalence of Diabetes will rise by 59.7 percent by 2050, as 1.3 billion people will have Diabetes. It suggests that 9.8% of the world's population may be diabetic at any one time, or around 1.31 billion individuals. Nearly half of the expected rise is attributable to changes in obesity (WHO, 2021), mostly driven by demographic shifts. By 2030, the World Health Organization aims to minimize the burden of Diabetes by halving the number of deaths caused by the disease and decreasing the number of people living with the disease by 10% (Rowley et al., 2017). Promoting better lifestyles, preventing obesity, and early identification and treatment of Diabetes are just some of the public health measures needed to combat the epidemic of Diabetes that is sweeping the world (Galaviz et al., 2018).

1.2.4 The Current Anti-Diabetic Therapies and Their Limitations

Antidiabetic medications for type 2 diabetes fall into many broad categories, including biguanides, sulfonylureas, alpha-glucosidase inhibitors, thiazolidinediones, dipeptidyl peptidase-4 (DPP-4) inhibitors, SGLT-2 inhibitors, and GLP-1 receptor agonists (Kumar et al., 2017; Yaribeygi et al., 2019). Different classes of drugs use different mechanisms to affect glucose metabolism, insulin secretion, and insulin sensitivity. Metformin is the most widely used biguanide, which decreases glucose synthesis in the liver and increases insulin sensitivity in muscle cells (Giannarelli et al., 2003). The quick postprandial rise in blood sugar can be avoided with sulfonylureas, which increase insulin secretion from the pancreas, and alpha-glucosidase inhibitors, reducing the digestion of carbohydrates in the gut (Pernicova & Korbonits, 2014).

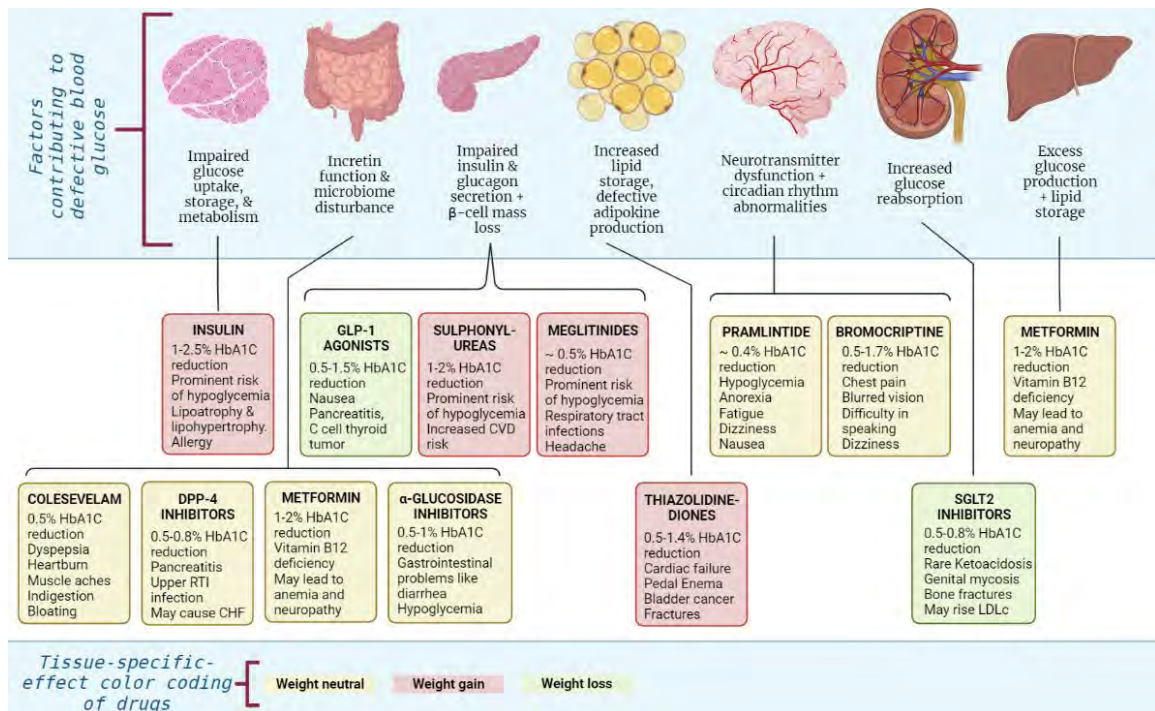


Figure 1.2: Current drug classes against diabetes and their therapeutic efficacy. Adapted from the works of Tahrani et al. (2016) and Chaudhury et al. (2017).

DPP-4 inhibitors prevent the breakdown of glucagon-like peptide-1 (GLP-1), and thiazolidinediones increase insulin sensitivity in muscle and fat cells (Khan et al., 2019). These antidiabetic medications are effective. However, there are some difficulties with using them in their current dose forms (Makrilakis, 2019). Barnett (2006) reported very

early that these inhibitors have variable bioavailability. Therefore, they need to be dosed often to maintain their therapeutic benefits. Some medications may also cause undesirable side effects such as nausea, vomiting, diarrhea, or drowsiness (Fletcher, 2023). These constraints may impede patient compliance, which may prevent optimum glycemic control from being attained.

1.2.4.1 Beta-Cell Substitution Therapy and Pancreas Transplantation

Surgical treatments for Diabetes include pancreas transplantation and beta cell replacement therapy. The long-term cure for type 1 diabetes is pancreatic transplantation, which entails implanting the pancreas of a dead donor into a diabetic patient. The patient's ability to produce insulin is restored, and he or she may no longer need insulin injections after this surgery. The goal of beta cell replacement treatment, which is currently in the research and development phase, is to restore insulin production by transplanting functioning beta cells into a diabetic patient (Odorico et al., 2018). Nanotechnology's potential use in organ preservation and transplantation holds promise for boosting success rates and decreasing graft rejection rates.

Beyond conventional medication administration, promising new technologies such as the bioartificial pancreas and stem cell therapy provide exciting new avenues for treating Diabetes. Automated insulin dosing in response to fluctuating blood sugar levels is made possible by the bioartificial pancreas (Latres et al., 2019), which consists of glucose sensors, insulin pumps, and computer algorithms. Type 1 diabetics may benefit from this approach since it makes monitoring and controlling their blood sugar easier and more accurate (Perkins et al., 2021). Both type 1 and type 2 diabetes may be curable thanks to stem cell treatment, which entails using stem cells to repair or replace damaged pancreatic cells.

1.2.4.2 Nanotechnology as the New Promising Frontier

Drug delivery technologies based on nanotechnology promise to improve the shortcomings of current diabetes treatments. Some interesting nanocarriers that may increase medication stability, bioavailability, and site-specific delivery include nanoparticles, liposomes, micelles, and hydrogels. These carriers may encapsulate

antidiabetic medicines, allowing for their regulated release and distribution to particular tissues like the pancreas or muscles (Singh et al., 2019). This method not only decreases adverse effects but also allows for less frequent dosage, which in turn increases patient compliance. Diabetes immunotherapy may be made more individualized and targeted using nanotechnology-based carriers like liposomes or nanoparticles to inhibit or enhance immune responses. Conversely, gene therapy aims to fix the underlying genetic causes of Diabetes (Nigam et al., 2022). Therapeutic genes may be delivered to pancreatic cells through nanocarriers to replace or repair faulty genes. Because it targets the underlying genetic variables in Diabetes, this strategy has promising applications for type 1 and type 2 diabetes.

1.2.4.3 Diet and Lifestyle Modifications

Modifying one's diet and level of physical activity is still the cornerstone of diabetes care, despite the many promising new antidiabetic medication therapies and cutting-edge technology (Vairavamurthy et al., 2017; Galaviz et al., 2018). Maintaining a healthy weight and engaging in regular physical activity have been shown to significantly impact diabetes management, insulin sensitivity, and complication risk (Colberg et al., 2010). For best diabetic management, professionals propose a multi-pronged strategy that includes pharmaceutical treatments and behavioral modifications (Shrivastava et al., 2013; Parati et al., 2022).

1.3 *Trigonella foenum-graecum* (Fenugreek): Bioactive Compounds and Anti-Diabetic Properties

Traditional medical practices worldwide have long recognized the usefulness of plant-based medicines. The wide variety of bioactive substances they generate offers medicinal promise. These compounds include polyphenols, flavonoids, alkaloids, and terpenoids. Antioxidant, anti-inflammatory, and anti-diabetic benefits are just a few of how these substances improve human health (Rahman et al., 2022). Scientists have therefore begun investigating these plant-derived chemicals as diabetic therapy options. Plant-derived chemicals have been shown to have antidiabetic effects in several investigations.

For example, berberine, a bioactive component in many plants, has been demonstrated to improve insulin sensitivity, decrease diabetes complications, and reduce blood glucose levels (Kong et al., 2009). A polyphenolic component found in turmeric called curcumin has also been demonstrated to reduce insulin resistance and inflammation in people with Diabetes (Zheng et al., 2018). Improved glycemic control and reduced risk of Diabetes complications have also been associated with using plant-based substances such as quercetin, resveratrol, and epigallocatechin gallate (EGCg) (Loureiro & Martel, 2019). These findings demonstrate the tremendous therapeutic potential of plant biochemistry in treating Diabetes.

1.3.1 *Trigonella foenum-graecum and its Bioactive Compounds*

Trigonella foenum-graecum, widely recognized as Fenugreek, is a perennial plant classified within the *Fabaceae* botanical family (Goyal et al., 2016). The cultivation of this plant is prevalent in diverse regions across the globe, encompassing Asia, Europe, and North Africa. Due to its therapeutic attributes, Fenugreek has historically been employed in Ayurveda, Chinese medicine, and other traditional healing systems (Nagulapalli Venkata et al., 2017). The botanical specimen possesses a substantial abundance of bioactive constituents, substantiating its therapeutic efficacy in a diverse range of health ailments encompassing the realm of Diabetes. Fenugreek seeds are widely recognized for their therapeutic attributes and encompass many biologically active constituents. Fenugreek seeds contain several bioactive compounds, including saponins, alkaloids, flavonoids, polyphenols, and sterols (Mallik et al., 2020). It is worth mentioning that the primary bioactive compounds responsible for its anti-diabetic properties are 4-hydroxy isoleucine, which is a derivative of an amino (Sauvaire et al., 1998), and L-arginine, an amino acid (Forzano et al., 2023). The anti-diabetic effects of Fenugreek are believed to be the result of the combined action of its bioactive compounds.

1.3.2 *The Anti-Diabetic Potential of Trigonella foenum-graecum*

The utilization of in vitro studies has played a crucial role in elucidating the underlying mechanisms by which *Trigonella foenum-graecum* exerts its anti-diabetic

effects. The studies have consistently exhibited the plant's capacity to impede the activity of alpha-glucosidase, an enzyme accountable for the hydrolysis of carbohydrates into glucose (Dirir et al., 2021). The process of enzyme inhibition by fenugreek results in a deceleration of glucose absorption into the circulatory system, thereby causing a reduction in blood glucose levels. Furthermore, it has been demonstrated in a study (Semwal et al., 2020) that fenugreek extract possesses the ability to augment the synthesis of insulin by beta cells located in the pancreas. The augmented insulin secretion facilitates the transportation of glucose molecules into cellular structures, enabling their utilization as an energy source. Consequently, this process plays a significant role in regulating blood sugar levels.

Animal studies have further substantiated the anti-diabetic potential of Fenugreek. The findings from these studies consistently indicate that fenugreek extract can decrease blood glucose levels in animal models with Diabetes. For example, a study conducted by Verma et al. (2016) demonstrated a significant decrease of approximately 40% in blood glucose levels among diabetic rats following the administration of fenugreek extract. A separate investigation emphasized the beneficial effect of Fenugreek on insulin sensitivity in rats with Diabetes, providing additional support for its potential as a therapeutic agent for Diabetes (Hosseini et al., 2020). The results obtained from animal studies are consistent with the observations made in laboratory experiments, thereby strengthening the potential of Fenugreek as a therapeutic option for managing Diabetes.

Although there is a scarcity of human studies investigating the anti-diabetic effects of Fenugreek, the existing evidence demonstrates encouraging outcomes. For example, the efficacy of fenugreek extract in lowering fasting blood glucose levels was observed in a study conducted on individuals diagnosed with type 2 diabetes (Gaddam et al., 2015). These findings offer significant insights into the potential clinical significance of Fenugreek as a supplementary treatment for Diabetes.

1.3.3 Mechanisms Underlying Fenugreek's Anti-Diabetic Effects

The anti-diabetic properties of fenugreek extract are primarily attributed to its ability to inhibit alpha-glucosidase, as stated in a study Palanuvej (2009). The enzyme

alpha-glucosidase plays a crucial role in the hydrolysis of complex carbohydrates into glucose within the small intestine (Dirir et al., 2021). The activity of this enzyme is impeded by Fenugreek, resulting in a deceleration of the conversion process whereby carbohydrates are transformed into glucose. Consequently, glucose is released into the bloodstream gradually and regulated. This phenomenon leads to a decrease in postprandial blood glucose spikes (Goff et al., 2018), which confers particular advantages for individuals diagnosed with Diabetes in achieving and sustaining stable blood sugar levels and mitigating abrupt hyperglycemic episodes.

The capacity of fenugreek extract to enhance insulin production by pancreatic beta cells is also a crucial factor contributing to its anti-diabetic (Hussain et al., 2020). The synthesis and secretion of insulin, a vital hormone for cellular glucose uptake, is carried out by beta cells located in the pancreas. The bioactive compounds found in Fenugreek have been observed to augment the sensitivity of beta cells toward fluctuations in blood glucose levels (Semwal et al., 2020). The increased sensitivity observed in beta cells leads to augmented insulin secretion in the presence of elevated glucose levels in the bloodstream, thereby guaranteeing a sufficient amount of insulin to facilitate the transportation of glucose into cells. Fenugreek facilitates improved glucose utilization and aids in reducing blood sugar levels in individuals with Diabetes by promoting heightened insulin secretion (Uemura et al., 2010).

Furthermore, the influence of Fenugreek on insulin sensitivity in peripheral tissues, including skeletal muscle and adipose tissue, serves to augment its therapeutic effects in managing Diabetes (Avalos-Soriano et al., 2016). The bioactive constituents of Fenugreek, such as 4-hydroxy isoleucine, can regulate the signaling pathways of insulin, specifically the insulin receptor substrate-1 (IRS-1) and Akt pathways, within specific tissues (Srinivasa & Naidu, 2021). According to Kiss et al. (2018), Fenugreek has been found to enhance insulin sensitivity, leading to an increase in the uptake and utilization of glucose by cells. This mechanism ultimately contributes to improved glycemic control and reduced blood glucose levels.

1.4 L-Arginine: A Potential Anti-Diabetic Agent

L-arginine, a crucial amino acid, has attracted considerable interest in diabetes research due to its potential therapeutic properties against Diabetes. It is a precursor for synthesizing nitric oxide (NO), a potent vasodilator pivotal in regulating blood flow and vascular function. The investigation of L-arginine's implications in diabetes management has extended beyond its well-established role in cardiovascular health.

1.4.1 *The Role of L-Arginine in Diabetes Management*

The anti-diabetic properties of L-arginine have been elucidated through *in vitro* studies, yielding significant insights. A study has shown that L-arginine supplementation can enhance insulin secretion from pancreatic beta cells. This finding suggests that L-arginine may improve the regulation of glucose levels in the body (Carvalho et al., 2016). Furthermore, previous studies have demonstrated that L-arginine can mitigate the detrimental effects of glucotoxicity and lipotoxicity on pancreatic beta-cell dysfunction and apoptosis (Araujo et al., 2017; Forzano et al., 2023). The results of this study highlight the potential of L-arginine in preserving the function of beta cells and facilitating insulin secretion.

The anti-diabetic effects of L-arginine have been further substantiated by *in vivo* studies. L-arginine supplementation was observed to improve insulin resistance and decrease fasting blood glucose levels in the rat model of Diabetes (Clemmensen et al., 2011). Furthermore, the administration of L-arginine has been linked to enhanced endothelial function and decreased oxidative stress in animal models with Diabetes (Forzano et al., 2023). These effects underscore the potential of L-arginine in mitigating the vascular complications frequently linked to Diabetes.

1.4.2 *Proposed Mechanisms of Action*

The anti-diabetic effects of L-arginine are complex and involve a combination of direct and indirect mechanisms. One of the principal mechanisms is the involvement of L-arginine in the synthesis of nitric oxide (NO). The supplementation of L-arginine serves as a precursor for nitric oxide (NO), thereby augmenting NO availability (Janaszak-Jasiecka

et al., 2023). This, in turn, results in heightened vasodilation and enhanced blood flow. The impact described is especially pertinent in Diabetes, characterized by endothelial dysfunction and impaired nitric oxide synthesis, contributing to vascular complications (Nikolaeva & Johnstone, 2023). Promoting vasodilation by L-arginine has the potential to enhance blood flow to peripheral tissues, thereby facilitating the transport and utilization of glucose.

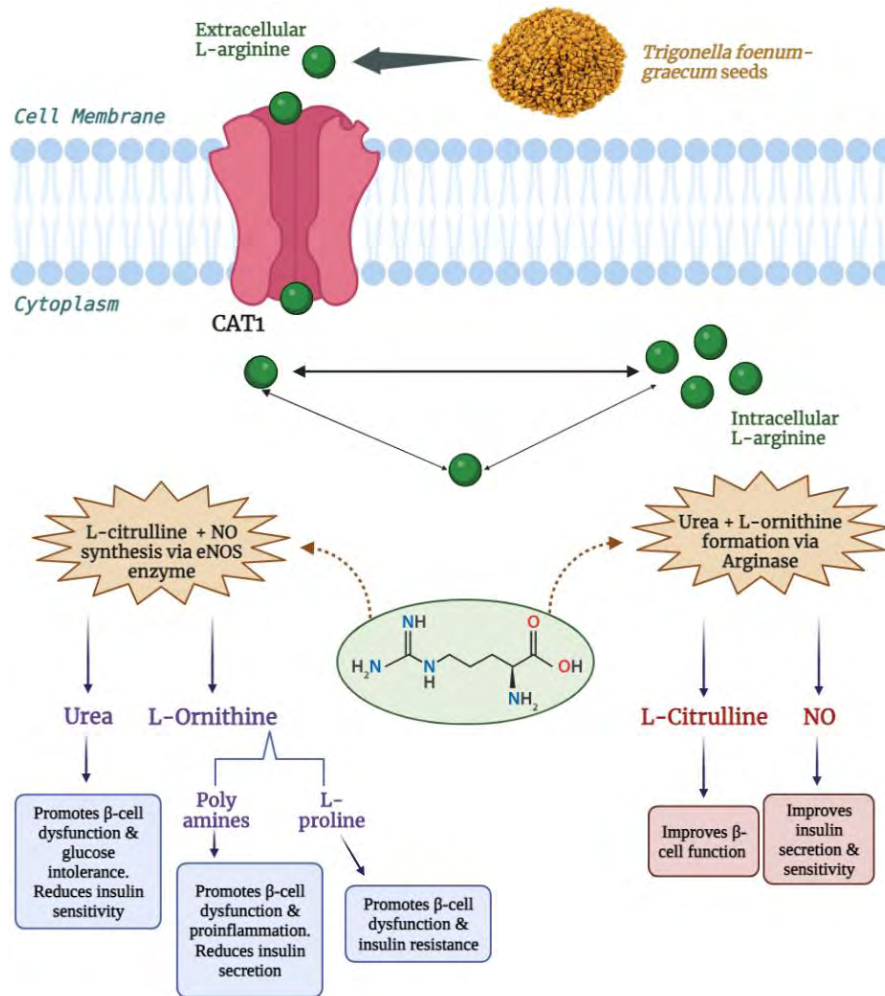


Figure 1.3: Anti-diabetic effects of L-arginine derived from *Trigonella foenum-graecum*.

Moreover, the impact of L-arginine on insulin secretion is associated with its function in regulating pancreatic beta cell activity. Research has indicated that L-arginine can augment insulin secretion from beta cells when exposed to glucose stimulation (Cho et al., 2020). The observed phenomenon is facilitated by initiating calcium-dependent

signaling pathways within beta cells, leading to insulin release through exocytosis (Ježek et al., 2021). Enhancing insulin secretion through administering L-arginine can improve glycemic control and decrease blood glucose levels in individuals diagnosed with Diabetes.

Also, it is worth noting the potential of L-arginine in mitigating oxidative stress. Oxidative stress plays a significant role in the development and progression of Diabetes and its related complications (Bhatti et al., 2022). The augmentation of nitric oxide (NO) availability through the administration of L-arginine has been shown to mitigate oxidative damage and diminish the generation of reactive oxygen species (ROS) (Incalza et al., 2018).

The antioxidative effect of this phenomenon has the potential to safeguard pancreatic beta cells against dysfunction and apoptosis caused by oxidative stress. Consequently, this may lead to enhanced insulin secretion and improved control over glycemic levels.

1.5 Lipid Nanocarriers for Drug Delivery

The investigation of different approaches for incorporating L-arginine in the human body has been driven by recognizing its therapeutic potential in diabetes management. L-arginine has the potential to be orally administered as a dietary supplement, serving as a direct source for its utilization in the synthesis of nitric oxide (Chen et al., 2020). Nevertheless, the effectiveness of the treatment may be constrained due to obstacles such as inconsistent bioavailability and swift elimination when utilized in isolation.

Farkhani et al. (2014) have noted that using L-arginine in conjunction with nanoparticles improves its stability and facilitate transportation to specific tissues has emerged as a promising strategy. Table 1.1 provides a comparative analysis of different nanoparticles in anti-diabetic research. Based on the analysis, it is presumed that an effective strategy that can be employed against Diabetes involves the utilization of lipid nanocarriers to deliver L-arginine.

Table 1.1: Comparison of different nanoparticles and their anti-diabetic efficacy.

Type of Nanoparticles	Size Range (nm)	Potential Anti-Diabetic Applications	Anti-diabetic efficacy	Cited Works
Lipid-based	20-200	Drug delivery carriers for anti-diabetic medications	Upto 99%	Rawat et al., 2011
Polymeric	10-500	Controlled release of insulin or other anti-diabetic agents	Upto 90%	Singh et al., 2018
Gold	2-100	Photothermal therapy, targeted drug delivery, and sensing	Upto 85%	Ayyoub et al., 2022
Silver	5-100	Antibacterial properties, wound healing, and glucose sensing	Upto 75%	Bagyalakshmi & Haritha, 2017
Quantum Dots	1-10	Fluorescent imaging, glucose sensing	Not available (N/A)	NA
Carbon-based (e.g., graphene)	1-100	Glucose monitoring, drug delivery	Upto 80%	Shao et al., 2019
Ceramics (e.g., silica)	5-200	Drug delivery and imaging applications	Upto 70%	Angel Rose Rajan et al., 2019
Zinc-based	5-50	Potential role in insulin signaling and glucose regulation	Upto 90%	Malaikozhundan et al., 2020
Iron-based	5-100	Iron oxide nanoparticles: Drug delivery and imaging	Upto 80%	Ali et al., 2020
Other Metabolic	Varies	Nanoparticles with specific metabolic functions and effects	NA	NA

Lipid-based nanocarriers, including liposomes and lipid nanoparticles, have garnered attention as multifunctional drug delivery platforms promising for treating Diabetes. Lipid-based carriers possess numerous advantages, such as biocompatibility, controlled drug release, and enhanced drug stability (Khosa et al., 2018). Encapsulating L-arginine within lipids, nanocarriers protect against enzymatic degradation and enable precise targeting of particular tissues or organs, such as the pancreas and vasculature (Huang et al., 2016). Table 1.2 summarizes the different approaches to delivering L-arginine in the human body.

There is a substantial body of evidence from both preclinical and clinical studies that strongly support the effectiveness of lipid nanocarriers in facilitating the delivery of L-arginine. The findings of a research study involving diabetic rats demonstrated that utilizing L-arginine-loaded lipid nanoparticles improved insulin secretion and glucose homeostasis more than free L-arginine administration (Kamoun et al., 2021). The utilization of lipid nanocarriers resulted in the facilitation of a sustained release mechanism for L-arginine, thereby extending its presence in the bloodstream and amplifying its

therapeutic efficacy. Lipid nanocarriers refer to nanoscale particles that consist of lipids, which are molecules exhibiting amphiphilic properties characterized by the presence of both hydrophobic and hydrophilic areas. The nanocarriers are created in several configurations, including liposomes, solid lipid nanoparticles (SLNs), nanostructured lipid carriers (NLCs), and lipid-drug conjugates.

Table 1.2: *L-arginine drug delivery approaches to treat Diabetes.*

Delivery System	Description	Advantages	References
Polymeric Nanoparticles	Composed of biocompatible and biodegradable polymers. Can protect L-arginine and facilitate its controlled release.	Prolongs circulation time. Enables specific delivery to target tissues via surface modification.	Sur et al., 2019
Microparticles	L-arginine-loaded microparticles range from micrometers to hundreds of micrometers.	Sustained and controlled release. Flexibility in administration routes.	Agüero et al., 2017
Prodrug Conjugation	Conjugates L-arginine with specific moieties forming prodrugs.	Enhances stability and solubility. Provides sustained release.	Li et al., 2020
Nanogels	Three-dimensional cross-linked networks of polymers. Encapsulates L-arginine and protects it from degradation.	High stability. Tunable platform for controlled release.	Suhail et al., 2019
Nano complexes	Complexes L-arginine with biocompatible polymers or surfactants.	Protects L-arginine from degradation. Facilitates delivery to target sites.	Narmani et al., 2019
Oral Delivery Systems	Includes enteric-coated formulations to protect L-arginine from stomach acidity.	Improves L-arginine's bioavailability. Facilitates release in the intestines for effective absorption.	Ma & Williams, 2017
Lipid Nanoparticles	Composed of lipids and encapsulated L-arginine. Offer improved drug stability and controlled release.	Enhanced drug penetration and cellular uptake. Facilitates targeted delivery to specific tissues.	Mohammadi-Samani & Ghasemiyeh, 2018
Nanocarriers	Utilizes various nanocarriers, such as liposomes, dendrimers, and solid lipid nanoparticles.	Enhanced drug stability and solubility. Controlled and sustained drug release.	Mura, 2020

The lipid nanocarriers possess remarkable adaptability, allowing the encapsulation of diverse drug molecules, including hydrophobic and hydrophilic medicines. This attribute enables the achievement of effective drug delivery.

1.5.1 Enhanced Solubility and Stability

A significant obstacle encountered in medication delivery is the inadequate water solubility shown by several therapeutic medicines. Lipid nanocarriers can entrap hydrophobic pharmaceutical compounds inside their lipid bilayer or core, substantially augmenting their solubility in the circulatory system (Tran et al., 2014). The enhanced solubility results in an augmented medication bioavailability, facilitating a greater proportion of the provided dosage to reach the intended location (Chenthamara et al., 2019). Furthermore, lipid nanocarriers serve as protective barriers, effectively shielding medicines from enzymatic breakdown, extending their stability and therapeutic efficacy.

1.5.2 Focused Drug Administration

One notable benefit of lipid nanocarriers is their capacity to selectively target certain tissues or cells. The use of ligands, antibodies, or peptides to modify the surface of nanocarriers facilitates the active targeting of these carriers to locations that exhibit certain receptors or indicators (Zhang et al., 2012). As a result, the medicine is administered in a targeted manner, minimizing the occurrence of unintended consequences and optimizing its therapeutic effectiveness. According to Farkhani et al., (2014), lipid nanocarriers have significant potential in the field of personalized medicine due to their ability to enhance therapeutic efficacy and reduce the occurrence of adverse events.

1.5.3 Preservation from Degradation

Lipid nanocarriers provide a safeguarding milieu for enclosed pharmaceutical agents, effectively safeguarding them from enzymatic degradation and other potentially detrimental elements inside the biological system (Mura, 2020). Implementing this safeguard guarantees to preserve the drug's stability and efficacy throughout its journey until it reaches its intended destination. Consequently, lipid nanocarriers facilitate sustained and regulated drug release, resulting in extended therapeutic outcomes and decreased frequency of administration.

The use of lipid nanocarriers has introduced novel opportunities for the administration of drugs, hence presenting noteworthy ramifications for both the

pharmaceutical sector and the provision of patient care. The potential of nanotechnology to improve medication solubility, stability, and targeted administration presents a significant opportunity for the therapeutic management of many ailments, such as cancer, infectious illnesses, and inflammatory disorders (Chenthamara et al., 2019). Furthermore, the adaptability of lipid nanocarriers enables the customization of medication formulations, enhancing the efficacy of therapeutic interventions for particular patients. Despite these encouraging benefits, obstacles still need to be addressed, such as large-scale manufacturing, obtaining regulatory permission, and conducting comprehensive long-term safety evaluations (Milewska et al., 2021). Additional research and development endeavors are needed to effectively tackle these concerns and fully use lipid nanocarriers' capabilities in the medication delivery field.

1.5.4 Findings on Lipid Nanocarriers in Diabetic Therapy

The use of lipid nanocarriers in diabetic therapy has been investigated in research, revealing its potential to transform the treatment of Diabetes significantly. For example, Böttger et al. (2020) investigated insulin administration by lipid nanocarriers that are selectively targeted to the liver. The study's findings exhibited enhanced regulation of blood sugar levels in mice with Diabetes, emphasizing the prospective use of lipid nanocarriers to precisely administer insulin to vital organs implicated in maintaining glucose balance (Böttger et al., 2020). A separate inquiry was conducted to examine the administration of the anti-diabetic medication gliclazide to the pancreas using lipid nanocarriers (Kesharwani et al., 2018). The study's results demonstrated a decrease in insulin resistance, suggesting that lipid nanocarriers may be viable for delivering tailored treatments to the pancreas to manage Diabetes. Several nanocarriers, such as lipid-based and polymeric-based insulin nanomedicines, have been created to deliver insulin orally. The nanomedicines demonstrated enhanced oral absorption and elevated bioavailability of insulin, resulting in efficient regulation of blood sugar levels *in vivo* models (Kesharwani et al., 2018).

The administration of orally delivered solid lipid nanoparticles (SLN) encapsulating insulin to diabetic rats resulted in a notable and sustained hypoglycemic

impact for 24 hours (Fonte et al., 2011). Patel et al. (2021) posit that using solid lipid nanoparticles (SLNs) may facilitate the oral absorption of insulin, presenting a viable and patient-centric alternative to traditional modes of insulin administration. The investigation of the combination of Methocel with solid lipid nanoparticles (SLNs) to create Methocel-lipid hybrid nanocarriers (MLNs) was undertaken by Boushra et al. (2016) as a means to improve the efficiency of insulin encapsulation (EE%). The research presented encouraging findings, as using MLNs resulted in a significant enhancement in insulin EE% while maintaining the properties of SLNs. It suggests that MLNs can serve as effective nanocarriers for the oral administration of peptides in treating Diabetes (Boushra et al., 2016). The increasing worldwide prevalence of Diabetes has also prompted exploration into the use of lipid nanocarriers to transform diabetic treatment by facilitating the oral administration of insulin and GLP-1 RA (Glucagon-like peptide-1 receptor agonists) (Poudwal et al., 2021). It has the potential for streamlined treatment protocols and enhanced patient compliance.

1.5.5 Critical Evaluation of Safety and Efficacy of Lipid Nanocarriers

As discussed, using lipid-based nanocarriers for oral medication delivery has significant potential in diabetes therapy. Nevertheless, several physicochemical barriers that are encountered throughout the gastrointestinal system provide noteworthy obstacles that must be overcome to achieve effective medication delivery.

1.5.5.1 Addressing Physicochemical Challenges

Lipid-based nanocarriers encounter challenges, including exposure to stomach acidic content, the presence of an intestinal mucus layer, and susceptibility to enzymatic degradation (Milewska et al., 2021). These factors affect the stability of drugs and impede their efficient delivery. However, it is possible to transform these constraints into favorable circumstances using a logical and systematic approach to developing nanocarriers. Various strategies, such as using mucoadhesive agents or pH-responsive coatings, have shown the potential to augment the release and penetration of medications through the mucus layer (Osman et al., 2022). Consequently, these approaches can enhance the bioavailability of loaded pharmaceuticals.

1.5.5.2 The Promising Application of Lipid Nanocarriers in the Treatment of Diabetes

Extensive investigation into lipid-based nanocarriers has yielded notable progress, ultimately resulting in the creation of Doxil®, which stands as the pioneering nanocarrier to get approval from the Food and Drug Administration (FDA) (De et al., 2022). This achievement has enabled further exploration in cancer research and peptide delivery. Although the clinical trials assessing the use of lipid nanocarriers in diabetes treatment are incomplete, promising outcomes have been shown in animal research (Costa et al., 2021). The findings of this research indicate that lipid nanocarriers have the potential to serve as a secure and efficient method for medication delivery in the context of diabetes therapy.

1.5.5.3 The Benefits of Lipid Components

The remarkable characteristics of lipid constituents in nanocarriers, including their exceptional adaptability, biocompatibility, and little toxicity, have greatly contributed to their widespread use and promising prospects in drug delivery systems (Mishra et al., 2018). Lipids can effectively encapsulate medications with hydrophobic and hydrophilic properties, making them a highly adaptable medium for drug delivery. This characteristic enables lipids to accommodate the wide-ranging therapeutic requirements of treating Diabetes.

1.5.5.4 Safety Considerations

Despite the encouraging preclinical findings, the issue of safety remains a significant consideration in the use of lipid nanocarriers for the delivery of drugs in diabetic patients (Ungaro et al., 2012). Examining lipid nanocarriers' long-term effects in human beings, namely their potential for accumulation in the body and immunogenicity, necessitates meticulous assessment in clinical studies. Furthermore, it is important to conduct comprehensive investigations into the possible interactions between lipid nanocarriers and other drugs or underlying health issues to guarantee the safety of patients.

1.5.5.5 Translating to Clinical Applications

It is essential to conduct meticulous and tightly regulated clinical trials. These studies should aim to assess the effectiveness and safety of lipid nanocarriers in various

groups of patients with Diabetes. In addition, it is necessary to conduct extended surveillance and subsequent investigations to evaluate any possible negative consequences and guarantee the comprehensive safety characteristics of treatments using lipid nanocarriers, as noted by Ettliger et al. (2022).

1.5.5.6 Future Perspectives

The use of lipid nanocarriers in diabetic medication delivery has great promise, as seen by notable progress made in recent years (Fonte et al., 2011; Boushra et al., 2016; Costa et al., 2021). Nevertheless, to fully exploit their advantages, it is essential to do more research to optimize their design, ensure their safety, and understand their mechanism of action. In addition, the investigation of combination medicines and personalized treatment regimens using lipid nanocarriers has the potential to provide better therapeutic results and greater adherence among patients.

1.6 Network Pharmacology in Diabetes Research

In recent years, there have been notable developments in the area of Diabetes research about the comprehension of intricate molecular pathways and signaling networks that contribute to the development and progression of the illness. In our investigation of the possible anti-diabetic properties of *Trigonella foenum-graecum* and its bioactive constituents, alongside an examination of the effectiveness of lipid nanocarrier systems in drug administration, it becomes evident that the treatment of Diabetes necessitates a complete and multidimensional strategy. Network pharmacology is a potent methodology combining systems biology, bioinformatics, and pharmacology to examine the comprehensive connections among medications, targets, and biological processes (Zhang et al., 2016). It enhances our investigation of natural bioactive chemicals and lipid nanocarriers and facilitates the translation of these discoveries into clinically significant and influential treatments for individuals with Diabetes.

1.6.1 The Applications of Network Pharmacology in Diabetes Research

Network pharmacology has emerged as a robust and influential methodology that has garnered significant attention in diabetes research. Integrating molecular, genetic, and

pharmacological data, the systems biology method fully comprehends the complex interplay of medications, genes, and illnesses (Zhang, Sun, et al., 2012). In the domain of Diabetes, network pharmacology has emerged as a valuable tool for identifying prospective therapeutic targets, predicting medication effectiveness, and developing innovative drug combinations (Noor et al., 2022). It has provided researchers with significant insights into the underlying processes of diabetic nephropathy, a very consequential condition associated with Diabetes. For example, novel pharmacological targets have been identified by examining the interplay between genetic elements and processes implicated in this ailment (Li et al., 2014), presenting promising treatment prospects.

Furthermore, the field of network pharmacology has facilitated the discovery and characterization of medication combinations that exhibit synergistic effects, therefore optimizing therapeutic outcomes while limiting the occurrence of adverse reactions (Nogales et al., 2022). Using an integrated method facilitates a full comprehension of the etiology of Diabetes beyond examining individual gene or medication interactions (Zięba et al., 2022). This technique allows for a thorough analysis of the linked network of biological pathways. Through network pharmacology, researchers have the potential to facilitate the advancement of novel and precise therapeutic approaches for the control of Diabetes.

1.6.2 Network Pharmacology Studies in Diabetes Treatment

The use of network pharmacology in the exploration of bioactive compounds and their mechanisms of action for the management of diabetes mellitus (DM) has garnered considerable interest owing to its capacity to account for the multifaceted character of natural products, which include several components and targets, while also minimizing adverse effects. A thorough analysis has been conducted on network pharmacology research for treating diabetes mellitus (DM), specifically targeting type 2 DM (Li et al., 2014). This study offers valuable insights into the many bioactive elements, relevant databases, and their applications in the field of inquiry.

A different research endeavor using network pharmacology-based methodologies to investigate the mechanisms of action of anti-diabetic triterpenoids derived from

Cyclocarya paliurus (Lin et al., 2020). Through active ingredient screening and target prediction methodologies, the investigation effectively discerned the precise constituents of *C. paliurus* that are accountable for its anti-diabetic properties and comprehensively defined their corresponding target proteins. Furthermore, bioinformatics and molecular docking analysis were employed to understand the fundamental processes responsible for the anti-diabetic benefits of triterpenoids (Lin et al., 2020). Likewise, a summary of relevant studies conducted in the last two years is provided in Table 1.3.

Table 1.3: Network pharmacology studies in natural products for diabetes mellitus treatment: mechanisms, targets, and active compounds.

Sr. No.	Study Title	Summary	Approach Used	Target	Cited Work
1	Network Pharmacology Study to Reveal the Potentiality of a Methanol Extract of <i>Caesalpinia sappan</i> L. Wood against Type-2 Diabetes Mellitus	Exploring the interrelationship of 33 bioactive compounds from CS wood with T2DM-associated signaling pathways and target receptors using network pharmacology, with fisetin tetramethyl ether identified as a potential drug for T2DM management.	Network Pharmacology, Compound Identification, Protein-Protein Interactions, Pathway Analysis, Molecular Docking	Peroxisome proliferator-activated receptor gamma (PPARG)	Adnan et al., 2022
2	Network Pharmacology and Bioinformatics Approach Reveals the Multi-Target Pharmacological Mechanism of <i>Fumaria indica</i> in the Treatment of Liver Cancer	Characterizing <i>Fumaria indica</i> 's mechanism in treating liver cancer using network pharmacology, identifying active ingredients, targets, and pathways, and validating active ingredients' binding efficacy on target genes.	Network Pharmacology, Molecular Docking	MTOR, MAPK3, PIK3R1, EGFR	Batool et al., 2022
3	Network pharmacology, molecular docking, and molecular dynamics simulation to elucidate the mechanism of anti-aging action of <i>Tinospora cordifolia</i>	Investigating anti-aging mechanisms of <i>Tinospora cordifolia</i> using network pharmacology, molecular docking, and molecular dynamics simulation, identifying key compounds, targets, and AKT1 binding affinity, highlighting potential	Network Pharmacology, Molecular Docking, Molecular Dynamics Simulation	AKT1, GAPDH, TP53	Bisht et al., 2023

		phytochemicals for future age-related disease prevention.			
4	Integrating network pharmacology and non-targeted metabolomics to explore the common mechanism of Coptis Categorized Formula improving T2DM zebrafish	Exploring Coptis Categorized Formula's mechanism in treating T2DM using network pharmacology and non-targeted metabolomics in zebrafish models, highlighting its role in regulating glycolipid metabolism and insulin resistance.	Network Pharmacology, Non-Targeted Metabolomics, UPLC-QTOF/MS, Gene Ontology, KEGG Pathway Enrichment, Molecular Docking	DPP-4, CASP3, NOS2, NOS3, AGE-RAGE Signaling, MAPK Signaling, HIF-1 Signaling, Glycolipid Metabolism, Insulin Resistance, Cell Apoptosis, Anti-Oxidation	He et al., 2022
5	Effect of metformin on nonalcoholic fatty liver based on meta-analysis and network pharmacology	Meta-analysis and network pharmacology study linking metformin to NAFLD, revealing decreased ALT, AST, TG, TC, and IR levels, and suggesting HIF1A, NFE2L2, NOS3, NR3C1, PIK3CA, and SIRT1 as core targets.	Meta-Analysis, Network Pharmacology, Cytoscape, R Software	HIF1A, NFE2L2, NOS3, NR3C1, PIK3CA, SIRT1	Huang et al., 2022
6	Hepatoprotective mechanism of Silybum marianum on nonalcoholic fatty liver disease based on network pharmacology and experimental verification	Revealing Silybum marianum's hepatoprotective mechanism on NAFLD through network pharmacology, experimental verification, and pathway analysis, demonstrating silymarin's effectiveness on NAFLD and key signaling pathways.	Network Pharmacology, Experimental Verification, KEGG, GO Enrichment, Western Blot Experiments, H&E Pathological Analysis	AKT1, IL-6, MAPK1, Caspase 3, p53, VEGFA	Jiang et al., 2022
7	A network pharmacology-based strategy to explore the pharmacological mechanisms of Antrodia camphorata and antcin K for treating type II diabetes mellitus	Investigating A. camphorata and antcin K's anti-diabetic activities using network pharmacology, identifying core targets and enriched pathways, and suggesting potential mechanisms for	Network Pharmacology, Protein-Protein Interactions, KEGG Pathway Enrichment, <i>In vivo</i> Experiments, qPCR	Insulin Resistance-related targets, Key Compound: Antcin K	Kuang et al., 2022

		Diabetes mellitus-linked Alzheimer's treatment.			
8	Network pharmacology prediction and molecular docking-based strategy to explore the potential mechanism of Huanglian Jiedu Decoction against sepsis	Exploring HLJDD's mechanism in treating sepsis through network pharmacology and molecular docking, identifying active components, targets, and pathways, with potential for positive regulation of transcription and involvement in PI3K-AKT and MAPK signaling.	Network Pharmacology, Molecular Docking	Sepsis Targets, HLJDD Components	Li et al., 2022
9	Defining the Role of Isoeugenol from <i>Ocimum tenuiflorum</i> against Diabetes Mellitus-Linked Alzheimer's Disease through Network Pharmacology and Computational Methods	Investigating phytochemicals from <i>Ocimum tenuiflorum</i> against diabetes-linked Alzheimer's using network pharmacology and phytoinformatics, identifying key genes and AGE-RAGE pathway, and suggesting isoeugenol as a potential ameliorative agent.	Network Pharmacology, Molecular Docking Simulations, GO Analysis, Molecular Dynamics Simulations, Binding Free Energy Analyses	GAPDH, AKT1	Martiz et al., 2022
10	Network pharmacology: curing causal mechanisms instead of treating symptoms	Discussing limitations of current disease classification and single target treatments for complex diseases, emphasizing the need for network pharmacology and systems medicine to enable precise therapeutic interventions.	Systems and Network Medicine, Network Pharmacology	Multitarget Signaling Modules, Disease Endotypes	Nogales et al., 2021
11	Integrating Network Pharmacology and Molecular Docking Approaches to Decipher the Multi-Target Pharmacological Mechanism of <i>Abrus precatorius</i> L. Acting on Diabetes	Uncovering the potentiality of <i>Abrus precatorius</i> in treating T2DM using network pharmacology and molecular docking, identifying active compounds and core targets, and suggesting its preventive effect on T2DM through diabetes-associated signaling pathways.	Network Pharmacology, Molecular Docking, In Vitro Experiments	AKT1, MAPK3, TNFalpha, MAPK1, Insulin Sensitivity, T2DM	Fatima et al., 2022

12	Network Pharmacology Approach for Medicinal Plants: Review and Assessment	Providing a comprehensive review of network pharmacology in medicinal plants research, discussing active ingredients, techniques, databases, and drug discovery applications for exploring traditional plant-based remedies.	Review of Network Pharmacology in Medicinal Plants Research	Not Applicable	Noor et al., 2022
13	Integrated lipidomics, transcriptomics and network pharmacology analysis to reveal the mechanisms of Danggui Buxue Decoction in the treatment of diabetic nephropathy in type 2 diabetes mellitus	Investigating DBT's therapeutic effects on DN in mice through lipidomics, transcriptomics, and network pharmacology, identifying altered lipid metabolites, pathways, and potential targets, and validating active components' binding with target receptors.	Lipidomics, Transcriptomics, Network Pharmacology, Molecular Docking	Cers, Phosphatidyl ethanolamines, Phosphatidylcholines, Degs2, Acers, Pdk1, Akt	Sun et al., 2022
14	The mechanism of action of the combination of Astragalus membranaceus and Ligusticum chuanxiong in the treatment of ischemic stroke based on network pharmacology and molecular docking	Investigating Astragalus membranaceus and Ligusticum chuanxiong's mechanism in treating IS through network pharmacology and molecular docking, identifying active ingredients, targets, and inflammatory response control in IS.	Network Pharmacology, Molecular Docking, Gene Ontology, KEGG, Molecular Docking	IL-17 Signaling, MAPK Signaling, PI3K-AKT Signaling, TNF Signaling, Toll-like Receptor Signaling, EGFR	Wang et al., 2022
15	Progress and Prospects of Research Ideas and Methods in the Network Pharmacology of Traditional Chinese Medicine	Reviewing the progress and prospects of network pharmacology in traditional Chinese medicine research, emphasizing the need for precise therapeutic interventions based on multi-target signaling modules.	Review of Network Pharmacology Research Ideas and Methods in Traditional Chinese Medicine (TCM)	Not Applicable	Yuan et al., 2022
16	Exploring the synergistic and complementary effects of berberine and paeoniflorin in the treatment of type 2 diabetes mellitus by network pharmacology	Exploring the synergistic and complementary effects of BBR and PF in treating T2DM using network pharmacology and molecular docking, identifying core targets,	Network Pharmacology, Molecular Docking, <i>In vivo</i> Experiments	JAK2, ESRI, IFG1R, STAT3, EGFR, MAPK1, AKT1, AGE-	Zhang et al., 2022

		and validating the therapeutic effect in a diabetic model.		RAGE, FOXO, AMPK, VEGF	
17	Screening and identification of a novel antidiabetic peptide from collagen hydrolysates of Chinese giant salamander skin: network pharmacology, inhibition kinetics and protection of IR-HepG2 cells	Identifying a novel peptide GPPGPA from Chinese giant salamander skin using network pharmacology and its potential in ameliorating T2DM-linked Alzheimer's through in vitro experiments.	Network Pharmacology, Inhibition Kinetics, Molecular Docking, In Vitro Experiments	AKT1, MAPK8, MAPK10, JUN, PI3K-Akt, AGE-RAGE, TNF, Insulin Resistance	Zhou et al., 2022
18	Potential Molecular Mechanism of Yishen Capsule in the Treatment of Diabetic Nephropathy Based on Network Pharmacology and Molecular Docking	Revealing the mechanism of Yishen Capsule in treating DN using network pharmacology and molecular docking, identifying active components, targets, and pathways, with experimental verification confirming its effect on diabetic kidney tissue.	Network Pharmacology, Molecular Docking, In Vitro and <i>In vivo</i> Experiments	AR, AKT1, TP53, ESR1, JUN, AGE-RAGE, PI3K/Akt, MAPK, NF- κ B	Hu et al., 2022

These studies showcase the considerable potential of network pharmacology in enhancing our comprehension of the intricate interplay between bioactive molecules and their targets. This approach proves to be invaluable in the identification of innovative therapeutic agents for the management of diabetes mellitus. The amalgamation of network pharmacology with bioinformatics and molecular docking methodologies offers a comprehensive and systematic framework for investigating the processes that underlie the anti-diabetic properties of natural compounds. These methodologies exhibit potential in identifying novel therapeutic targets and their contribution toward advancing more efficient and focused therapies for diabetes mellitus.

1.6.2.1 Potential Drug Targets and Pathways

The network pharmacology research discussed in table 1.2 reveals many pharmacological targets and pathways that have potential implications for treating Diabetes. Numerous investigations have examined the underlying processes by which diverse natural products and traditional medicines have therapeutic effects on diabetes

mellitus (DM), focusing on type 2 diabetes (T2DM). The inherent characteristics of these natural compounds, consisting of many components and targeting multiple sites, render them viable contenders for developing innovative therapeutic approaches with fewer adverse effects.

Peroxisome proliferator-activated receptor gamma (PPARG) has been identified as a significant therapeutic target in the discussed investigations (Adnan et al., 2022; Zhou et al., 2022). The peroxisome proliferator-activated receptor gamma (PPARG) is crucial in regulating insulin sensitivity and glucose metabolism, making it a significant therapeutic target for treating type 2 diabetes mellitus (T2DM) (Adnan et al., 2022). The compounds derived from *Coptis* Categorized Formula (CCF) have shown interactions with PPARG and other molecular targets implicated in insulin resistance, glycolipid metabolism, and anti-oxidation (He et al., 2022). These findings indicate the potential of CCF as a promising therapeutic approach for treating type 2 diabetes mellitus (T2DM).

Nonalcoholic fatty liver disease (NAFLD) has identified several fundamental targets, including HIF1A, NFE2L2, NOS3, NR3C1, PIK3CA, and SIRT1 (Huang et al., 2022; Jiang et al., 2022). Metformin, a frequently prescribed medication for the treatment of Diabetes, has been seen to regulate these specific targets and enhance hepatic function in individuals diagnosed with non-alcoholic fatty liver disease (Huang et al., 2022). In a similar vein, previous studies have shown that *Silybum marianum*, together with its active constituent silymarin, selectively modulates the activity of AKT1, IL-6, MAPK1, Caspase 3, p53, and VEGFA, hence exhibiting hepatoprotective properties in cases of NAFLD (Jiang et al., 2022).

Identifying crucial targets, including GAPDH and AKT1 and the AGE-RAGE signaling pathway, has been significant in the therapeutic approach to Alzheimer's disease associated with Diabetes (Kuang et al., 2022; Martiz et al., 2022; Zhou et al., 2022). Isoeugenol, a chemical constituent derived from the plant *Ocimum tenuiflorum*, has shown notable affinity for binding to glyceraldehyde-3-phosphate dehydrogenase (GAPDH), hence indicating its potential therapeutic use in mitigating the onset of Alzheimer's disease associated with diabetes mellitus (Martiz et al., 2022). Moreover, the investigations on the mechanisms of *Tinospora cordifolia* in combating aging (Bisht et al., 2023) and the

preventive properties of *Abrus precatorius* against Type 2 Diabetes Mellitus (Fatima et al., 2022) have underscored the significance of AKT1 as a pivotal focal point.

The AKT1 protein also plays a significant role in several physiological processes, such as insulin signaling, glucose absorption, and cell survival. Consequently, it is considered a pivotal target for controlling Diabetes (Hu et al., 2022; Zhang et al., 2022). These network pharmacology studies emphasize the significance of incorporating multi-target signaling modules into creating precise and successful pharmacological approaches for managing Diabetes. These studies provide significant insights into the possible processes by which natural products and conventional pharmaceuticals may effectively treat Diabetes. Moreover, they lay the foundation for future investigations and the creation of innovative therapeutic agents to manage Diabetes.

1.7 Purpose of the Thesis Research: Integration of L-Arginine and Lipid Nanocarriers

Diabetes mellitus is a multifaceted metabolic condition characterized by compromised insulin production or function, resulting in elevated blood glucose levels and related consequences. Given the increasing incidence of Diabetes and its consequential implications for public health, there is an urgent need to develop novel and efficacious treatment modalities. L-arginine, an amino acid, has shown promise in enhancing glucose metabolism and insulin sensitivity, making it a possible contender for the control of Diabetes.

The primary objective of this thesis study is to investigate the incorporation of L-arginine into lipid nanocarriers synthesized from *Trigonella foenum-graecum* as a potential therapeutic approach for managing Diabetes. Lipid nanocarriers have several benefits, such as heightened medication administration efficacy, increased body absorption, and extended-release kinetics. The use of lipid nanocarriers for encapsulating L-arginine presents a promising approach to improve its stability, boost its bioavailability, and facilitate its targeted distribution to certain tissues or cells pertinent to the pathophysiology of Diabetes.

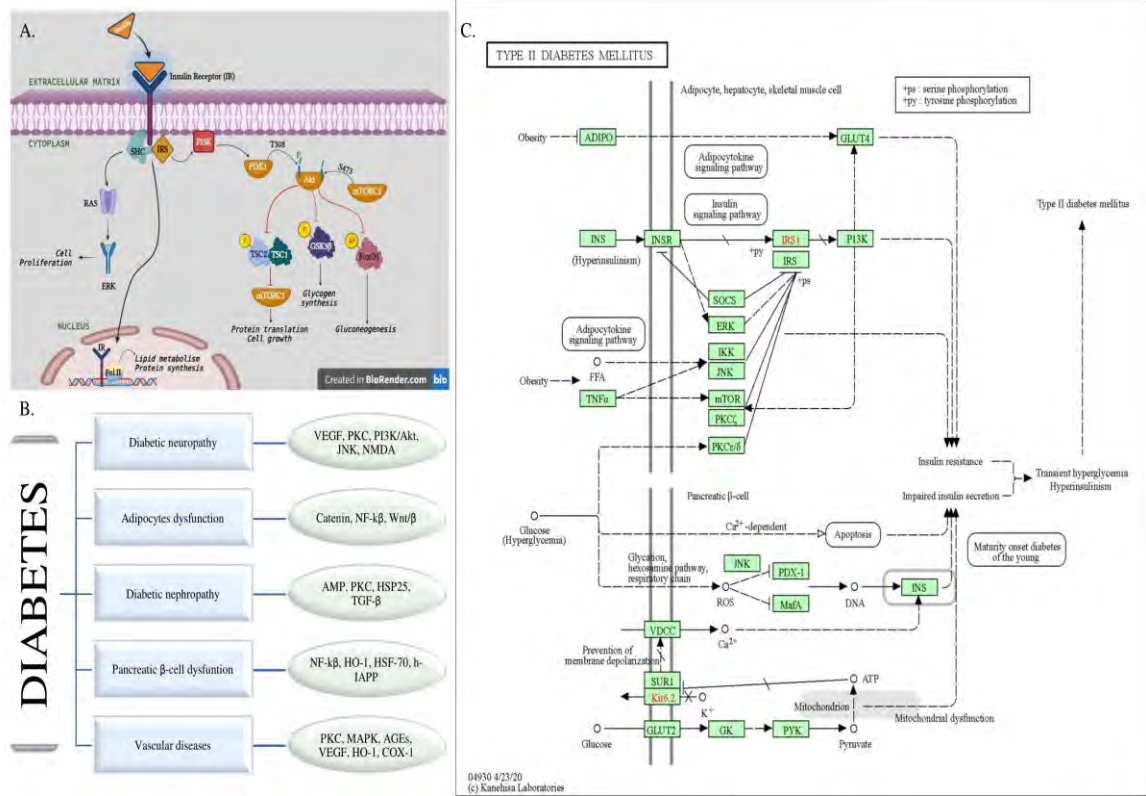


Figure 1.4: Potential therapeutic pathway targets in anti-diabetic research; A. The insulin signaling pathway; B. Protein targets of diabetes and its comorbidities; C. Diabetes pathway and therapeutic targets adapted from the work of Kanehisa Laboratories (2023).

The potential for boosting diabetes treatment results is great via the combination of L-arginine and lipid nanocarriers. The convergence of these two entities has the potential to enhance glycemic control, mitigate complications, and facilitate comprehensive diabetes treatment. Previous studies have used network pharmacology methodologies and molecular docking analyses to understand better the essential targets and signaling pathways implicated in treating Diabetes. These findings have subsequently informed the rational development and composition of lipid nanocarriers loaded with L-arginine.

1.8 Research Rationale

The rationale for using lipid nanocarriers to encapsulate L-arginine is rooted in the advantageous outcomes that may be achieved by integrating these two methodologies in the context of diabetes therapy. L-arginine has been found to be a significant

pharmaceutical agent for treating Diabetes via network pharmacology investigations. This compound exhibits its effectiveness by participating in several pathways that are closely linked to the management of Diabetes, such as the insulin signaling route, PI3K-AKT pathway, and MAPK signaling pathway (Chen et al., 2020). Moreover, it has been shown that L-arginine has antioxidant and anti-inflammatory characteristics, which play a crucial role in alleviating oxidative stress and inflammation often seen with the advancement of Diabetes (Cho et al., 2020). The use of lipid nanocarriers to encapsulate L-arginine has the potential to augment its stability and boost its bioavailability. It, in turn, facilitates prolonged and regulated release at the intended location, promoting therapeutic interventions' efficacy and specificity.

The selection of *Trigonella foenum-graecum* as the focal plant for this research was based on its examination using network pharmacology. The investigation findings indicate that Fenugreek has noteworthy quantities of L-arginine and daidzein, which have been recognized as crucial bioactive constituents with anti-diabetic properties. The selection of L-arginine for the study was based on its greater accessibility and advantageous ADMET (Absorption, Distribution, Metabolism, Excretion, and Toxicity) characteristics. These characteristics render L-arginine a more viable contender for incorporation inside lipid nanocarriers since it can potentially provide amplified therapeutic benefits in the context of diabetes management.

There is a wide array of therapies for controlling Diabetes; nonetheless, the advancement of nanocarrier medication delivery bears considerable importance. Nanocarriers have several benefits compared to traditional drug delivery methods, making them a compelling strategy for treating Diabetes (Fonte et al., 2011; Costa et al., 2021).

- Using lipid nanocarriers to encapsulate L-arginine can effectively safeguard the medication from degradation and enzymatic inactivation. Consequently, this approach enhances the stability of the drug during storage and transportation.
- Nanocarriers can augment the solubility and permeability of L-arginine, resulting in increased bioavailability and enhanced absorption within the physiological system.

- Controlled and sustained release of L-arginine can be achieved by the use of nanocarriers. This approach can maintain a consistent and longer therapeutic impact, minimize the need for frequent dosage, and promote improved patient compliance.
- Targeted drug delivery involves integrating targeting ligands onto the surface of nanocarriers, enabling their precise localization to certain tissues or cells pertinent to the pathogenesis of Diabetes. This strategy enhances drug accumulation at the intended location while simultaneously reducing the occurrence of off-target effects.
- Nanocarrier medication delivery can minimize systemic adverse effects by reducing drug exposure to non-target tissues.
- Combination therapy with nanocarriers presents a promising avenue for integrating various medications or therapeutic agents into a singular formulation, facilitating a synergistic approach to treating Diabetes.

The combination of L-arginine and lipid nanocarriers derived from *Trigonella foenum-graecum* has great potential in diabetes treatment. This technique offers a more efficient and focused therapeutic strategy characterized by better drug stability, improved bioavailability, and regulated release of the medication. This research aims to use these two entities' combined advantages to contribute to developing new and effective therapies for Diabetes.

1.9 Scope and Limitations of the Study

The scope of this study lies in exploring the potential of L-arginine encapsulated in lipid nanocarriers from *Trigonella foenum-graecum* for diabetes treatment. The combination of network pharmacology research and phyto informatics has yielded significant findings on the principal anti-diabetic chemicals found in fenugreeks. Among these molecules, L-arginine has emerged as a particularly promising candidate. This work aims to increase L-arginine's stability, bioavailability, and targeted distribution by encapsulating it in lipid nanocarriers. This improvement in L-arginine's properties is expected to boost its therapeutic effectiveness for the control of Diabetes.

The study's comprehensive methodology, which integrates network pharmacology, phyto informatics, and *in vitro* comparative trials with metformin, significantly advances diabetes research. The investigation of the combined advantages of L-arginine and lipid nanocarriers emphasizes the possibility of creating novel and effective treatments for Diabetes. The results of this study provide a foundation for future *in vivo* investigations aimed at confirming the therapeutic efficacy of L-arginine when encapsulated in lipid nanocarriers, both in preclinical and clinical contexts.

Even with the promising potential of our investigation, it is imperative to realize several constraints. The main constraint is the need for *in vivo* investigations. Due to limited resources and time, the research could not continue with animal tests to assess the therapeutic benefits of L-arginine encapsulated in lipid nanocarriers *in vivo*. Using *in vivo* investigations is essential to effectively translate the identified potential advantages from *in vitro* experiments into a more realistic physiological environment. Additionally, these studies provide valuable insights into the safety and effectiveness of drugs inside live creatures.

Another constraint is the need for comprehensive *in vitro* investigations. While some comparable *in vitro* experiments have been undertaken with metformin, a more extensive examination, including diverse cell lines and varying doses of encapsulated L-arginine, would have yielded a more thorough knowledge of its cellular impacts. Furthermore, further mechanistic investigations to elucidate the signaling pathways affected by the nanocarriers and L-arginine might have yielded a more comprehensive understanding of the fundamental processes at play.

In addition, it is worth noting that the research did not include direct comparative trials, including established medications. Such trials would have provided more insights into the possible benefits and drawbacks of utilizing lipid nanocarriers to encapsulate L-arginine compared to current treatment methods. The inclusion of comparison trials with anti-diabetic medicines other than metformin would have for a more thorough evaluation of the therapeutic potential of the innovative method.

1.10 Research Objectives

This study aims:

- To computationally investigate the effects of L-arginine from *Trigonella foenum-graecum* on key targets and pathways implicated in diabetes management.
- To greenly synthesize lipid nanocarriers from *Trigonella foenum-graecum* seed oil extract.
- To encapsulate L-arginine in lipid nanocarriers and characterize the physicochemical properties of the formulation.
- To assess the *in vitro* safety and biocompatibility potential of L-arginine-conjugated lipid nanocarriers and evaluate their stability.

CHAPTER TWO

MATERIAL & METHODS

MATERIAL AND METHODS

2.1 Plant Selection

A comprehensive review informed the plant selection process for this study of relevant literature. Notably, the research conducted by Tariq et al. (2020) concerning the utilization of herbal medicines for diabetes treatment in the Southern regions of Pakistan, along with its associated pharmacological evidence, served as a pivotal reference. This literature review facilitated the identification of a suitable plant candidate.

2.1.1 *Rationale for *Trigonella foenum-graecum* Selection*

From the pool of identified plants, *Trigonella foenum-graecum*, commonly known as fenugreek, emerged as the primary focus of this study. The rationale behind this selection was multi-faceted. Firstly, fenugreek had received comparatively limited research attention, rendering it a promising subject for in-depth investigation. Moreover, its local availability near Wazirabad was pivotal in its selection.

2.1.2 *Exploration of Fenugreek's Therapeutic Potential*

A comprehensive exploration of the therapeutic potential associated with fenugreek was undertaken to reinforce its selection for this research endeavor. A thorough review of scholarly sources (Verma et al., 2016; Kiss et al., 2018; Srinivasa & Naidu, 2021) provided substantive evidence suggesting that fenugreek seeds harbor significant therapeutic attributes.

2.2 Seed Collection

The acquisition of research-grade fenugreek seeds was executed to ensure the integrity and reliability of the subsequent investigative phases. Two hundred fifty grams of fenugreek seeds were procured from a reputable local source, namely the Kashmiri Dawa Khana establishment in Wazirabad. The choice of this source was underpinned by its reputation for supplying genuine and unadulterated botanical specimens. The collected seeds were stored in an air tight jar at room temperature.

The imperative for sourcing pure fenugreek seeds arises from the fundamental necessity to maintain the authenticity and consistency of the experimental process. The quality and genetic makeup of seeds profoundly influence the reliability of research outcomes, as any extraneous contaminants or genetic variations could potentially introduce confounding factors.

2.3 Network Pharmacology for Active Compound Identification

A pivotal phase of the research involved employing network pharmacology analysis to identify the target compound within fenugreek that holds the potential for mitigating diabetes. This advanced computational methodology systematically integrates multifaceted interactions between biological entities, elucidating intricate molecular networks through an interplay of computational algorithms and biological databases.

2.3.1 Therapeutic Potential of the Plant

We harnessed the Collective Molecular Activities of Useful Plants (CMAUP) database, accessible at <https://bidd.group/CMAUP/>, to assess fenugreek's therapeutic potential systematically. We elucidated its global distribution, specific disease targets, gene ontology attributes, and target pathways. These findings, obtained from the CMAUP database (Zeng et al., 2019), constituted a foundational framework for identifying a target compound within fenugreek that holds promise for anti-diabetic properties, guiding subsequent phases of this study.

2.3.2 Active Compound Screening

The compound screening was conducted to identify the bioactive chemical constituents of fenugreek. Extracted from the CMAUP database, these compounds formed the foundational basis for exploring potential anti-diabetic attributes. Concurrently, identifying biological targets associated with these active compounds was also achieved through data from the CMAUP database. We utilized the UniProt database to ensure data standardization and coherence (Bateman et al., 2022; accessible at <https://www.uniprot.org/>) to convert target protein names into standardized target gene

names. This integration of resources not only streamlined our research process but enhanced precision and consistency, priming us for subsequent phases dedicated to solving the intricate mechanisms underpinning fenugreek's potential therapeutic efficacy against diabetes.

2.3.3 Identification of T2DM Gene Targets & Collective Targets

T2DM-associated targets were systematically searched within the GeneCards platform (Stelzer et al., 2016; accessible at <https://www.genecards.org/>), employing "type 2 diabetes mellitus" and "T2DM" as primary keywords, with a focus on the Homo sapiens species. Subsequently, these curated targets, originating from the identified fenugreek compounds and those linked to type 2 diabetes mellitus, were merged using Microsoft Excel. This step also encompassed the removal of duplicate entries. The pinpointing of shared targets among the fenugreek compounds and T2DM targets was achieved through a comparative analysis aided by VENNY 2.1 (Oliveros, 2015; accessible at <https://bioinfogp.cnb.csic.es/tools/venny/>), which enabled the visual representation of overlapping elements for enhanced comprehension and interpretation.

2.3.4 Network Visualization of Target Genes and Active Compounds

In line with the preceding analyses, Cytoscape 3.9.1 (accessible at <http://www.cytoscape.org/>) was crucial in constructing a comprehensive network diagram. This diagram served as a dynamic visual representation, elucidating the interplay between the bioactive compounds present in Fenugreek and the T2DM-associated targets.

The common T2DM-related and active compound target genes were systematically arranged in Excel sheets. The common genes were typed individually for each entry. Subsequently, the data was imported into Cytoscape, with the circular network layout being chosen. Multi-colored cells displayed the common targets between fenugreek compounds and T2DM. Leveraging Cytoscape's established proficiency in network analysis and visualization (Shannon, 2003), this approach depicted intricate molecular interactions.

2.3.5 Protein-Protein Network Analysis

The overlapping targets, resulting from the earlier analysis, were subjected to interaction assessment using STRING 11.0 (Search Tool for the Retrieval of Interacting Genes/Proteins), accessible at <https://string-db.org/>. We utilized the "multiple protein" module within STRING to ensure a focused examination of the protein-protein associations. In this process, we input the compiled list of shared targets between the active compounds of fenugreek and T2DM, ensuring a systematic consideration of each common category. For instance, interactions involving compound 1 and T2DM-associated targets and those of compound 2 and T2DM-associated targets were independently extracted and visualized. The gene type was specified as *Homo sapiens* to ensure a relevant context. The generated network visualization distinguished nodes by color and content to convey critical information (Szklarczyk et al., 2022). Colored nodes encompassed both the query proteins and the initial shell of interacting proteins, while white nodes represented the secondary shell of interactors. The status of nodes was characterized by content, where empty nodes denoted proteins with an unknown 3D structure. In contrast, filled nodes indicated instances where some level of 3D structure was either known or predicted.

2.3.5.1 The Analysis of Edges in the STRING Network

The edges within the network held distinct significance, reflecting diverse aspects of protein-protein associations. These associations were purposeful and contextually meaningful, indicating shared contributions to specific functions. Importantly, an edge did not necessarily signify a physical binding between proteins. The network nodes encapsulated proteins, accounting for splice isoforms or post-translational modifications. Nodes collectively represented all proteins produced by a single, protein-coding gene locus.

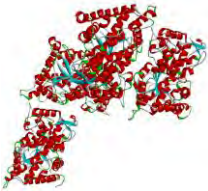


In interpreting the interactions, distinct edge colors conveyed their nature and origin. Blue edges denoted known interactions sourced from curated databases, while pink edges represented interactions that had been experimentally determined. Green edges indicated predicted interactions derived from gene neighborhood analysis, while orange edges signified predicted interactions originating from gene fusions. Additionally, purple

edges denoted predicted interactions based on gene co-occurrence analysis. Light-green edges represented text-mining-derived interactions, while black edges indicated co-expression-based interactions. Violet edges highlighted interactions grounded in protein homology.

2.4 Molecular Docking of Target Proteins and Active Compounds

We explored molecular interactions between the core gene targets and Fenugreek's active compounds using the sophisticated Molecular Operating Environment (MOE) software (Vilar et al., 2008). Central to this analysis was procuring critical protein structures, a foundational step accomplished by retrieving common proteins shared by active fenugreek compounds and the designated T2DM targets. These protein structures, acquired from the Protein Data Bank (PDB), accessible at: <https://www.rcsb.org/>, comprised the three-dimensional (3D) structures essential for the docking study (Berman, 2000). The specifics of these target proteins are detailed in Table 2.1.

Table 2.1: Core protein targets selected for molecular docking.

Target Protein	PDB ID	Length	Molecular Weight	3D Structure
CYP2C19	4GQS	477 amino acids	222.19 kDa	
CYP1A2	2HI4	495 amino acids	57.18 kDa	
NFKB-1	1NFK	325 amino acids	79.89 kDa	

Before the docking analysis, a rigorous protein preparation phase was undertaken. Using the Discovery Studio software 2021 client (downloaded from

<https://discover.3ds.com/discovery-studio-visualizer-download>), we purified the protein structures of extraneous elements, notably water molecules, and ligands. This purification process was quintessential in ensuring a pristine environment for subsequent docking investigations, eliminating any potential sources of interference.

The induced fit model was chosen for the docking refinement within the Molecular Operating Environment (MOE). The initial scoring method was chosen as London dG, whereas the final scoring function was chosen as GBVI/WSA dG with 5 docking poses.

This docking strategy allowed us to explore the inherent flexibility of ligands and proteins, providing a more comprehensive assessment of potential binding interactions. For each of the bioactive compounds, a total of ten docking poses were generated. Considering the dynamic nature of molecular interactions, this strategic approach offered a thorough exploration of binding orientations.

To explore the molecular intricacies underlying the docking poses, we embarked on detailed 2D visualizations. Identifying the most promising docking pose and compound was grounded in two pivotal criteria: evaluating minimum free energy and quantifying hydrogen bonds formed within the intricate complex. These guiding parameters collectively directed us toward the compounds exhibiting the most favorable binding interactions, illuminating their potential therapeutic efficacy.

To ascertain the relative docking energies and benchmark our findings, we extended our analysis to encompass metformin, a well-established antidiabetic agent. By including metformin (accessed at: <https://pubchem.ncbi.nlm.nih.gov/compound/Metformin>, PubChem ID: 4091) in our docking exploration, we gained a valuable reference point for comparing the relative binding affinities of the identified fenugreek compounds.

2.5 Absorption, Distribution, Metabolism, Excretion, and Toxicity (ADMET) Analysis

ADMET analysis was performed to evaluate our target compounds' pharmacokinetic properties comprehensively. Drawing upon established literature reports

and pharmacokinetic parameters outlined by Xu et al. (2012), we navigated the intricate landscape of compound characteristics to discern their suitability for potential drug development.

2.5.1 Oral Bioavailability and Drug-Likeness Criteria

Leveraging insights from the literature, we introduced two pivotal criteria: compounds with oral bioavailability (OB) greater than or equal to 30% were considered to possess favorable absorption and metabolism characteristics following oral administration. Compounds with a drug-likeness (DL) score equal to or exceeding 0.18 were deemed chemically suitable for drug development. These parameters were crucial in refining our selection process and advancing compounds with promising pharmacokinetic profiles.

2.5.2 Optimal Solubility and Penetration

The optimal solubility of compounds in both aqueous and lipid environments emerged as a paramount consideration. The logarithm of the octanol/water partition coefficient ($\log P_{ow}$) provided an estimate of solubility, particularly relevant for cellular membrane penetration. Moreover, balancing the water-solubility of the compound, as influenced by the ratio of hydrogen bond donors to alkyl sidechains (Ermondi et al., 2020), was imperative to ensure efficient transport within aqueous media like blood and intracellular fluid.

2.5.3 Molecular Weight and Pharmacophores

Molecular weight, a direct determinant of diffusion, has significance, with compounds exhibiting lower molecular weights under 450 Dalton being favored (Zhang et al., 2006). Recognition of substructures with known pharmacological properties further enhanced the assessment, offering insights into the compound's therapeutic potential.

2.5.4 Lipinski's Rule of Five and Toxicity Considerations

Lipinski's Rule of Five, a traditional heuristic guideline, was applied to assess parameters such as molecular weight, lipophilicity, and hydrogen bond donors/acceptors,

providing a rapid filter to identify compounds with desirable pharmacokinetic properties (Pollastri, 2010). Additionally, vigilance was exercised in identifying substructures with known toxic, mutagenic, or teratogenic effects, thereby ensuring the safety and viability of designed molecules.

2.5.5 Online Tools for Comprehensive Analysis

To thoroughly evaluate these critical pharmacokinetic characteristics, we harnessed the capabilities of SwissADME (Daina et al., 2017; accessed at: <http://www.swissadme.ch/>) and ADMET LAB 2.0 (Xiong et al., 2021; <https://admetmesh.scbdd.com/>) online platforms.

These tools enabled the calculation of a spectrum of parameters, encompassing solubility, molecular weight, and various other ADMET-related attributes. Through these platforms, we gained a comprehensive understanding of the pharmacokinetic viability of our target compounds, enhancing our ability to make informed decisions in selecting a compound with the most promising drug-like characteristics.

2.6 Seed Extract Preparation

Twenty grams of Fenugreek seeds were washed thrice with distilled water and subsequently air-dried. The desiccated seeds were then finely powdered utilizing an electric grinder. Subsequently, in a 250 mL beaker, a mixture of 100 mL of methanol and 20 gm of finely ground Fenugreek seeds was prepared. The beaker was subjected to ultrasonication at 50 °C for 60 minutes to facilitate the preparation of the seed extract. After the sonication process, the resulting extract was filtered through Whatman filter paper No. 1, employing a conical flask. The filtrate was then stored at a temperature of 4 °C in a laboratory refrigerator for subsequent employment in the production of lipid nanoparticles.

2.7 Seed Oil Preparation

Dried and ground fenugreek seeds, weighing 30 gm, were employed in the oil extraction process. The fenugreek seeds accurately weighed, were introduced into the thimble.

2.7.1 Apparatus Setup

The assembly of the Soxhlet apparatus was carried out, configuring the extraction chamber. The thimble, containing the fenugreek seeds, was introduced into the extraction chamber, ensuring precise fitting. Secure attachment of the condenser and round-bottom flask to the extraction chamber was performed to ensure hermetic connections.

2.7.2 Solvent Addition

A volume of 300 ml of chloromethane, the selected solvent, was added to the round-bottom flask. The solvent level was maintained below the thimble in the fully assembled apparatus.

2.7.3 Extraction Process

The extraction process was initiated by gently heating the round-bottom flask using a heating mantle. As chloromethane vaporized, it ascended into the extraction chamber. Upon encountering the cooled condenser walls, the vapor underwent condensation, forming liquid droplets that returned to the fenugreek seeds within the thimble. This iterative process facilitated the efficient extraction of oil from the seeds. The extraction procedure was allowed to proceed overnight, approximately for 12 hours.

2.7.4 Post-Extraction Steps

2.7.4.1 Desiccation

Following the completion of the oil extraction, a desiccation step was implemented to ensure the complete removal of residual solvent from the extracted oil. This step involved the utilization of a vacuum pump, accompanied by applying gentle heat, thereby effectively eliminating any traces of chloromethane.

2.7.4.2 Oil Transfer and Filtration

A transfer of the extracted oil from the round-bottom flask was performed upon the thorough removal of residual solvent. The oil was subjected to filtration through filter paper to eliminate any solid particulates.

2.7.4.3 Storage and Preservation

The refined and filtered oil was subsequently carefully transferred to a reagent bottle, ensuring protection against light exposure and ambient air and preserving its structural integrity over extended durations.

2.8 Phytochemical Screening

The phytochemical screening of plant extracts plays a crucial role in identifying the diverse array of biologically active compounds present within botanical specimens. Through a series of systematic tests, the presence or absence of specific classes of phytochemicals can be discerned, providing valuable insights into the plant material's potential pharmacological and therapeutic attributes. This study conducted a comprehensive phytochemical screening on both seed extract and oil extract derived from fenugreek seeds. The objective was to explore these extracts' phytochemical composition, laying the foundation for a comprehensive understanding of their potential applications in various fields.

2.8.1 *Wagner's Test for Alkaloid Identification*

Wagner's test was conducted to ascertain the presence of alkaloids. In this context, separate seed and oil extract samples (2–3 mL) were introduced into individual test tubes. Subsequently, the seed tincture was supplemented with 1 mL of HCl and several drops of Wagner's reagent. Vigorous agitation of the test tube resulted in the appearance of a reddish-brown hue, which served as an indicative marker of the alkaloid presence.

2.8.2 *Foam Test for Saponin Differentiation*

The foam test differentiated saponins within the seed and oil extract solution. Equal volumes of seed and oil extract (5 mL) were combined with purified water (5 mL) and subjected to vigorous shaking. A stable foam formation was observed, indicating the presence of saponins.

2.8.3 Ferric Chloride Test for Phenol Detection

The ferric chloride test facilitated the detection of phenols within the seed tincture and oil extract. Five mL of seed and oil extract were introduced into separate test tubes, followed by a few drops of neutral 5% ferric chloride solution. The resulting interaction led to a distinctive blue-green coloration, confirming the presence of phenols.

2.8.4 Braymer's Test for Tannin Recognition

The identification of tannins was accomplished through Braymer's test. It involved the addition of 2 mL of purified water and several drops of ferric chloride solution to 2 mL of seed tincture and oil extract. The appearance of green precipitates within the solutions signified the presence of tannins.

2.8.5 Salkowski's Test for Terpenoid Demonstration

To demonstrate the existence of terpenoids within the extracted seed tincture and oil extract, Salkowski's test was conducted. To this end, 2 mL of seed tincture and oil extract were combined with 2 mL of chloroform and 2 mL of concentrated H₂SO₄. The development of a discernible yellow coloration served as an indication of the presence of terpenoids.

2.8.6 Bontrager's Test for Quinone Assessment

Phytochemical quinones were assessed using Bontrager's test. A distinct layer was separated by adding 3 mL of chloroform to 3 mL of seed tincture and oil extract. The subsequent addition of 5% potassium hydroxide to the formed layer resulted in a pronounced red coloration, confirming the presence of quinones.

2.8.7 Keller Killian's Test for Cardiac Glycoside Screening

Screening cardiac glycosides within the prepared seed extract and oil extract involved Keller-Killian's test. It combined 2 mL of HCl, sodium nitroprusside, and sodium hydroxide with 2 mL of seed extract and oil extract. The emergence of a pink to crimson coloration indicated the presence of cardiac glycosides.

2.8.8 Glycosides Test for Phytochemical Identification

The identification of phytochemical glycosides was executed through the glycosides test. In this process, 2 mL of seed tincture and oil extract were combined with 3 mL of chloroform and 10% alkali solution. The manifestation of a pink coloration confirmed the presence of glycosides.

2.8.9 Alkaline Reagent Test for Flavonoid Detection

The alkaline reagent test ascertained the presence of flavonoids within the seed tincture and oil extract. A distinct yellow coloration emerged by introducing NaOH to 2 mL of seed extract and oil extract, signifying the presence of flavonoids.

2.8.10 Precipitate Test for Phlobatannin Screening

The screening for phytochemical phlobatannins was conducted through the precipitate test. Adding a few drops of 2% HCl to 1 mL of seed extract and oil extract resulted in the formation of red precipitates, thereby confirming the presence of phlobatannins within the extracted seed tincture and oil extract.

2.9 Evaluation of Total Flavonoid Content

The total flavonoid content was quantified following a methodology stipulated by Singleton et al. (1999) employing the aluminum chloride colorimetric technique. Quercetin, chosen as a standard reference, was solubilized in methanol to establish a standard curve across a concentration range of 50–250 µg/mL. In a volumetric flask, a solution containing 0.5 mL of both fenugreek seed and oil extracts was combined with 0.1 mL of a 10% w/v aluminum chloride solution, 0.1 mL of a 10% w/v aluminum chloride solution, and 0.1 mL of a 0.1 mM potassium acetate solution. The final volume was adjusted to 5 mL with distilled water, and the resultant solution was incubated at 37 °C for 30 minutes. Subsequently, absorbance measurements were ascertained utilizing a UV–Vis spectrophotometer at a wavelength of 715 nm.

The quantification of total flavonoid content was achieved by utilizing the quercetin calibration curve, as the equation $y = 0.0042x - 0.1149$, demonstrating a commendable

coefficient of determination (R^2) value of 0.998. The outcomes were expressed in terms of the extract's quercetin equivalent (QE) per milligram per gram (mg/g).

The computation of the total flavonoid content (T) was performed using the formula:

$$TFC \left(\frac{mg}{g} \right) = \frac{C \times V}{M}$$

Where:

TFC represents the total flavonoid content in milligrams per gram (mg/g) of the extract in terms of quercetin equivalent.

C signifies the concentration of the determined fractions derived from the quercetin calibration curve.

V indicates the volume of the extract in milliliters (mL).

M denotes the weight of the dry fenugreek seed and oil extract in grams (g).

This approach allowed for a comprehensive assessment of the flavonoid content within the fenugreek seed and oil extracts, providing valuable insights into their potential bioactive properties.

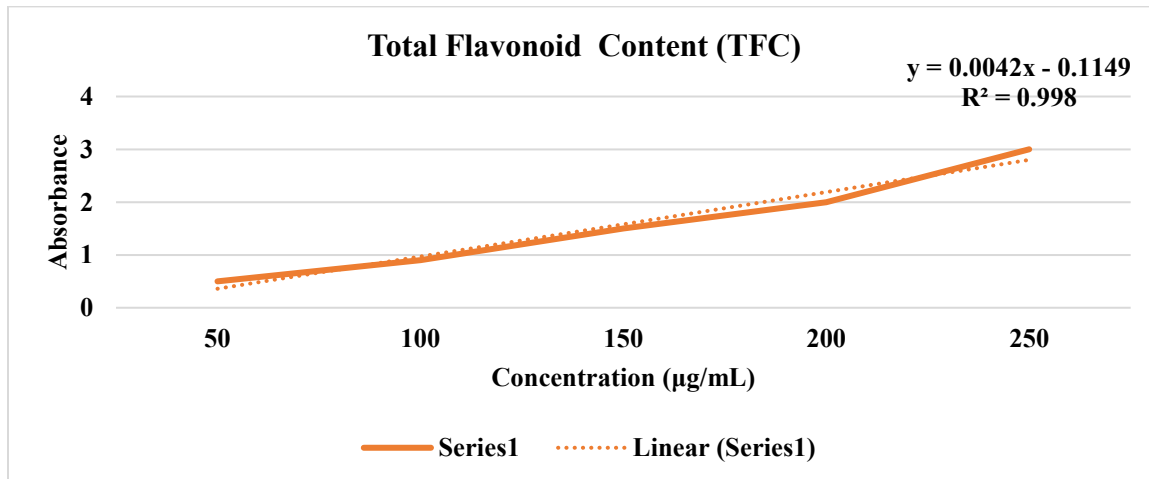


Figure 2.1: TFC content of *Trigonella foenum-graecum*

2.10 Evaluation of Total Phenolic Content

Singleton et al. (1999) elucidated the utilization of the Folin–Ciocalteu reagent in quantifying the total phenolic content (TPC). Within this analytical procedure, 0.5 mL of

fenugreek seed and oil extracts were admixed with 2.5 mL of the Folin–Ciocalteu reagent. The resultant mixtures underwent an incubation period of 15 minutes at 37 °C. Following this, 2 mL of sodium carbonate (Na₂CO₃) solution (7.5% w/v) was added, followed by a volume adjustment to 10 mL with distilled water. A subsequent 30-minute incubation transpired before triplicate spectrophotometric measurements were conducted at a wavelength of 760 nm.

A standard curve was established using gallic acid as a reference compound. The concentrations of gallic acid ranged from 50 to 250 µg/mL. The quantification of total phenols was expressed as gallic acid equivalents (GAE) in milligrams per gram (mg/g) of dry weight, employing the equation $y = 0.0037x - 0.094$, which yielded an impressive coefficient of determination (R^2) value of 0.999.

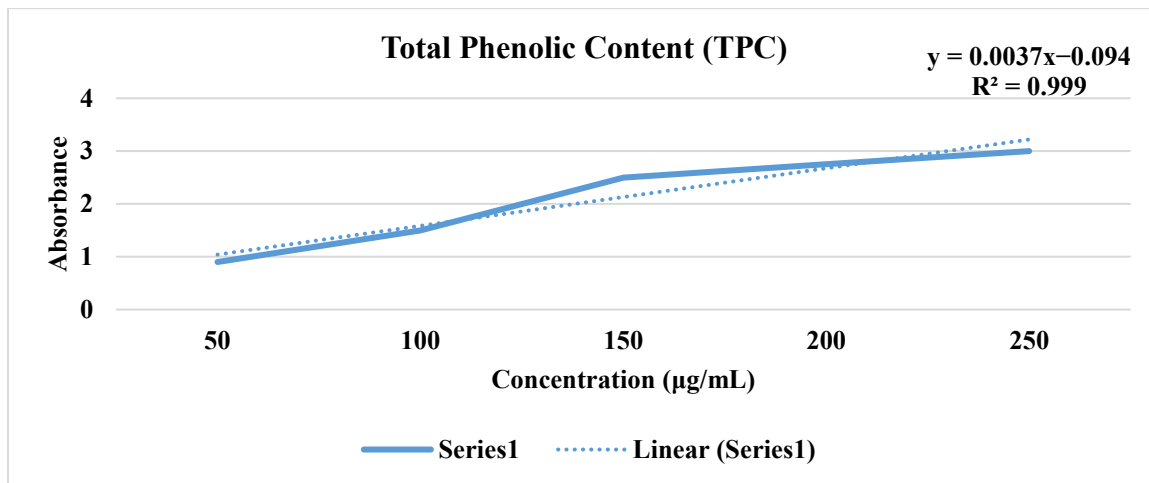


Figure 2.2: TPC content of *Trigonella foenum-graecum*

The computation of the total phenolic content (T) was performed utilizing the formula:

$$TPC \left(\frac{mg}{g} \right) = \frac{C \times V}{M}$$

Where:

TPC denotes the total phenolic content in milligrams per gram (mg/g) of extract in terms of gallic acid equivalent.

C signifies the concentration of the determined fractions extrapolated from the gallic acid calibration curve.

V represents the volume of the extract in milliliters (mL).

M indicates the weight of the dry plant extract in grams (g).

2.11 Synthesis of Lipid Nanoparticles

Lipid nanoparticles were synthesized through the controlled mixing of methanolic seed extract and seed oil derived from Fenugreek seeds, adhering to a fixed 1:1 ratio. To mitigate the potential influence of light exposure during the reaction, the sequential addition of seed extract and seed oil was administered dropwise while maintaining a consistent stirring rate of 1500 rpm on a magnetic stirrer. After the complete incorporation of seed extract and seed oil following the predetermined ratio, the solution was subjected to continuous stirring in darkness at room temperature for 30 minutes.

The synthesized solution was then examined within a UV-Vis spectrophotometer across the defined wavelength range of 450 nm to 800 nm. This evaluation aimed to ascertain the precise attributes of the resulting lipid nanocarriers, consequently validating the successful synthesis of the intended lipid nanoparticles. Upon the conclusive confirmation of lipid nanoparticle synthesis, the subsequent phase involved the encapsulation of the L-arginine metabolite within these nanostructures.

2.12 Encapsulation of L-Arginine in Lipid Nanoparticles

Following the successful preparation of lipid nanoparticles, an aqueous solution of L-arginine was prepared using distilled water. Subsequently, a controlled combination of the lipid nanoparticles and the L-arginine solution was achieved at a ratio of 2:1 respectively. This mixing was executed through high-speed stirring at 1500 rpm, inducing the formation of a pre-emulsion. The resulting pre-emulsion was introduced drop by drop into an aqueous solution containing a stabilizer while maintaining constant stirring. This process led to forming a water-in-oil-in-water (W/O/W) emulsion. The subsequent step involved the gradual evaporation of the organic solvent, culminating in the desired outcome of lipid nanoparticles encapsulating L-arginine.

A centrifugation process was employed to ensure the purity of the obtained nanoparticles, operating at a speed of 40,000 rpm for 30 minutes. The supernatant was

discarded, and the resultant pellet underwent a thorough washing procedure involving three cycles with distilled water. The cleaned pellet was then transferred to an evaporating dish and subjected to a drying process, which spanned 6 to 7 hours, within a hot air oven set at 80 °C. After the drying phase, the resulting pellet underwent further examination. This assessment was carried out after the pellet had been maintained at room temperature within an Eppendorf tube, thereby facilitating a comprehensive evaluation of the encapsulated L-arginine within the lipid nanoparticles.

2.13 Characterization of the Synthesized Nanoparticles

The nanoparticle characterization validated successful synthesis and provided essential insights for tailored applications. These findings are pivotal for optimizing the nanoparticles' performance in diverse fields, from drug delivery to nanomedicine, ensuring their effective integration into cutting-edge research and technological advancements.

2.13.1 UV-Visible Spectrophotometry

The validation of the presence of synthesized lipid nanoparticles encapsulating L-arginine was accomplished through the utilization of a UV-visible spectrophotometer. The evaluation involved the assessment of the surface plasmon resonance band across the wavelength range spanning from 200 to 800 nm. This band manifests maximum absorption and indicates the successful synthesis of lipid nanoparticles encapsulating L-arginine, thereby signifying the activation of surface plasmon vibration.

2.13.2 Scanning Electron Microscopy (SEM)

The structural characteristics of the acquired nanoparticles were elucidated via Scanning Electron Microscopy (SEM). Samples of the synthesized L-arginine encapsulated lipid nanoparticles, in their dried state, were positioned on double-conductive tape affixed to a designated sample holder. After this preparation, a platinum–gold coating was applied to enhance electrical conductivity. The examination of these samples transpired under a voltage of 12.50 kV, thereby revealing insights into the morphological attributes of the nanoparticles.

2.13.3 Fourier Transform Infrared Spectroscopy (FTIR)

Distinctive functional groups intrinsic to the synthesis of L-arginine encapsulated lipid nanoparticles were ascertained through Fourier Transform Infrared Spectroscopy (FTIR). The solution containing the resultant lipid nanoparticles underwent prior centrifugation at 10,000 rpm for 30 minutes before acquiring FTIR measurements.

2.13.4 Energy-Dispersive X-Ray Spectroscopy (EDX)

Energy-Dispersive X-ray Spectroscopy (EDX) analysis was employed to discern the elemental composition within the synthesized L-arginine encapsulated lipid nanoparticles. This analytical methodology involved the irradiation of the sample with specific X-rays, resulting in the emission of subsequent radiations, which were then amplified and recorded. The ensuing diffracted rays were measured to identify the elemental constitution of the nanoparticles.

2.13.5 Particle Size Distribution Analyzer

The particle size analysis used a Laser Scattering Particle Size Distribution Analyzer (Model: LA-300, Manufacturer: Horiba, Japan). The principle employed was Dynamic Light Scattering (DLS), which measured particle sizes through their Brownian motion. This technique capitalized on the relationship between particle size and their speed in Brownian motion - smaller particles exhibited higher speeds (Stetefeld et al., 2016).

The analyzer, operating with a 650nm Laser diode (5mW) as the light source and a photomultiplier tube as the detector, determined particle size and distribution state. The solvent used for sample preparation was Dimethyl Sulfoxide (DMSO), and a dilute sample of 10 mL was prepared. We sonicated the samples for 20 minutes to prevent aggregation. The measurements were conducted using a cuvette cell as the container, and each measurement lasted approximately 2 minutes.

2.13.6 Zeta (ζ) Potential Analysis

The Zetasizer Nano ZSP (Model: Malvern Zetasizer Nano ZSP, Manufacturer: Malvern Panalytical, Malvern, UK) was employed for the measurement of particle size,

electrophoretic mobility of proteins, zeta potential of nanoparticles and surfaces, and optionally, microrheology of protein and polymer solutions. The solvent of choice was Dimethyl Sulfoxide (DMSO), and a dilute sample of 10 mL was meticulously prepared. Each sample was processed through a 20-minute sonication process to prevent aggregation. The instrument's measurement range spanned from 3.8nm to 100 microns (diameter), accommodating a broad spectrum of particle sizes. The measurement principle involved Electrophoretic Light Scattering, wherein particles experience an electric field that induces motion, resulting in scattered light patterns that are subsequently analyzed to determine electrophoretic mobility and zeta potential (McNeil-Watson, 2013). The minimum sample volume required was 150 μ L, although the diffusion barrier method allowed a reduced volume of 20 μ L.

2.13.7 X-Ray Diffraction (XRD) Analysis

The crystalline nature of the biosynthesized arginine-encapsulated lipid nanoparticles was investigated through X-ray diffraction (XRD) analysis. A powdered sample of the nanoparticles was employed, and XRD measurements were conducted in scanning mode using a current of 30 mA and a voltage of 40 kV. Cu/K α radiation was utilized, and the diffraction pattern was recorded over a 2θ angle range of 20° to 70°. To determine the average crystalline size of the lipid nanoparticles, the Debye–Scherrer equation was applied.

$$D = \frac{k\lambda}{\beta \cos\theta}$$

In this equation:

D represents the average crystalline size of the nanoparticles.

k is the shape factor with a value of 0.94.

λ stands for the X-ray wavelength ($\lambda = 1.5418 \text{ \AA}$) for Cu/K α radiation.

β corresponds to the full width at half maximum (FWHM) of the diffraction peak in radians.

θ represents Bragg's angle, which is the angle at which constructive interference occurs for a specific lattice plane.

2.14 Assessing the Biological Potential of the Encapsulated Nanoparticles

2.14.1 Anti-Oxidant Activity

Employing a 2,2-diphenyl-1-picrylhydrazyl radical (DPPH)-based assay, we investigated the capacity of methanolic seed extract, seed oil, and synthetically encapsulated L-arginine lipid nanoparticles to scavenge free radicals. The examination encompassed varying concentrations of 100, 200, 300, 400, and 500 L for each methanolic seed extract, seed oil, and encapsulated lipid nanoparticle. Initially, 3.94 mg of DPPH was dissolved in 100 mL of methanol, yielding a 0.1 mM solution stored in darkness at room temperature to prevent light exposure. Subsequently, individual combinations of the prepared methanolic seed extract, seed oil, and encapsulated lipid nanoparticles were each treated with 0.1 mL of 0.1 mM DPPH solution. After a 30-minute incubation period, the absorbance at 517 nm was measured against the positive control, DPPH. The free radical scavenging analysis was conducted in triplicate, and the percentage of DPPH inhibition was calculated using the formula:

$$\% \text{ DPPH Inhibition} = \frac{A_o - A_s}{A_o} \times 100$$

Here, **A_o** denotes the absorbance of the control, and **A_s** represents the absorbance of the test sample, measured through UV-visible spectroscopy at 517 nm.

2.14.2 Anti-Inflammatory Activity

Following the protocol of Naveed et al. (2023), mitigating effects were assessed through the protein denaturation method, evaluating the influence of methanolic seed extract, seed oil, and synthetic L-arginine encapsulated lipid nanoparticles. The procedure involved the combination of the following constituents: 2.8 mL of phosphate-buffered saline solution (pH 6.4), 0.2 mL of hen's egg white, and varying concentrations of 150, 250, 350, 450, and 550 g/mL of the respective methanolic seed extract, seed oil, and synthetic L-arginine encapsulated lipid nanoparticles. After an incubation period of 20 minutes at 37 °C, the mixture was further subjected to a temperature of 70 °C for 5 minutes.

Post-cooling, the turbidity was quantified at 660 nm using a UV-Vis spectrophotometer. An anti-inflammatory medication (acetylsalicylic acid) was employed for comparative purposes at concentrations mirroring the experimental samples (150, 250, 350, 450, and 550 g/mL). The anti-inflammatory analysis was executed in triplicate, and the protein inhibition percentage was calculated utilizing the formula:

$$\% \text{ Inhibition of Protein Denaturation} = 1 - \frac{A_s}{A_o} \times 100$$

A_o signifies the absorbance of the control, and A_s represents the absorbance of the test sample, both measured via UV-Visible spectroscopy at 660 nm. This protein denaturation method provided a comprehensive insight into the potential mitigating effects of the tested samples, enhancing our understanding of their anti-inflammatory properties.

2.14.3 Anti-Diabetic Assay

The antidiabetic activity was assessed utilizing the alpha-amylase test, wherein the methanolic seed extract, seed oil, and synthetic L-arginine encapsulated lipid nanoparticles were subjected to varying concentrations (200, 400, 600, 800, and 1000 μ L). The protocol involved the creation of an alpha-amylase solution in a separate falcon tube, with metformin solution serving as the control for this antidiabetic evaluation. Separate test tubes were allocated for the control, methanolic seed extract, seed oil, and synthetic L-arginine encapsulated lipid nanoparticles (at the concentrations specified above). In each test tube, 10 μ L of the alpha-amylase solution was introduced, followed by thorough mixing and subsequent incubation at 30 °C for 10 minutes. Following the initial incubation, a 50 μ L aliquot of a 1% starch solution was added, and the mixture underwent an additional incubation period of 1 hour at 37 °C.

Subsequently, each test tube was supplemented with 50 μ L of a 1% iodine solution, followed by further incubation for 30 minutes at 37 °C. The absorbance measurement was subsequently conducted utilizing an ELISA reader set to a wavelength of 630 nm. This method facilitated the evaluation of the antidiabetic potential of the tested substances, providing insights into their capacity to inhibit alpha-amylase activity, a key factor in glucose metabolism and diabetes management, using the following equation.

$$\% \text{ Inhibition} = \frac{Abs_{control} - Abs_{sample}}{Abs_{control}} \times 100$$

2.14.4 Hemolytic Activity

This analysis aimed to evaluate the potential cytotoxic impacts of the test samples on cellular viability. A 3 mL aliquot of human blood was drawn and introduced into an EDTA vial, followed by inversion for thorough mixing. The resulting sample was then carefully transferred to a 15 mL tube and subjected to centrifugation at an acceleration of 850 g for approximately 5 minutes. The ensuing pellet underwent a rigorous washing process involving three cycles with phosphate-buffered saline (PBS) at approximately 4 °C, while the supernatant was subsequently discarded.

A suspension was then prepared by adding chilled PBS to achieve a final volume of 20 mL within a Falcon tube. Subsequently, varying volumes of 150, 250, 350, 450, and 550 µL of the methanolic seed extract, seed oil, and synthetic L-arginine encapsulated lipid nanoparticles were combined with 0.2 mL of the blood suspension within microcentrifuge tubes. After a 30-minute incubation at 37 °C, the absorbance was measured at 630 nm using an ELISA reader. This measurement was conducted after a 15-minute centrifugation at 16,000 rpm, followed by collecting and mixing 100 µL of the resulting supernatant. For comparative assessment, 0.1% Triton X-100 was utilized as the positive control, while PBS served as the reference standard in these experiments. The hemolysis percentage was calculated using the following formula:

$$\% \text{ Hemolysis} = \frac{Abs_{sample} - Abs_{negative control}}{Abs_{positive control}} \times 100$$

2.14.5 Anti-bacterial Activity

The disc diffusion method evaluated the antibacterial activity of L-arginine conjugated nanoparticles against *Bacillus anthrax* and *Vibrio cholera*. Fresh bacterial strains were introduced into prepared and autoclaved nutrient broth. Subsequently, 5 mL of nutrient broth was dispensed into each falcon tube, yielding three tubes, and one colony of *Vibrio cholera* and *Bacillus anthrax* was inoculated onto separate plates. The colonies were then subjected to an incubation period of 24 hours at 37 °C within an incubator shaker.

On a subsequent day, culture plates were established by introducing sterile LB agar media. To ensure the absence of contamination, 25 mL of the medium was added to autoclaved petri plates and allowed to stand at room temperature for one day. The overnight grown cultures of each strain were then spread across 200 μL of LB agar plates, along with 500 μL of the methanolic seed extract, seed oil, and synthetic L-arginine encapsulated lipid nanoparticles. The petri dishes were subsequently incubated overnight.

On the ensuing day, the inhibition zone encircling the discs was quantified and compared with the positive control. The presence of an inhibition zone around the disc signifies the antibacterial attributes of the respective solution. Notably, an inhibition zone measuring 12 mm or above holds significance (Balouiri et al., 2016), highlighting the substantial antibacterial potential of the sample under assessment.

CHAPTER THREE

RESULTS & ANALYSIS

RESULTS AND ANALYSIS

3.1 Seed Collection

The initial phase encompassed gathering fenugreek seeds, characterized by their distinct mustard hue and irregular form. This collection process occurred in two stages, each contributing to the acquisition of 250 grams. The first stage involved the procurement of 150 grams of seeds, earmarked specifically for subsequent seed oil extraction and nanoparticle synthesis processes. Subsequently, an additional 100 grams of seeds were acquired in the second stage, fulfilling the requisites for concurrent extraction, nanoparticle synthesis, and comprehensive bioactive potential characterization and assessment. These seeds, emblematic of the research's foundational components, are visually depicted in Figure 3.1.

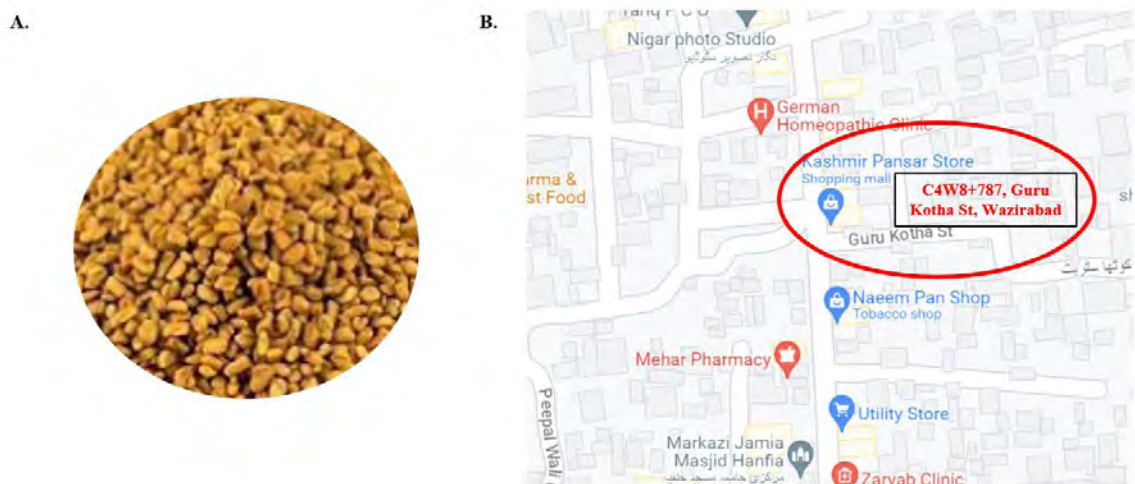


Figure 3.1: Seeds collection from the local shop ‘Kashmiri Dawa Khana’ of Wazirabad. A. Seed Texture; B. Map of Kashmiri Dawa Khana.

3.2 Network Pharmacology Analysis

The subsequent pivotal stage involved an elaborate network pharmacology analysis. The comprehensive outcomes of this analysis have been expounded upon in subsequent sections. Through scrutiny, L-arginine emerged as the designated target compound sourced from fenugreek in combatting type 2 diabetes mellitus. This finding

was arrived at through a series of analyses, the details of which are outlined in the ensuing sections.

3.2.1 Therapeutical Potential of the Plant

The investigation into the plant's therapeutic potential has yielded insightful findings, succinctly depicted in Figures 3.2 and 3.3. The intricacies of these findings are delineated below, shedding light on the multifaceted aspects of fenugreek's medicinal attributes. Figure 3.2A elucidates the distribution pattern of fenugreek across different regions of Europe and Asia, excluding southwest Asia, and its presence in North and South America. Remarkably, while fenugreek boasts a wide geographic presence, its exploitation for therapeutic purposes remains relatively limited, primarily finding prominence in North and South America and select Asian regions. Notably, while fenugreek holds medicinal significance in India, it is under-utilized therapeutically in Pakistan, as per current knowledge.

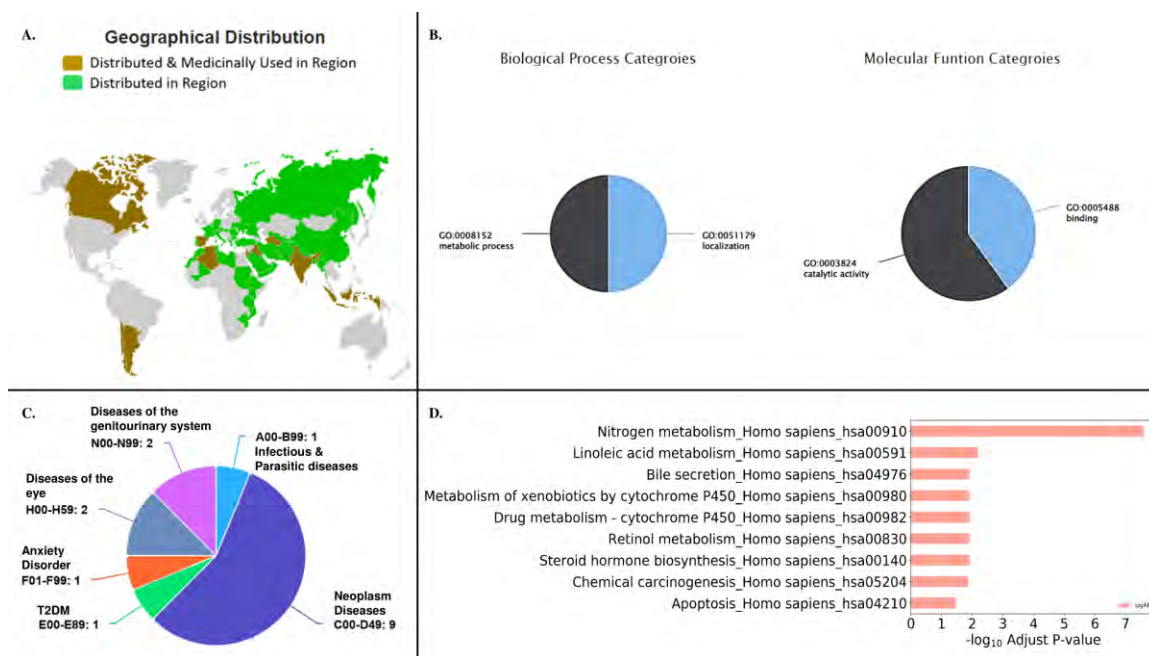


Figure 3.2: Information about *Trigonella foenum-graecum*. A. Geographical distribution; B. Gene ontology targets; C. Disease targets; D. Target processes and pathways.

Figure 3.2B highlights the predominant involvement of fenugreek compounds in vital human biological and metabolic processes, with limited influence on cellular

processes. The malleability of these compounds offers prospects for broad catalytic activities, encompassing pivotal mechanisms such as drug metabolism. In a noteworthy representation, Figure 3.2C employs a pie chart to delineate the breadth of fenugreek's therapeutic impact across diverse diseases. The synthesis of this categorical insight finds further articulation in Table 3.1, wherein the summarized therapeutic effects against various diseases are discussed. These findings emphasize fenugreek's pronounced role in combatting type 2 diabetes mellitus, our target disease.

Table 3.1: A detailed insight into the disease targets of *Trigonella foenum-graecum*.

ICD10 Disease Category	Disease Name	ICD10 Code	Associated Targets
<i>(Association Ref: TTD database)</i>			
A00-B99: Certain infectious and parasitic diseases	Bacterial infections	A00-B99	CYP2C9
C00-D49: Neoplasms	Clear cell renal cell carcinoma	C64	CA9
C00-D49: Neoplasms	Breast cancer	C50	CYP19A1; CA9
C00-D49: Neoplasms	Cancer	C00-C96	NFKB1; CA9
C00-D49: Neoplasms	Advanced breast cancer	C50	CYP19A1
C00-D49: Neoplasms	Renal cancer	C64	CA9
C00-D49: Neoplasms	Solid tumours	C00-D48	CA9
C00-D49: Neoplasms	Lymphoma	C81-C86	CA9
C00-D49: Neoplasms	Hormonally-responsive breast cancer	C50	CYP19A1
C00-D49: Neoplasms	Bladder cancer	C67	CYP19A1
E00-E89: Endocrine, nutritional and metabolic diseases	Type 2 diabetes	E11	NFKB1
F01-F99: Mental, Behavioral and Neurodevelopmental disorders	Anxiety disorder	F32, F40-F42	CYP3A4
H00-H59: Diseases of the eye and adnexa	Open-angle glaucoma	H40-H42	CA4
H00-H59: Diseases of the eye and adnexa	Ocular hypertension	H40.0	CA4
N00-N99: Diseases of the genitourinary system	Endometriosis	N80	CYP19A1
N00-N99: Diseases of the genitourinary system	Prostate disease	N42.9	CYP19A1

Expanding upon the prior visualizations, Figure 3.2D orchestrates an integration of diverse mechanisms, each calibrated by adjusted P-values. This figure accentuates the relevance of fenugreek's therapeutic potential in addressing type 2 diabetes mellitus. The

maximal log AP value attributed to nitrogen metabolism is particularly noteworthy, signifying the plant's remarkable potential in diabetes management. Figure 3.3A categorizes the diseases fenugreek targets, encapsulating its versatility in healthcare interventions.

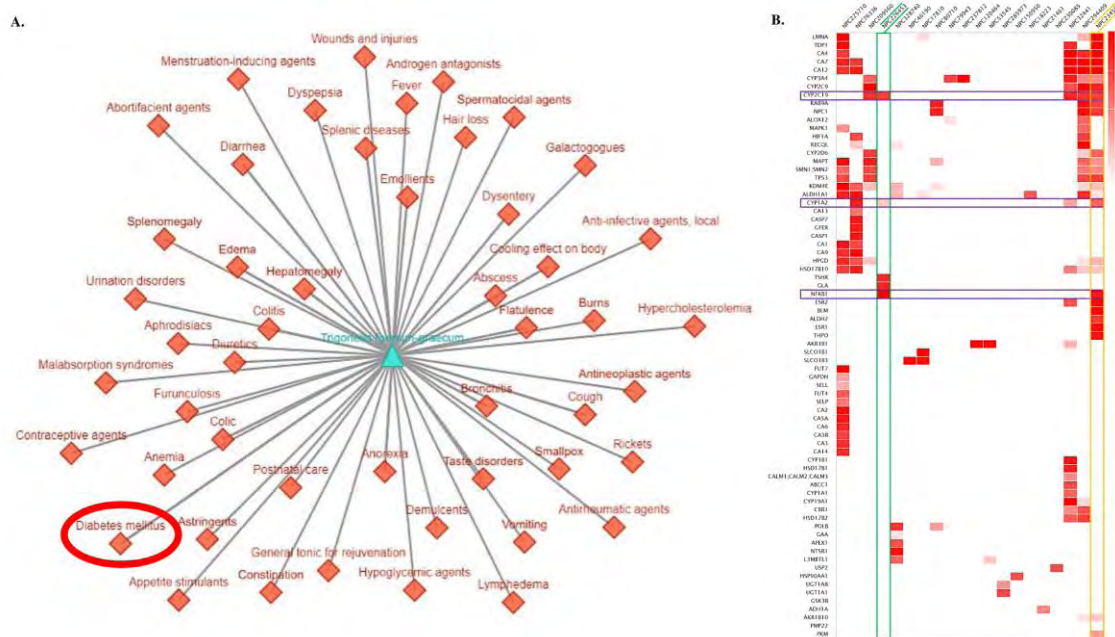


Figure 3.3: Therapeutic activity of fenugreek. A. Diseases targeted by *Trigonella foenum-graecum*; Our target disease is highlighted in the red circle; B. Activity profiles of fenugreek's active compounds. The green box highlights L-arginine's activity profile, the yellow box highlights Daidzein's activity profile and the purple boxes highlights the common gene targets of these compounds.

Figure 3.3B presents an intricate compound-target activity chart, elucidating the dynamic interplay between fenugreek compounds and gene/protein targets. The varying intensities of red boxes denote the respective therapeutic potentials, wherein deeper hues correlate with heightened efficacy, progressively attenuating as the color lightens.

3.2.2 Active Compound Screening

An exploration of the CMAUP database revealed the identification of 172 distinct compounds inherent to fenugreek, the detailed compilation of which is presented in Table 3.2. Figure 3.4 assumes a central role in elucidating the therapeutic potential of these compounds. Figure 3.4A provides an intricate portrayal of the distribution of molecular

weights within this compound cohort. Meanwhile, Figure 3.4B employs a dynamic visualization of the Topological Polar Surface Area (TPSA) juxtaposed against XlogP activities. TPSA, encompassing the collective influence of polar entities such as oxygen and nitrogen, articulates a molecule's propensity to permeate cell membranes (Milkovic et al., 2007). Similarly, XlogP, symbolic of lipophilicity, exercises a commanding influence over absorption, transport, distribution, and dosing considerations (Bruno et al., 2021). The salient interplay between these parameters emerges as pivotal, fostering an equilibrium essential for compound viability as prospective drugs.

Table 3.2: Identification of active compounds present in *Trigonella foenum-graecum*, provided by the CMAUP database. The target compounds are highlighted in Yellow.

No.	Compound_ID	Formula	Common_Name
1	NPC101785	C27H44O4	Neogitogenin
2	NPC102256	C24H32O7	Schizandrin
3	NPC103209	C33H42O19	Troloxerutin
4	NPC10559	C40H56O4	Nostoxanthin
5	NPC112819	C56H42O12	Vitisin C
6	NPC114289	C27H42O4	Nuatigenin
7	NPC116280	C45H74O18	N.A.
8	NPC117295	C44H74O19	N.A.
9	NPC117418	C21H20O11	2-(3,4-dihydroxyphenyl)-5,7-dihydroxy-8-[(2S,3R,4R,5S,6R)-3,4,5-trihydroxy-6-(hydroxymethyl)oxan-2-yl]chromen-4-one
10	NPC118773	C35H42O22	N.A.
11	NPC120464	C17H14O7	Tricin
12	NPC121509	C51H82O22	N.A.
13	NPC129185	C27H30O15	N.A.
14	NPC130530	C27H42O4	N.A.
15	NPC132904	C33H40O21	N.A.
16	NPC139075	C44H74O18	N.A.
17	NPC140310	C21H20O10	N.A.
18	NPC141357	C16H10O5	N.A.
19	NPC142108	C63H104O33	N.A.
20	NPC144229	C45H72O17	N.A.
21	NPC148235	C27H42O4	N.A.
22	NPC14970	C45H76O19	N.A.
23	NPC150324	C27H44O3	N.A.
24	NPC150950	C12H17N4OS	Thiamine
25	NPC151808	C30H26O12	N.A.

26	NPC156694	C52H86O23	N.A.
27	NPC15825	C12H22O11	N.A.
28	NPC163209	C52H88O23	N.A.
29	NPC16366	C51H84O23	N.A.
30	NPC165410	C51H84O23	N.A.
31	NPC166225	C51H84O23	N.A.
32	NPC170052	C27H30O16	3-[(2S,3R,4S,5R,6R)-4,5-dihydroxy-6-(hydroxymethyl)-3-[(2S,3R,4S,5S,6R)-3,4,5-trihydroxy-6-(hydroxymethyl)oxan-2-yl]oxyoxan-2-yl]oxy-5,7-dihydroxy-2-(4-hydroxyphenyl)chromen-4-one
33	NPC17230	C47H78O17	N.A.
34	NPC1769	C21H20O11	N.A.
35	NPC17810	C40H56	Beta
36	NPC180145	C44H74O19	N.A.
37	NPC18223	C6H9N3O2	D-Histidine
38	NPC18326	C27H42O4	N.A.
39	NPC183359	C51H82O22	N.A.
40	NPC184054	C10H9NO2	N.A.
41	NPC185137	C27H40O2	N.A.
42	NPC186179	C68H110O37	N.A.
43	NPC190385	C6H13NO3	(2S,3R,4S)-2-azaniumyl-4-hydroxy-3-methylpentanoate
44	NPC194293	C50H82O22	N.A.
45	NPC194701	C68H114O37	N.A.
46	NPC19513	C51H86O23	N.A.
47	NPC196638	C17H14O7	N.A.
48	NPC20790	C15H10O7	N.A.
49	NPC209560	C16H12O4	Formononetin
50	NPC209846	C21H20O10	Vitexin
51	NPC21461	C21H27N7O14P2	5'-Ester
52	NPC214758	C18H32O16	N.A.
53	NPC217741	C45H76O18	N.A.
54	NPC21937	C68H112O37	N.A.
55	NPC220125	C35H42O22	N.A.
56	NPC220270	C24H32O7	N.A.
57	NPC225710	C7H6O5	Gallic
58	NPC226453	C6H14N4O2	L-Arginine
59	NPC227260	C27H44O4	N.A.
60	NPC22845	C33H40O22	N.A.
61	NPC230085	C7H7NO2	Trigonelline
62	NPC233124	C45H76O18	N.A.
63	NPC234106	C32H52O6	N.A.
64	NPC234560	C15H10O4	Daidzein

65	NPC235126	C27H42O3	N.A.
66	NPC236203	C45H76O19	N.A.
67	NPC237804	C27H42O3	N.A.
68	NPC237812	C6H9N3O2	Histidine
69	NPC239416	C30H26O12	N.A.
70	NPC239788	C44H74O19	N.A.
71	NPC242419	C27H42O3	Disogenin
72	NPC243645	C26H28O14	N.A.
73	NPC245554	C45H74O18	N.A.
74	NPC24556	C27H42O3	N.A.
75	NPC250751	C44H72O18	N.A.
76	NPC252085	C44H74O18	N.A.
77	NPC254772	C56H92O27	N.A.
78	NPC254894	C52H86O23	N.A.
79	NPC254942	C44H74O19	N.A.
80	NPC255204	C6H13NO3	N.A.
81	NPC255885	C10H11NO3	N.A.
82	NPC256078	C51H82O22	N.A.
83	NPC257040	C22H28O8	N.A.
84	NPC257296	C27H44O3	N.A.
85	NPC25913	C27H42O3	N.A.
86	NPC263031	C57H94O27	N.A.
87	NPC270077	C5H14NO	N.A.
88	NPC270735	C45H76O18	N.A.
89	NPC273855	C27H42O3	N.A.
90	NPC277677	C44H74O19	N.A.
91	NPC278976	C21H20O11	N.A.
92	NPC279120	C15H10O6	N.A.
93	NPC280102	C16H12O6	N.A.
94	NPC281255	C45H74O18	N.A.
95	NPC283736	C26H28O14	N.A.
96	NPC283790	C16H20O9	N.A.
97	NPC283923	C6H5NO2	N.A.
98	NPC285973	C16H10O6	9-Hydroxy-7-(4-Hydroxyphenyl)-[1,3]Dioxolo[4,5-G]Chromen-8-One
99	NPC287295	C33H40O22	N.A.
100	NPC288426	C23H24O12	N.A.
101	NPC292279	C45H76O18	N.A.
102	NPC292318	C44H74O18	N.A.
103	NPC293832	C27H40O2	N.A.
104	NPC294409	C16H12O5	Biochanin
105	NPC294656	C67H110O36	N.A.

106	NPC302370	C6H13NO3	N.A.
107	NPC302780	C63H104O33	N.A.
108	NPC304909	C15H20O3	N.A.
109	NPC305227	C68H112O37	N.A.
110	NPC309585	C68H114O38	N.A.
111	NPC310098	C51H86O23	N.A.
112	NPC311473	C22H28O7	N.A.
113	NPC311485	C15H12O5	N.A.
114	NPC312416	C13H8S2	N.A.
115	NPC313179	C40H56O2	(1R)-4-[(1E,3E,5E,7E,9E,11E,13E,15E,17E)-18-[(1R,4R)-4-hydroxy-2,6,6-trimethylcyclohex-2-en-1-yl]-3,7,12,16-tetramethyloctadeca-1,3,5,7,9,11,13,15,17-nonaenyl]-3,5,5-trimethylcyclohex-3-en-1-ol
116	NPC32034	C28H50N2O4	N.A.
117	NPC32441	C15H12O5	Naringenin
118	NPC327103	C6H8O3	N.A.
119	NPC328740	C21H20O10	5,7-Dihydroxy-2-(4-Hydroxyphenyl)-6-[3,4,5-Trihydroxy-6-(Hydroxymethyl)Oxan-2-Yl]Chromen-4-One
120	NPC33747	C33H40O21	N.A.
121	NPC35067	C45H74O18	N.A.
122	NPC37578	C46H78O19	N.A.
123	NPC37691	C45H76O19	N.A.
124	NPC37852	C51H84O22	N.A.
125	NPC39591	C51H84O22	N.A.
126	NPC4268	C44H74O19	N.A.
127	NPC43094	C23H24O12	N.A.
128	NPC44321	C45H74O18	N.A.
129	NPC4538	C68H112O37	N.A.
130	NPC45677	C68H112O37	N.A.
131	NPC45782	C40H56O2	(1R)-4-[(1E,3E,5E,7E,9E,11E,13E,15E,17E)-18-[(4R)-4-hydroxy-2,6,6-trimethylcyclohexen-1-yl]-3,7,12,16-tetramethyloctadeca-1,3,5,7,9,11,13,15,17-nonaenyl]-3,5,5-trimethylcyclohex-3-en-1-ol
132	NPC46190	C45H72O16	Dioscin
133	NPC46801	C40H56O4	N.A.
134	NPC47319	C27H44O3	N.A.
135	NPC47517	C27H44O4	N.A.
136	NPC52956	C44H74O18	N.A.
137	NPC53545	C21H20O11	Isoorientin
138	NPC53558	C21H20O11	N.A.
139	NPC54538	C27H40O2	N.A.
140	NPC54764	C45H76O18	N.A.
141	NPC56867	C6H13NO3	N.A.

142	NPC60175	C16H14O5	N.A.
143	NPC61139	C51H84O23	N.A.
144	NPC6298	C27H42O3	N.A.
145	NPC63318	C56H112N36O11	N.A.
146	NPC67541	C44H74O18	N.A.
147	NPC71458	C45H72O17	N.A.
148	NPC72093	C51H84O22	N.A.
149	NPC72194	C51H84O23	N.A.
150	NPC7479	C27H44O3	N.A.
151	NPC75322	C56H92O27	N.A.
152	NPC76336	C10H8O4	Scopoletin
153	NPC77349	C27H42O3	N.A.
154	NPC77869	C27H30O15	N.A.
155	NPC79943	C15H12O5	5,7-Dihydroxy-2-(4-Hydroxyphenyl)-2,3-Dihydrochromen-4-One
156	NPC80334	C29H44O4	N.A.
157	NPC80710	C16H12O5	Calycosin
158	NPC81063	C27H43NO8	N.A.
159	NPC81792	C44H74O19	N.A.
160	NPC82839	C46H76O18	N.A.
161	NPC84956	C51H84O22	N.A.
162	NPC8526	C45H72O17	N.A.
163	NPC86688	C45H74O18	N.A.
164	NPC8747	C21H20O10	N.A.
165	NPC94250	C51H84O23	N.A.
166	NPC97700	C50H82O22	Gitonin
167	NPC97824	C9H19NO3	N.A.
168	NPC98257	C30H26O13	N.A.
169	NPC98555	C17H14O7	N.A.
170	NPC98696	C45H74O18	N.A.
171	NPC99016	C12H12O2	N.A.

Figure 3.4C elaborates on the count of hydrogen bond acceptors and donors intrinsic to the identified compounds, unraveling additional facets of their pharmacological characteristics. Subsequently, Figure 3.4D offers a comprehensive summary regarding the degree of adherence to the Rule of Five. This representation elucidates the extent of non-compliance, and the number of rules violated, serving as a concise distillation of compound properties. Building upon the insights from Table 3.1, identifying NFK β 1 as the target gene in fenugreek's anti-diabetic potential informed further analysis of Figure 3.3B. This examination sought to identify compounds of substantive activity against NFK β 1.

172 Known Ingredients in Total

Unique ingredients have been isolated from this plant. Plant-Ingredients Associations were manually curated from publications or collected from other databases.

24 Ingredients with Available Activity

Unique ingredients have activity data available.

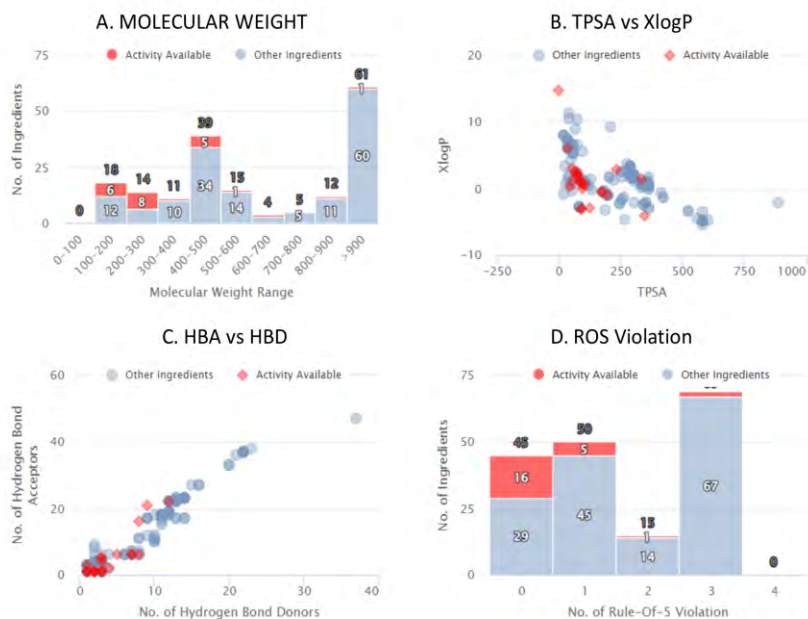


Figure 3.4: Fenugreek's active compounds and their therapeutic profiling. A. Molecular weight distribution graph of the compounds; B. TPSA vs XlogP distribution chart of the active compounds; C. Hydrogen bond donors vs acceptors graph; D. Rule-of-5 violation graph.

Outlined by distinctive green boxes, compound no. 58, NPC226453 (L-arginine), and no. 64, NPC234560 (Daidzein), emerged as consequential target compounds. These are concurrently yellow-highlighted in Table 3.2. Moreover, the alignment of their common gene targets is depicted through the medium of purple boxes in Figure 3.3B.

3.2.3 Identification of Gene/Protein Targets

The target identification phase involved a systematic exploration, commencing with the screening of GeneCards, which yielded a comprehensive assembly of 14,327 targets associated with Type 2 Diabetes Mellitus (T2DM). From the CMAUP database, the search identified 10 targets attributed to L-arginine and 55 targets linked to Daidzein, as presented in Tables 3.3 and Table 3.4, respectively. After a rigorous alignment of the 65 compound targets with the entirety of T2DM-related targets, a discerning analysis revealed a convergence of 3 distinct targets. A Venn diagram in Figure 3.5 illustrates this visually informative synthesis.

Table 3.3: Potential gene targets of L-arginine.

No.	Target Name	Target Gene	UNIPROT ID	CHEMBL ID
1	Nitric Oxide Synthase, Inducible	NOS2	P35228	CHEMBL4481
2	Nitric Oxide, Synthase, Endothelial	NOS3	P29474	CHEMBL4803
3	Nitric Oxide Synthase, Brain	NOS1	P29475	CHEMBL3568
4	Muscarinic Acetylcholine Receptor, M4	CHRM4	P08173	CHEMBL1821
5	Muscarinic Acetylcholine Receptor, M2	CHRM2	P08172	CHEMBL211
6	Muscarinic Acetylcholine Receptor, M1	CHRM1	P11229	CHEMBL216
7	Carboxypeptidase B2 Isoform A	CPB2	Q961Y4	CHEMBL3419
8	Cytochrome P450 Family 2 Subfamily C Member 19	CPY2C19	F717T9	CHEMBL3622
9	Cytochrome P450 Family 1 Subfamily A Member 2	CYP1A2	Q3LFT9	CHEMBL3356
10	Nuclear Factor Kappa β , Subunit 1	NFKB1	P19838	CHEMBL209425

A noteworthy observation emerges from the evaluation of Daidzein targets. Among the 55 identified Daidzein targets, 52 (94.5%) were discernibly associated with T2DM, thus emphasizing a substantial overlap between the compound's targeting spectrum and the disease in question. Similarly, within the ambit of L-arginine, a substantial nexus was discerned, with 7 out of the 10 identified targets (70%) distinctly implicated in T2DM.

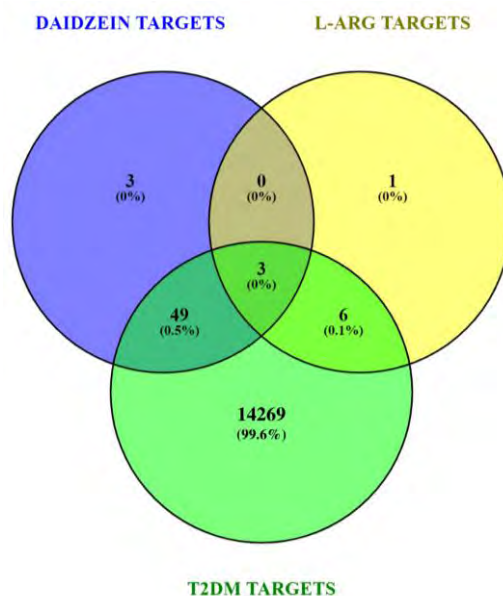


Figure 3.5: Venn diagram showcasing the common gene/protein targets of T2DM and the active compounds.

Table 3.4: Potential gene targets of Daidzein.

No.	Target Name	Target Gene	UNIPROT ID	CHEMBL ID
1	6-phosphofructo-2-kinase/fructose-2,6-bisphosphatase 3	PFKFB3	Q16875	CHEMBL2331053
2	Acetylcholinesterase	ACHE	P22303	CHEMBL220
3	Adenosine A1 receptor (by homology)	ADORA1	P30542	CHEMBL226
4	Adenosine A2a receptor	ADORA2A	P29274	CHEMBL251
5	Aldehyde dehydrogenase	ALDH2	P05091	CHEMBL1935
6	Arachidonate 12-lipoxygenase	ALOX12	P18054	CHEMBL3687
7	Arachidonate 15-lipoxygenase	ALOX15	P16050	CHEMBL2903
8	Arachidonate 5-lipoxygenase	ALOX5	P09917	CHEMBL215
9	ATP-binding cassette sub-family G member 2	ABCG2	Q9UNQ0	CHEMBL5393
10	Carbonic anhydrase I	CA1	P00915	CHEMBL261
11	Carbonic anhydrase II	CA2	P00918	CHEMBL205
12	Carbonic anhydrase IV	CA4	P22748	CHEMBL3729
13	Carbonic anhydrase IX	CA9	Q16790	CHEMBL3594
14	Carbonic anhydrase VB	CA5B	Q9Y2D0	CHEMBL3969
15	Carbonic anhydrase VII	CA7	P43166	CHEMBL2326
16	Carbonic anhydrase XII	CA12	O43570	CHEMBL3242
17	Carbonyl reductase [NADPH] 1	CBR1	P16152	CHEMBL5586
18	Cyclooxygenase-1	PTGS1	P23219	CHEMBL221
19	Cytochrome P450 19A1	CYP19A1	P11511	CHEMBL1978
20	Cytochrome P450 Family 1 Subfamily A Member 2	CYP1A2	Q3LFT9	CHEMBL3356
21	Cytochrome P450 family 2 subfamily C member 19	CYP2C19	F7I7T9	CHEMBL3622
22	Epidermal growth factor receptor erbB1	EGFR	P00533	CHEMBL203
23	Estradiol 17-beta-dehydrogenase 1	HSD17B1	P14061	CHEMBL3181
24	Estradiol 17-beta-dehydrogenase 2	HSD17B2	P37059	CHEMBL2789
25	Estrogen receptor alpha	ESR1	P03372	CHEMBL206
26	Estrogen receptor beta	ESR2	Q92731	CHEMBL242
27	Estrogen-related receptor alpha	ESRRA	P11474	CHEMBL3429
28	Estrogen-related receptor beta	ESRRB	O95718	CHEMBL3751
29	Induced myeloid leukemia cell differentiation protein Mcl-1	MCL1	Q07820	CHEMBL4361
30	Interleukin-2	IL2	P60568	CHEMBL5880
31	Macrophage migration inhibitory factor	MIF	P14174	CHEMBL2085
32	Maltase-glucoamylase	MGAM	O43451	CHEMBL2074
33	Monoamine oxidase A	MAOA	P21397	CHEMBL1951
34	Monoamine oxidase B	MAOB	P27338	CHEMBL2039
35	NADPH oxidase 4	NOX4	Q9NPH5	CHEMBL1250375
36	Norepinephrine transporter	SLC6A2	P23975	CHEMBL222
37	Nuclear factor Kappa β , Subunit 1	NFKB1	P19838	CHEMBL2094258
38	Peroxisome proliferator-activated receptor alpha	PPARA	Q07869	CHEMBL239
39	Peroxisome proliferator-activated receptor gamma	PPARG	P37231	CHEMBL235
40	P-glycoprotein 1	ABCB1	P08183	CHEMBL4302

41	Protein-tyrosine phosphatase 1B	PTPN1	P18031	CHEMBL335
42	Receptor-type tyrosine-protein phosphatase S	PTPRS	Q13332	CHEMBL2396508
43	Serotonin 2a (5-HT2a) receptor	HTR2A	P28223	CHEMBL224
44	Serotonin 2c (5-HT2c) receptor	HTR2C	P28335	CHEMBL225
45	Serum paraoxonase/arylesterase 1	PON1	P27169	CHEMBL3167
46	Steryl-sulfatase	STS	P08842	CHEMBL3559
47	Tankyrase-1	TNKS	O95271	CHEMBL6164
48	Tankyrase-2	TNKS2	Q9H2K2	CHEMBL6154
49	Thrombin and coagulation factor X	F10	P00742	CHEMBL244
50	Thromboxane-A synthase	TBXAS1	P24557	CHEMBL1835
51	Tissue-type plasminogen activator	PLAT	P00750	CHEMBL1873
52	Toll-like receptor (TLR7/TLR9)	TLR9	Q9NR96	CHEMBL5804
53	Tyrosinase (by homology)	TYR	P14679	CHEMBL1973
54	Urokinase-type plasminogen activator	PLAU	P00749	CHEMBL3286
55	Xanthine dehydrogenase	XDH	P47989	CHEMBL1929

3.2.4 Network Visualization of Common Genes

The analytical stride involved translating shared gene targets spanning L-arginine, Daidzein, and T2DM into a coherent network representation. This interplay is portrayed in Figure 3.6, encapsulating the convergence of biological interactions within the context of these compounds and their shared association with Type 2 Diabetes Mellitus (T2DM). A chromatic differentiation adeptly distinguishes the collective gene targets within this network. Targets shared between T2DM and Daidzein are rendered in hues of pink, a visual testament to their coalescence and consequential interactions. In parallel, the nexus between L-arginine and T2DM targets finds expression in verdant shades of green, embodying their shared influence terrain. Most notably, the tripartite juncture of L-arginine, Daidzein, and T2DM gene targets is impeccably illuminated by a warm expanse of yellow, encapsulating their harmonized intersection within the complex network.

3.2.5 Protein-Protein Network Analysis

The culmination of our exploration is encapsulated within the confines of the STRING network analysis, unveiling a nexus of interactions elucidated through an interplay of protein targets. As a summation, Table 3.5 distills the common targets harnessed from the preceding sections, affording a consolidated perspective on these pivotal interactions.

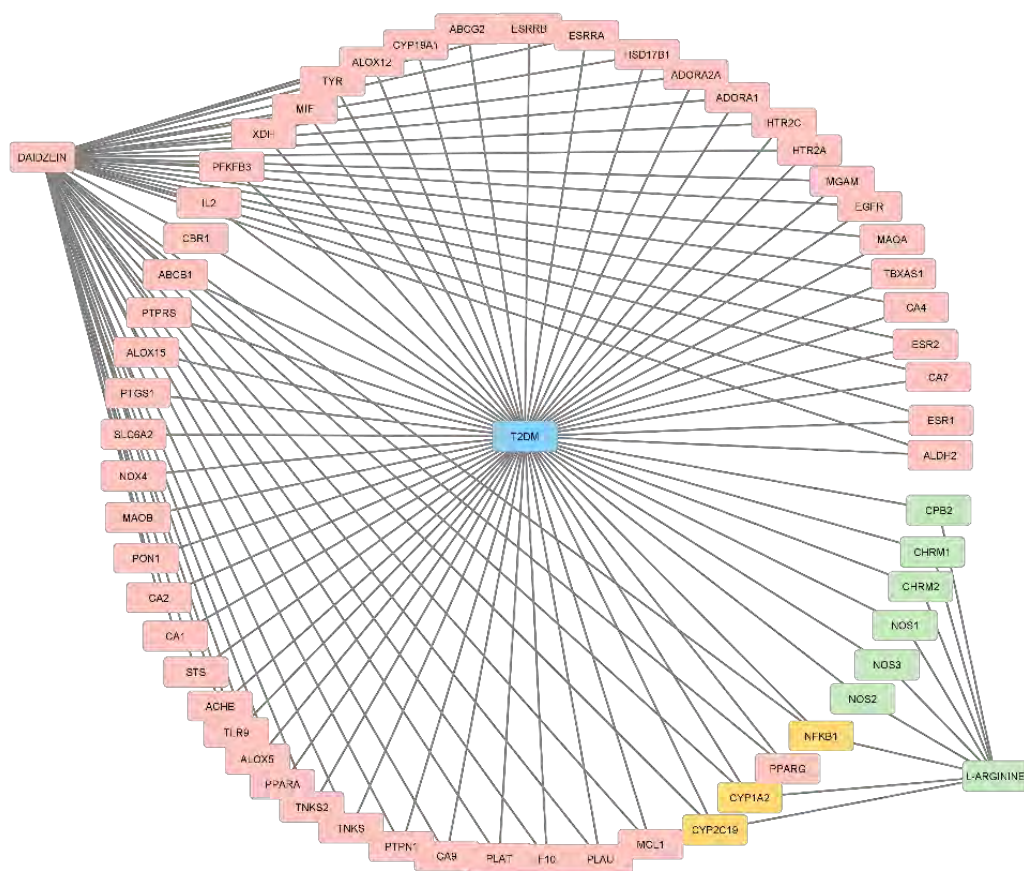


Figure 3.6: Cytoscape network of gene/protein targets of the active compounds. Genes in pink are targeted by Daidzein, genes in green are targeted by L-arginine, while those in yellow are targeted by both.

Table 3.5: Details of the Gene/Protein Targets of the Active Compounds.

DAIDZEIN TARGETS	
CA1	Carbonic anhydrase 1; Reversible hydration of carbon dioxide. Can hydrates cyanamide to urea. (261 aa)
MAOA	Amine oxidase [flavin-containing] A; Catalyzes the oxidative deamination of biogenic and xenobiotic amines and has important functions in the metabolism of neuroactive and vasoactive amines in the central nervous system and peripheral tissues. MAOA preferentially oxidizes biogenic amines such as 5-hydroxytryptamine (5-HT), norepinephrine and epinephrine. (527 aa)
TYR	Tyrosinase; This is a copper-containing oxidase that functions in the formation of pigments such as melanins and other polyphenolic compounds. Catalyzes the initial and rate limiting step in the cascade of reactions leading to melanin production from tyrosine. In addition to hydroxylating tyrosine to DOPA (3,4-dihydroxyphenylalanine), also catalyzes the oxidation of DOPA to DOPA-quinone, and possibly the oxidation of DHI (5,6-dihydroxyindole) to indole-5,6 quinone. Belongs to the tyrosinase family. (529 aa)

<i>F10</i>	Activated factor Xa heavy chain; Factor Xa is a vitamin K-dependent glycoprotein that converts prothrombin to thrombin in the presence of factor Va, calcium and phospholipid during blood clotting. (488 aa)
<i>PON1</i>	Serum paraoxonase/arylesterase 1; Hydrolyzes the toxic metabolites of a variety of organophosphorus insecticides. Capable of hydrolyzing a broad spectrum of organophosphate substrates and lactones, and a number of aromatic carboxylic acid esters. Mediates an enzymatic protection of low density lipoproteins against oxidative modification and the consequent series of events leading to atheroma formation; Belongs to the paraoxonase family. (355 aa)
<i>ESR1</i>	Estrogen receptor; Nuclear hormone receptor. The steroid hormones and their receptors are involved in the regulation of eukaryotic gene expression and affect cellular proliferation and differentiation in target tissues. Ligand-dependent nuclear transactivation involves either direct homodimer binding to a palindromic estrogen response element (ERE) sequence or association with other DNA-binding transcription factors, such as AP-1/c-Jun, c-Fos, ATF-2, Sp1 and Sp3, to mediate ERE- independent signaling. (595 aa)
<i>MCL1</i>	Induced myeloid leukemia cell differentiation protein Mcl-1; Involved in the regulation of apoptosis versus cell survival, and in the maintenance of viability but not of proliferation. Mediates its effects by interactions with a number of other regulators of apoptosis. Isoform 1 inhibits apoptosis. Isoform 2 promotes apoptosis. Belongs to the Bcl-2 family. (350 aa)
<i>ALOX12</i>	Arachidonate 12-lipoxygenase, 12S-type; Catalyzes the regio and stereo-specific incorporation of a single molecule of dioxygen into free and esterified polyunsaturated fatty acids generating lipid hydroperoxides that can be further reduced to the corresponding hydroxy species. Mainly converts arachidonic acid to (12S)-hydroperoxyeicosatetraenoic acid/(12S)-HPETE but can also metabolize linoleic acid. In contrast does not react towards methyl esters of linoleic and arachidonic acids (By similarity). (663 aa)
<i>CBR1</i>	Carbonyl reductase [NADPH] 1; NADPH-dependent reductase with broad substrate specificity. Catalyzes the reduction of a wide variety of carbonyl compounds including quinones, prostaglandins, menadione, plus various xenobiotics. Catalyzes the reduction of the antitumor anthracyclines doxorubicin and daunorubicin to the cardiotoxic compounds doxorubicinol and daunorubicinol. Can convert prostaglandin E2 to prostaglandin F2- alpha. Can bind glutathione, which explains its higher affinity for glutathione-conjugated substrates. Catalyzes the reduction of S- nitrosoglutathione. (277 aa)
<i>PTGS1</i>	Prostaglandin G/H synthase 1; Converts arachidonate to prostaglandin H2 (PGH2), a committed step in prostanoid synthesis. Involved in the constitutive production of prostanoids in particular in the stomach and platelets. In gastric epithelial cells, it is a key step in the generation of prostaglandins, such as prostaglandin E2 (PGE2), which plays an important role in cytoprotection. In platelets, it is involved in the generation of thromboxane A2 (TXA2), which promotes platelet activation and aggregation, vasoconstriction and proliferation of vascular smooth muscle cells. (599 aa)
<i>ADORA2A</i>	Adenosine receptor A2a; Receptor for adenosine (By similarity). The activity of this receptor is mediated by G proteins which activate adenylyl cyclase (By similarity); Belongs to the G-protein coupled receptor 1 family. (412 aa)
<i>ACHE</i>	Acetylcholinesterase; Terminates signal transduction at the neuromuscular junction by rapid hydrolysis of the acetylcholine released into the synaptic cleft. Role in neuronal apoptosis. Belongs to the type-B carboxylesterase/lipase family. (617 aa)
<i>ABCB1</i>	ATP-dependent translocase ABCB1; Translocates drugs and phospholipids across the membrane. Catalyzes the flop of phospholipids from the cytoplasmic to the exoplasmic leaflet of the apical membrane. Participates mainly to the flop of phosphatidylcholine, phosphatidylethanolamine, beta-D-glucosylceramides and sphingomyelins. Energy-

	dependent efflux pump responsible for decreased drug accumulation in multidrug-resistant cells. (1280 aa)
CYP19A1	Aromatase; A cytochrome P450 monooxygenase that catalyzes the conversion of C19 androgens, androst-4-ene-3,17-dione (androstenedione) and testosterone to the C18 estrogens, estrone and estradiol, respectively. Catalyzes three successive oxidations of C19 androgens: two conventional oxidations at C19 yielding 19-hydroxy and 19-oxo/19-aldehyde derivatives, followed by a third oxidative aromatization step that involves C1-beta hydrogen abstraction combined with cleavage of the C10-C19 bond to yield a phenolic A ring and formic acid. (503 aa)
STS	Steryl-sulfatase; Catalyzes the conversion of sulfated steroid precursors, such as dehydroepiandrosterone sulfate (DHEA-S) and estrone sulfate to the free steroid. (583 aa)
HTR2A	5-hydroxytryptamine receptor 2A; G-protein coupled receptor for 5-hydroxytryptamine (serotonin). Also functions as a receptor for various drugs and psychoactive substances, including mescaline, psilocybin, 1-(2,5-dimethoxy-4-iodophenyl)-2-aminopropane (DOI) and lysergic acid diethylamide (LSD). Ligand binding causes a conformation change that triggers signaling via guanine nucleotide-binding proteins (G proteins) and modulates the activity of down-stream effectors. Beta-arrestin family members inhibit signaling via G proteins and mediate activation of alternative signaling pathways. (471 aa)
CA2	Carbonic anhydrase 2; Essential for bone resorption and osteoclast differentiation (By similarity). Reversible hydration of carbon dioxide. Can hydrate cyanamide to urea. Involved in the regulation of fluid secretion into the anterior chamber of the eye. Contributes to intracellular pH regulation in the duodenal upper villous epithelium during proton- coupled peptide absorption. Stimulates the chloride-bicarbonate exchange activity of SLC26A6. (260 aa)
CA7	Carbonic anhydrase 7; Reversible hydration of carbon dioxide; Belongs to the alpha-carbonic anhydrase family. (264 aa)
TNKS	Poly [ADP-ribose] polymerase tankyrase-1; Poly-ADP-ribosyltransferase involved in various processes such as Wnt signaling pathway, telomere length and vesicle trafficking. Acts as an activator of the Wnt signaling pathway by mediating poly-ADP-ribosylation (PARsylation) of AXIN1 and AXIN2, 2 key components of the beta-catenin destruction complex: poly-ADP-ribosylated target proteins are recognized by RNF146, which mediates their ubiquitination and subsequent degradation. Also mediates PARsylation of BLZF1 and CASC3, followed by recruitment of RNF146 and subsequent ubiquitination. (1327 aa)
PFKFB3	6-phosphofructo-2-kinase/fructose-2,6-bisphosphatase 3; Synthesis and degradation of fructose 2,6-bisphosphate; In the C-terminal section; belongs to the phosphoglycerate mutase family. (568 aa)
ABCG2	Broad substrate specificity ATP-binding cassette transporter ABCG2; Broad substrate specificity ATP-dependent transporter of the ATP-binding cassette (ABC) family that actively extrudes a wide variety of physiological compounds, dietary toxins and xenobiotics from cells. Involved in porphyrin homeostasis, mediating the export of protoporphyrin IX (PPIX) from both mitochondria to cytosol and cytosol to extracellular space, it also functions in the cellular export of heme. Also mediates the efflux of sphingosine-1-P from cells. (655 aa)
ESRRA	Steroid hormone receptor ERR1; Binds to an ERR-alpha response element (ERRE) containing a single consensus half-site, 5'-TNAAGGTCA-3'. Can bind to the medium-chain acyl coenzyme A dehydrogenase (MCAD) response element NRRE-1 and may act as an important regulator of MCAD promoter. Binds to the C1 region of the lactoferrin gene promoter. Requires dimerization and the coactivator, PGC-1A, for full activity. The ERRalpha/PGC1alpha complex is a regulator of energy metabolism. Induces the expression of PERM1 in the skeletal muscle. (423 aa)

CA4	Carbonic anhydrase 4; Reversible hydration of carbon dioxide. May stimulate the sodium/bicarbonate transporter activity of SLC4A4 that acts in pH homeostasis. It is essential for acid overload removal from the retina and retina epithelium, and acid release in the choriocapillaris in the choroid; Belongs to the alpha-carbonic anhydrase family. (312 aa)
MAOB	Amine oxidase [flavin-containing] B; Catalyzes the oxidative deamination of biogenic and xenobiotic amines and has important functions in the metabolism of neuroactive and vasoactive amines in the central nervous system and peripheral tissues. MAOB preferentially degrades benzylamine and phenylethylamine; Belongs to the flavin monoamine oxidase family. (520 aa)
PPARG	Peroxisome proliferator-activated receptor gamma; Nuclear receptor that binds peroxisome proliferators such as hypolipidemic drugs and fatty acids. Once activated by a ligand, the nuclear receptor binds to DNA specific PPAR response elements (PPRE) and modulates the transcription of its target genes, such as acyl-CoA oxidase. It therefore controls the peroxisomal beta-oxidation pathway of fatty acids. Key regulator of adipocyte differentiation and glucose homeostasis. ARF6 acts as a key regulator of the tissue-specific adipocyte P2 (aP2) enhancer. (505 aa)
TLR9	Toll-like receptor 9; Key component of innate and adaptive immunity. TLRs (Toll-like receptors) control host immune response against pathogens through recognition of molecular patterns specific to microorganisms. TLR9 is a nucleotide-sensing TLR which is activated by unmethylated cytidine- phosphate-guanosine (CpG) dinucleotides. Acts via MYD88 and TRAF6, leading to NF-kappa-B activation, cytokine secretion and the inflammatory response. Controls lymphocyte response to Helicobacter infection (By similarity). (1032 aa)
CA9	Carbonic anhydrase 9; Reversible hydration of carbon dioxide. Participates in pH regulation. May be involved in the control of cell proliferation and transformation. Appears to be a novel specific biomarker for a cervical neoplasia. (459 aa)
ALOX5	Arachidonate 5-lipoxygenase; Catalyzes the first step in leukotriene biosynthesis, and thereby plays a role in inflammatory processes. Belongs to the lipoxygenase family. (674 aa)
IL2	Interleukin-2; Produced by T-cells in response to antigenic or mitogenic stimulation, this protein is required for T-cell proliferation and other activities crucial to regulation of the immune response. Can stimulate B-cells, monocytes, lymphokine-activated killer cells, natural killer cells, and glioma cells. (153 aa)
ESR2	Estrogen receptor beta; Nuclear hormone receptor. Binds estrogens with an affinity similar to that of ESR1, and activates expression of reporter genes containing estrogen response elements (ERE) in an estrogen-dependent manner. Isoform beta-cx lacks ligand binding ability and has no or only very low ere binding activity resulting in the loss of ligand-dependent transactivation ability. (530 aa)
PTPRS	Receptor-type tyrosine-protein phosphatase S; Cell surface receptor that binds to glycosaminoglycans, including chondroitin sulfate proteoglycans and heparan sulfate proteoglycan. Binding to chondroitin sulfate and heparan sulfate proteoglycans has opposite effects on PTPRS oligomerization and regulation of neurite outgrowth. Contributes to the inhibition of neurite and axonal outgrowth by chondroitin sulfate proteoglycans, also after nerve transection. Plays a role in stimulating neurite outgrowth in response to the heparan sulfate proteoglycan GPC2. (1948 aa)
SLC6A2	Sodium-dependent noradrenaline transporter; Amine transporter. Terminates the action of noradrenaline by its high affinity sodium-dependent reuptake into presynaptic terminals. Belongs to the sodium:neurotransmitter symporter (SNF) (TC 2.A.22) family. SLC6A2 subfamily. (628 aa)
EGFR	Epidermal growth factor receptor; Receptor tyrosine kinase binding ligands of the EGF family and activating several signaling cascades to convert extracellular cues into appropriate cellular responses. Known ligands include EGF, TGFA/TGF-alpha, AREG, epigen/EPGN, BTC/betacellulin, epiregulin/EREG and HBEGF/heparin- binding EGF.

	Ligand binding triggers receptor homo- and/or heterodimerization and autophosphorylation on key cytoplasmic residues. The phosphorylated receptor recruits adapter proteins like GRB2 which in turn activates complex downstream signaling cascades. (1210 aa)
HTR2C	5-hydroxytryptamine receptor 2C; G-protein coupled receptor for 5-hydroxytryptamine (serotonin). Also functions as a receptor for various drugs and psychoactive substances, including ergot alkaloid derivatives, 1-2,5,- dimethoxy-4-iodophenyl-2-aminopropane (DOI) and lysergic acid diethylamide (LSD). Ligand binding causes a conformation change that triggers signaling via guanine nucleotide-binding proteins (G proteins) and modulates the activity of down-stream effectors. (458 aa)
PLAT	Tissue-type plasminogen activator chain A; Converts the abundant, but inactive, zymogen plasminogen to plasmin by hydrolyzing a single Arg-Val bond in plasminogen. By controlling plasmin-mediated proteolysis, it plays an important role in tissue remodeling and degradation, in cell migration and many other physiopathological events. Plays a direct role in facilitating neuronal migration; Belongs to the peptidase S1 family. (562 aa)
PTPNI	Tyrosine-protein phosphatase non-receptor type 1; Tyrosine-protein phosphatase which acts as a regulator of endoplasmic reticulum unfolded protein response. Mediates dephosphorylation of EIF2AK3/PERK; inactivating the protein kinase activity of EIF2AK3/PERK. May play an important role in CKII- and p60c- src-induced signal transduction cascades. May regulate the EFNA5-EPHA3 signaling pathway which modulates cell reorganization and cell-cell repulsion. May also regulate the hepatocyte growth factor receptor signaling pathway through dephosphorylation of MET. (435 aa)
NOX4	NADPH oxidase 4; Constitutive NADPH oxidase which generates superoxide intracellularly upon formation of a complex with CYBA/p22phox. Regulates signaling cascades probably through phosphatases inhibition. May function as an oxygen sensor regulating the KCNK3/TASK-1 potassium channel and HIF1A activity. May regulate insulin signaling cascade. May play a role in apoptosis, bone resorption and lipolysaccharide-mediated activation of NFkB. May produce superoxide in the nucleus and play a role in regulating gene expression upon cell stimulation. Isoform 3 is not functional. (578 aa)
ALOX15	Arachidonate 15-lipoxygenase; Non-heme iron-containing dioxygenase that catalyzes the stereo-specific peroxidation of free and esterified polyunsaturated fatty acids generating a spectrum of bioactive lipid mediators. Converts arachidonic acid into 12-hydroperoxyeicosatetraenoic acid/12- HPETE and 15-hydroperoxyeicosatetraenoic acid/15-HPETE. Also converts linoleic acid to 13-hydroperoxyoctadecadienoic acid. May also act on (12S)-hydroperoxyeicosatetraenoic acid/(12S)-HPETE to produce hepoxilin A3. Probably plays an important role in the immune and inflammatory responses. (662 aa)
MGAM	Maltase-glucoamylase, intestinal; May serve as an alternate pathway for starch digestion when luminal alpha-amylase activity is reduced because of immaturity or malnutrition. May play a unique role in the digestion of malted dietary oligosaccharides used in food manufacturing. (1857 aa)
ADORA1	Adenosine receptor A1; Receptor for adenosine. The activity of this receptor is mediated by G proteins which inhibit adenylyl cyclase; Belongs to the G-protein coupled receptor 1 family. (326 aa)
TNKS2	Poly [ADP-ribose] polymerase tankyrase-2; Poly-ADP-ribosyltransferase involved in various processes such as Wnt signaling pathway, telomere length and vesicle trafficking. Acts as an activator of the Wnt signaling pathway by mediating poly-ADP-ribosylation of AXIN1 and AXIN2, 2 key components of the beta-catenin destruction complex: poly- ADP-ribosylated target proteins are recognized by RNF146, which mediates their ubiquitination and subsequent degradation. Also mediates poly-ADP-ribosylation of BLZF1 and CASC3, followed by recruitment of RNF146 and subsequent ubiquitination. (1166 aa)

<i>PPARA</i>	Peroxisome proliferator-activated receptor alpha; Ligand-activated transcription factor. Key regulator of lipid metabolism. Activated by the endogenous ligand 1-palmitoyl-2-oleoyl-sn-glycerol-3-phosphocholine (16:0/18:1-GPC). Activated by oleylethanolamide, a naturally occurring lipid that regulates satiety. Receptor for peroxisome proliferators such as hypolipidemic drugs and fatty acids. Regulates the peroxisomal beta-oxidation pathway of fatty acids. Functions as transcription activator for the ACOX1 and P450 genes. (468 aa)
<i>XDH</i>	Xanthine dehydrogenase/oxidase; Key enzyme in purine degradation. Catalyzes the oxidation of hypoxanthine to xanthine. Catalyzes the oxidation of xanthine to uric acid. Contributes to the generation of reactive oxygen species. Has also low oxidase activity towards aldehydes (in vitro). (1333 aa)
<i>ESRRB</i>	Steroid hormone receptor ERR2; [Isoform 3]: Transcription factor that binds a canonical ESRRB recognition (ERRE) sequence 5'TCAAGGTCA-3' localized on promoter and enhancer of targets genes regulating their expression or their transcription activity. Plays a role, in a LIF-independent manner, in maintenance of self-renewal and pluripotency of embryonic and trophoblast stem cells through different signaling pathways including FGF signaling pathway and Wnt signaling pathways. (508 aa)
<i>PLAU</i>	Urokinase-type plasminogen activator short chain A; Specifically cleaves the zymogen plasminogen to form the active enzyme plasmin. (431 aa)
<i>TBXAS1</i>	Thromboxane A synthase 1; Belongs to the cytochrome P450 family. (580 aa)
<i>ALDH2</i>	Aldehyde dehydrogenase, mitochondrial; Aldehyde dehydrogenase 2 family member; Belongs to the aldehyde dehydrogenase family. (517 aa)
<i>MIF</i>	Macrophage migration inhibitory factor; Pro-inflammatory cytokine. Involved in the innate immune response to bacterial pathogens. The expression of MIF at sites of inflammation suggests a role as mediator in regulating the function of macrophages in host defense. Counteracts the anti-inflammatory activity of glucocorticoids. Has phenylpyruvate tautomerase and dopachrome tautomerase activity (in vitro), but the physiological substrate is not known. It is not clear whether the tautomerase activity has any physiological relevance, and whether it is important for cytokine activity. (115 aa)
<i>HSD17B1</i>	Estradiol 17-beta-dehydrogenase 1; Favors the reduction of estrogens and androgens. Also has 20- alpha-HSD activity. Uses preferentially NADH; Belongs to the short-chain dehydrogenases/reductases (SDR) family. (329 aa)
L-ARGININE TARGETS	
<i>CHRM2</i>	Muscarinic acetylcholine receptor M2; The muscarinic acetylcholine receptor mediates various cellular responses, including inhibition of adenylate cyclase, breakdown of phosphoinositides and modulation of potassium channels through the action of G proteins. Primary transducing effect is adenylate cyclase inhibition. Signaling promotes phospholipase C activity, leading to the release of inositol trisphosphate (IP3); this then triggers calcium ion release into the cytosol. (466 aa)
<i>NOS3</i>	Nitric oxide synthase, endothelial; Produces nitric oxide (NO) which is implicated in vascular smooth muscle relaxation through a cGMP-mediated signal transduction pathway. NO mediates vascular endothelial growth factor (VEGF)-induced angiogenesis in coronary vessels and promotes blood clotting through the activation of platelets; Belongs to the NOS family. (1203 aa)
<i>CPB2</i>	Carboxypeptidase B2; Cleaves C-terminal arginine or lysine residues from biologically active peptides such as kinins or anaphylatoxins in the circulation thereby regulating their activities. Down-regulates fibrinolysis by removing C-terminal lysine residues from fibrin that has already been partially degraded by plasmin. Belongs to the peptidase M14 family. (423 aa)
<i>NOS2</i>	Nitric oxide synthase, inducible; Produces nitric oxide (NO) which is a messenger molecule with diverse functions throughout the body. In macrophages, NO mediates tumoricidal and bactericidal actions. Also has nitrosylase activity and mediates cysteine S-nitrosylation of cytoplasmic target proteins such PTGS2/COX2 (By similarity). (1153 aa)

3.3 Molecular Docking Analysis

The subsequent analysis comprised the rigorous molecular docking of the selected compounds: L-Arginine (PubChem ID: 6322), Daidzein (PubChem ID: 5281708), and the comparator drug Metformin (PubChem ID: 4091). These compounds were systematically docked against the triumvirate of common protein targets harnessed from preceding investigations. The resultant docking energy scores, presented in Table 3.6, unravel a compelling narrative of molecular interactions, outlining the relative affinities of these compounds toward the identified protein targets.

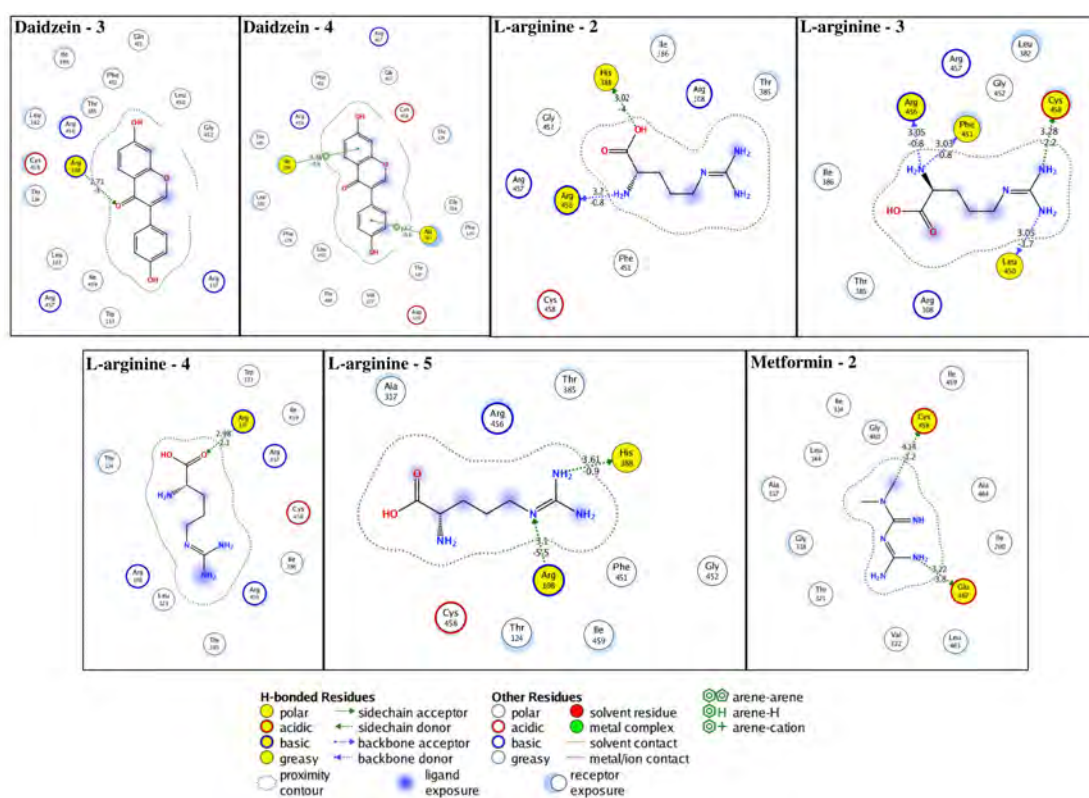


Figure 3.8: 2D interaction profiles of different poses of L-arginine, Daidzein, and Metformin (Control) with CYP1A2 protein. The ligands are present in the centre whereas the protein's surrounding amino acids are present around them. The amino acids shown in yellow are involved in direct molecular interaction with the ligands. The numbers represent the docking pose for each interaction.

The docking outcomes yield a distinctive revelation, accentuating the propensity of L-arginine and Daidzein to foster substantive interactions with the target proteins, thereby emphasizing their heightened binding affinities compared to Metformin. L-arginine

emerges as a potent lead compound, exhibiting more interaction and binding affinity than Daidzein and Metformin. A dissection within the precincts of NFKB-1 reveals a notable dissonance, wherein Daidzein appears devoid of interaction. In contrast, L-arginine espouses significant molecular entanglements that differentiate it from Metformin, further solidifying its potent role.

The crux of these interactions is vividly encapsulated through Figures 3.8, 3.9, and 3.10, an illustrative depiction that articulates the web of intermolecular interactions. Figure 3.8, for instance, exudes Daidzein's substantial arene interactions in the third and fourth pose, juxtaposed against Metformin's solitary sidechain hydrogen bonding in the second pose. L-arginine emerged as the best, weaving an elaborate tapestry of sidechain and backbone hydrogen bonding, an attribute exhibited prominently in four out of five docking poses, amplifying its potential.

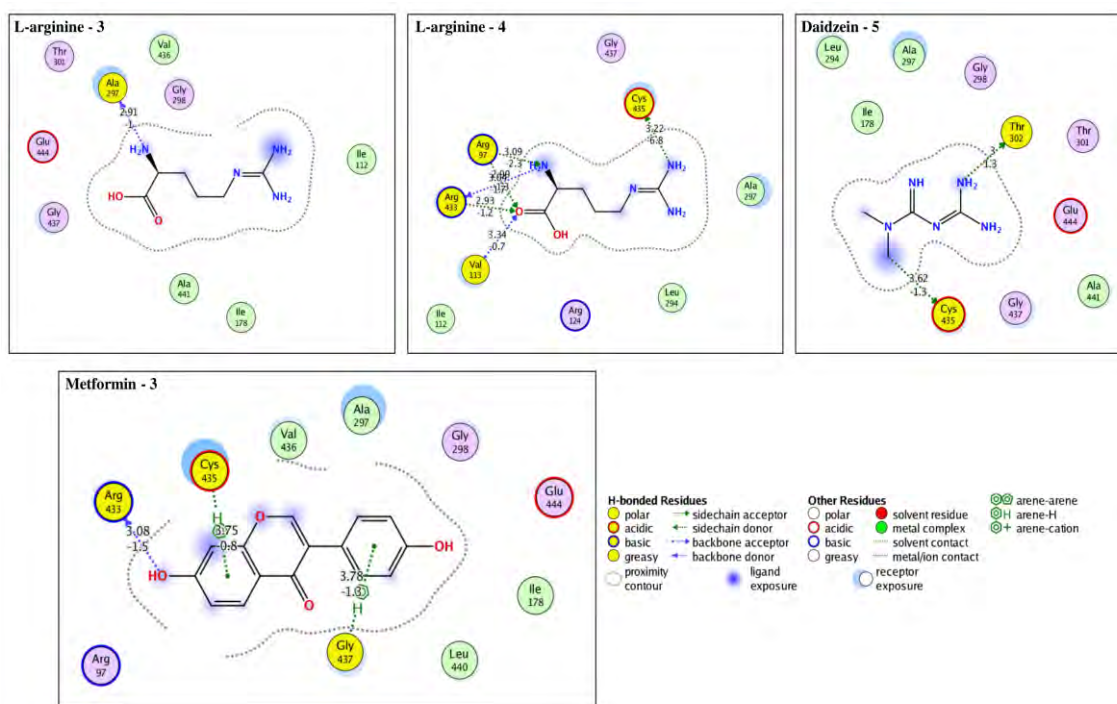


Figure 3.9: 2D interaction profiles of different poses of L-arginine, Daidzein, and Metformin (Control) with CYP2C19 protein. The ligands are present in the centre whereas the protein's surrounding amino acids are present around them. The amino acids shown in yellow are involved in direct molecular interaction with the ligands. The numbers represent the docking pose for each interaction.

Table 3.6: Molecular docking energy scores (indicated as *S*) of target compounds with the three common proteins.

Ligands	Poses	Energy
CYP1A2		
Daidzein - <chem>O=C1C(c2ccc(O)cc2)=COc2c1ccc(O)c2</chem>	1	-6.78727
	2	-6.71767
	3	-6.35044
	4	-6.29579
	5	-6.29216
L-Arginine - <chem>O=C(O)[C@@H](N)CCC/N=C(N)/N</chem>	1	-5.68231
	2	-5.51145
	3	-5.42317
	4	-5.41298
	5	-5.32958
Metformin - <chem>N(C)C(N)C(=N)N</chem>	1	-5.31141
	2	-5.24249
	3	-5.17449
	4	-5.17066
	5	-5.09862
CYP2C19		
Metformin - <chem>N(C)C(N)C(=N)N</chem>	1	-5.08931
	2	-4.88484
	3	-4.88281
	4	-4.78904
	5	-4.58654
L-Arginine - <chem>O=C(O)[C@@H](N)CCC/N=C(N)/N</chem>	1	-5.7561
	2	-5.56947
	3	-5.39879
	4	-5.18215
	5	-5.15937
Daidzein - <chem>O=C1C(c2ccc(O)cc2)=COc2c1ccc(O)c2</chem>	1	-6.55574
	2	-6.51544
	3	-6.38638
	4	-6.36012
	5	-6.21629
NFKB-1		
Metformin - <chem>N(C)C(N)C(=N)N</chem>	1	-4.50871
	2	-3.22173
	3	-3.07811
	4	-3.01871
	5	-2.90027

<i>L</i> -Arginine - <chem>O=C(O)[C@@H](N)CCC/N=C(N)/N</chem>	1	-4.97617
	2	-4.69486
	3	-4.57247
	4	-4.28701
	5	-4.24928
<i>Daidzein</i> - <chem>O=C1C(c2ccc(O)cc2)=COc2c1ccc(O)c2</chem>	1	4.738304
	2	6.864085
	3	7.248343
	4	8.795058
	5	9.027375

The narrative continues in Figure 3.9, where Daidzein and Metformin partake in singular sidechain hydrogen bonding instances with CYP2C19. At the same time, *L*-arginine engaged in multiple sidechain and backbone hydrogen bonding interactions in two out of five poses, affirming its enhanced promise.

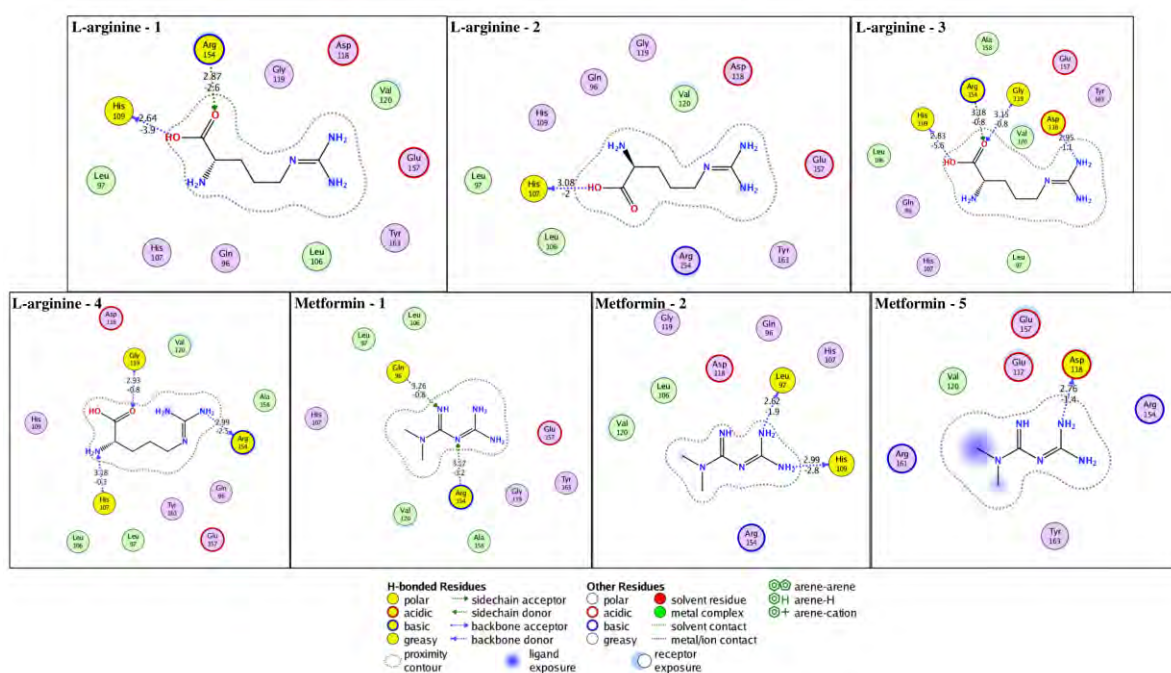


Figure 3.10: 2D interaction profiles of different poses of *L*-arginine, Daidzein, and Metformin (Control) with NFKB1 protein. The ligands are present in the centre whereas the protein's surrounding amino acids are present around them. The amino acids shown in yellow are involved in direct molecular interaction with the ligands. The numbers represent the docking pose for each interaction.

Finally, Figure 3.10 casts the spotlight on NFkB-1 interactions, portraying Daidzein's absence of engagement, Metformin's intermittent interactions in three poses, and the resolute predominance of L-arginine, orchestrating multiple hydrogen bondings in four out of five poses, reinforcing its elevated potency. Collectively, L-arginine emerged as a notably potent compound, poised to orchestrate intricate interactions that confer significant therapeutic implications.

3.4 ADMET Profiles of the Target Compounds

The completion of our network pharmacology investigation entails an assessment of Absorption, Distribution, Metabolism, Excretion, and Toxicity (ADMET) attributes gleaned through ADMETLab 2.0 analyses, thereby furnishing a comprehensive insight into the pharmacological potential of the compounds under study. Table 3.7 encapsulates the findings, providing a detailed perspective on the compounds' ADMET profiles. According to these analyses, Daidzein is commendably acceptable in 6 out of 8 medicinal chemistry analyses, albeit bearing a sole alert pertinent to thiol-reactive compounds. In stark contrast, L-arginine garners broader acclaim, rendering acceptability in 5 out of 8 analyses, notably without alarms.

Table 3.7: ADMET profiles of the target compounds of *Trigonella foenum-graecum*. The green sphere indicates favorable results, whereas spheres in red indicate non-favorable outcomes.

1. Physicochemical Property			
Property	Value Daidzein	Value L-arginine	Comment
<i>Molecular Weight</i>	254.06	174.11	Contain hydrogen atoms. Optimal:100~600
<i>Volume</i>	256.396	168.627	Van der Waals volume
<i>Density</i>	0.991	1.033	Density = MW / Volume
<i>nHA</i>	4	6	Number of hydrogen bond acceptors. Optimal:0~12
<i>nHD</i>	2	7	Number of hydrogen bond donors. Optimal:0~7
<i>nRot</i>	1	6	Number of rotatable bonds. Optimal:0~11
<i>nRing</i>	3	0	Number of rings. Optimal:0~6
<i>MaxRing</i>	10	0	Number of atoms in the biggest ring. Optimal:0~18
<i>nHet</i>	4	6	Number of heteroatoms. Optimal:1~15
<i>fChar</i>	0	0	Formal charge. Optimal:-4 ~4
<i>nRig</i>	18	2	Number of rigid bonds. Optimal:0~30
<i>Flexibility</i>	0.056	3.0	Flexibility = nRot /nRig
<i>Stereo Centers</i>	0	1	Optimal: ≤ 2
<i>TPSA</i>	70.67	125.22	Topological Polar Surface Area. Optimal:0~140

<i>logS</i>	-3.464	-1.286	Log of the aqueous solubility. Optimal: -4~-0.5 log mol/L		
<i>logP</i>	2.795	-3.533	Log of the octanol/water partition coefficient. Optimal: 0~3		
<i>logD</i>	2.626	-1.232	logP at physiological pH 7.4. Optimal: 1~3		
2. Medicinal Chemistry					
Property	Value Daidzein	Value L-arginine	Decision for Daidzein	Decision for L-Arginine	Comment
<i>QED</i>	0.7	0.2	●	●	A measure of drug-likeness based on the concept of desirability; Attractive: > 0.67; unattractive: 0.49~0.67; too complex: < 0.34
<i>SAscore</i>	2.071	2.774	●	●	Synthetic accessibility score is designed to estimate ease of synthesis of drug-like molecules. $SAscore \geq 6$, difficult to synthesize; $SAscore < 6$, easy to synthesize
<i>Fsp3</i>	0.0	0.667	●	●	The number of sp ³ hybridized carbons / total carbon count, correlating with melting point and solubility. $Fsp3 \geq 0.42$ is considered a suitable value.
<i>MCE-18</i>	16.0	3.0	●	●	MCE-18 stands for medicinal chemistry evolution. $MCE-18 \geq 45$ is considered a suitable value.
<i>NPscore</i>	0.83	1.027	-	-	Natural product-likeness score. This score is typically in the range from -5 to 5. The higher the score is, the higher the probability is that the molecule is a NP.
<i>Lipinski Rule</i>	Accepted	Accepted	●	●	$MW \leq 500$; $\log P \leq 5$; $Hacc \leq 10$; $Hdon \leq 5$. If two properties are out of range, poor absorption or permeability is possible, one is acceptable.

<i>Pfizer Rule</i>	Accepted	Accepted	●	●	logP > 3; TPSA < 75. Compounds with a high log P (>3) and low TPSA (<75) are likely to be toxic.
<i>GSK Rule</i>	Accepted	Accepted	●	●	MW ≤ 400; logP ≤ 4. Compounds satisfying the GSK rule may have a more favorable ADMET profile
<i>Golden Triangle</i>	Accepted	Rejected	●	●	200 ≤ MW ≤ 50; -2 ≤ logD ≤ 5. Compounds satisfying the Golden Triangle rule may have a more favorable ADMET profile.
<i>PAINS</i>	0 alerts	0 alerts	-	-	Pan Assay Interference Compounds, frequent hitters. Alpha-screen artifacts and reactive compound.
<i>ALARM NMR</i>	2 alerts	0 alerts	-	-	Thiol reactive compounds.
<i>BMS</i>	0 alerts	0 alerts	-	-	Undesirable, reactive compounds.
<i>Chelator Rule</i>	0 alerts	0 alerts	-	-	Chelating compounds.

3. Absorption

Property	Value Daidzein	Value L-arginine	Decision for Daidzein	Decision for L-arginine	Comment
<i>Caco-2 Permeability</i>	-4.643	-6.335	●	●	Optimal: higher than -5.15 Log unit
<i>MDCK Permeability</i>	1.2E-05	0.003066	●	●	low permeability: < 2 × 10 ⁻⁶ cm/s, medium permeability: 2–20 × 10 ⁻⁶ cm/s, high passive permeability: > 20 × 10 ⁻⁶ cm/s
<i>Pgp-inhibitor</i>	0.006	0.001	●	●	Category 1: Inhibitor; Category 0: Non-inhibitor. The output value is the probability of being Pgp-inhibitor
<i>Pgp-substrate</i>	0.937	0.988	●	●	Category 1: substrate; Category 0: Non-substrate. The output value is the probability of not being Pgp-substrate
<i>HIA</i>	0.008	0.033	●	●	Human Intestinal Absorption. Category 1: HIA+(HIA < 30%); Category 0: HIA-(HIA < 30%); The

					output value is the probability of being HIA+
$F_{20\%}$	0.23	0.011	●	●	20% Bioavailability. Category 1: F20%+ (bioavailability < 20%); Category 0: F20%- (bioavailability ≥ 20%); The output value is the probability of being F20%+
$F_{30\%}$	0.856	0.267	●	●	30% Bioavailability. Category 1: F30%+ (bioavailability < 30%); Category 0: F30%- (bioavailability ≥ 30%); The output value is the probability of not being F30%+

4. Distribution

Property	Value Daidzein	Value L-arginine	Decision for Daidzein	Decision for L-arginine	Comment
<i>PPB</i>	97.07%	6.073%	●	●	Plasma Protein Binding. Optimal: < 90%. Drugs with high protein-bound may have a low therapeutic index.
<i>VD</i>	0.495	0.677	●	●	Volume Distribution. Optimal: 0.04-20L/kg
<i>BBB Penetration</i>	0.054	0.538	●	●	Blood-Brain Barrier Penetration. Category 1: BBB+; Category 0: BBB-; The output value is the probability of being BBB+
<i>Fu</i>	1.960%	89.58%	●	●	The fraction unbound in plasms. Low: <5%; Middle: 5~20%; High: > 20%

5. Metabolism

Property	Value Daidzein	Value L-arginine	Comment
<i>CYP1A2 inhibitor</i>	0.976	0.004	-
<i>CYP1A2 substrate</i>	0.127	0.025	-
<i>CYP2C19 inhibitor</i>	0.808	0.031	-
<i>CYP2C19 substrate</i>	0.054	0.049	-
<i>CYP2C9 inhibitor</i>	0.375	0.015	-
<i>CYP2C9 substrate</i>	0.945	0.05	-
<i>CYP2D6 inhibitor</i>	0.929	0.012	-
<i>CYP2D6 substrate</i>	0.89	0.252	-

<i>CYP3A4 inhibitor</i>	0.908	0.003	-
<i>CYP3A4 substrate</i>	0.173	0.008	-

6. Excretion

Property	Value Daidzein	Value L-arginine	Decision for Daidzein	Decision for L-arginine	Comment
<i>CL</i>	7.802	5.289	●	●	Clearance. High: >15 mL/min/kg; moderate: 5-15 mL/min/kg; low: <5 mL/min/kg
<i>t_{1/2}</i>	0.846	0.614	-	-	Category 1: long half-life; Category 0: short half-life; long half-life: >3h; short half-life: <3h. The output value is the probability of having long half-life.

7. Toxicity

Property	Value Daidzein	Value L-arginine	Decision for Daidzein	Decision for L-arginine	Comment
<i>hERG Blockers</i>	0.072	0.066	●	●	Category 1: active; Category 0: inactive; The output value is the probability of being active.
<i>H-HT</i>	0.053	0.031	●	●	Human Hepatotoxicity. Category 1: H-HT positive(+); Category 0: H-HT negative(-); The output value is the probability of being toxic.
<i>DILI</i>	0.52	0.015	●	●	Drug Induced Liver Injury. Category 1: drugs with a high risk of DILI; Category 0: drugs with no risk of DILI. The output value is the probability of being toxic.
<i>AMES Toxicity</i>	0.061	0.024	●	●	Category 1: Ames positive(+); Category 0: Ames negative(-); The output value is the probability of being toxic.
<i>Rat Oral Acute Toxicity</i>	0.333	0.074	●	●	Category 0: low-toxicity; Category 1: high-toxicity; The output value is the probability of being highly toxic.

<i>FDAMDD</i>	0.188	0.016	●	●	Maximum Recommended Daily Dose Category 1: FDAMDD (+); Category 0: FDAMDD (-). The output value is the probability of being positive.
<i>Skin Sensitization</i>	0.895	0.527	●	●	Category 1: Sensitizer; Category 0: Non-sensitizer; The output value is the probability of being sensitizer.
<i>Carcinogenicity</i>	0.617	0.072	●	●	Category 1: carcinogens; Category 0: non-carcinogens; The output value is the probability of being toxic.
<i>Eye Corrosion</i>	0.019	0.003	●	●	Category 1: corrosives ; Category 0: noncorrosives. The output value is the probability of being corrosives.
<i>Eye Irritation</i>	0.97	0.038	●	●	Category 1: irritants ; Category 0: nonirritants. The output value is the probability of being irritants.
<i>Respiratory Toxicity</i>	0.101	0.294	●	●	Category 1: respiratory toxicants; Category 0: respiratory nontoxicants. The output value is the probability of being toxic.

8. Environmental Toxicity

Property	Value Daidzein	Value L-arginine	Comment
<i>Bioconcentration Factors</i>	1.133	-0.084	Bioconcentration factors are used for considering secondary poisoning potential and assessing risks to human health via the food chain. The unit is $-\log_{10}[(\text{mg/L})/(1000 \cdot \text{MW})]$
<i>IGC₅₀</i>	4.838	2.294	<i>Tetrahymena pyriformis</i> 50 percent growth inhibition concentration. The unit is $-\log_{10}[(\text{mg/L})/(1000 \cdot \text{MW})]$
<i>LC_{50FM}</i>	5.43	2.836	96-hour fathead minnow 50 percent lethal concentration. The unit is $-\log_{10}[(\text{mg/L})/(1000 \cdot \text{MW})]$
<i>LC_{50DM}</i>	5.626	3.179	48-hour daphnia magna 50 percent lethal concentration. The unit is $-\log_{10}[(\text{mg/L})/(1000 \cdot \text{MW})]$

9. Tox21 Pathway					
Property	Value Daidzein	Value L-arginine	Decision for Daidzein	Decision for L-arginine	Comment
<i>N+A9:F20R-AR</i>	0.721	0.021	●	●	Androgen receptor. Category 1: active; Category 0: inactive; The output value is the probability of being active.
<i>NR-AR-LBD</i>	0.35	0.002	●	●	Androgen receptor ligand-binding domain. Category 1: active; Category 0: inactive; The output value is the probability of being active.
<i>NR-AhR</i>	0.947	0.008	●	●	Aryl hydrocarbon receptor. Category 1: active; Category 0: inactive;. The output value is the probability of being active.
<i>NR-Aromatase</i>	0.732	0.004	●	●	Category 1: active; Category 0: inactive; The output value is the probability of being active.
<i>NR-ER</i>	0.991	0.143	●	●	Estrogen receptor. Category 1: active; Category 0: inactive; The output value is the probability of being active.
<i>NR-ER-LBD</i>	0.996	0.014	●	●	Estrogen receptor ligand-binding domain. Category 1: active; Category 0: inactive; The output value is the probability of being active.
<i>NR-PPAR-gamma</i>	0.058	0.003	●	●	Peroxisome proliferator-activated receptor gamma. Category 1: active; Category 0: inactive; The output value is the probability of being active.
<i>SR-ARE</i>	0.938	0.045	●	●	Antioxidant response element. Category 1: active; Category 0: inactive; The output

					value is the probability of being active.
<i>SR-ATAD5</i>	0.983	0.003	●	●	ATPase family AAA domain-containing protein 5. Category 1: active; Category 0: inactive; The output value is the probability of being active.
<i>SR-HSE</i>	0.781	0.003	●	●	Heat shock factor response element. Category 1: active; Category 0: inactive; The output value is the probability of being active.
<i>SR-MMP</i>	0.972	0.003	●	●	Mitochondrial membrane potential. Category 1: active; Category 0: inactive; The output value is the probability of being active.
<i>SR-p53</i>	0.881	0.007	●	●	Category 1: active; Category 0: inactive; The output value is the probability of being active.

10. Toxicophore Rules

Property	Value Daidzein	Value L-arginine	Comment
<i>Acute Toxicity Rule</i>	0 alerts	0 alerts	20 substructures; acute toxicity during oral administration
<i>Genotoxic Carcinogenicity Rule</i>	0 alerts	0 alerts	117 substructures; carcinogenicity or mutagenicity
<i>NonGenotoxic Carcinogenicity Rule</i>	0 alerts	0 alerts	23 substructures; carcinogenicity through nongenotoxic mechanisms
<i>Skin Sensitization Rule</i>	0 alerts	0 alerts	155 substructures; skin irritation
<i>Aquatic Toxicity Rule</i>	0 alerts	0 alerts	99 substructures; toxicity to liquid(water)
<i>NonBiodegradable Rule</i>	0 alerts	0 alerts	19 substructures; non-biodegradable
<i>SureChEMBL Rule</i>	0 alerts	0 alerts	164 substructures; MedChem unfriendly status

The absorption analysis highlights favorable prospects for Daidzein and L-arginine, as evidenced by satisfactory outcomes in 5 out of 7 evaluations. Regarding distribution, L-arginine forges ahead, securing 3 out of 4 satisfactory results compared to Daidzein's

3.5 Seed Extract Preparation

The solution obtained from the filtration and sonication of fenugreek seeds exhibited a distinctive light yellow to golden hue (visualized in figure 3.12A), providing a visual confirmation of its origin from the seeds of the fenugreek plant. Subsequently, we screened the seed extract to confirm the presence of diverse phytochemical constituents inherent to fenugreek.

3.6 Seed Oil Preparation

The seed oil extracted from fenugreek using the Soxhlet extraction method manifested a coloration ranging from dark yellow to a subdued golden hue, as shown in figure 3.12B. This coloration of the collected seed oil indicates its composition and origin. The harvested seed oil was preserved for subsequent analysis to synthesize and characterize lipid-based nanoparticles. This analysis was conducted in conjunction with evaluating phytochemical constituents from the methanolic seed extract of fenugreek.



Figure 3.12: Processing of *Trigonella foenum-graecum*; A. Seed extract; B. Oil Extract

3.7 Phytochemical Screening

3.7.1 Wagner's Test

The examination employing Wagner's reagent revealed the presence of alkaloids in both fenugreek seeds and oil extract. It was substantiated by the formation of a distinct reddish-brown coloration upon reaction.

3.7.2 Foam Test

The foam test implementation emphasized saponins' existence in both fenugreek seeds and the extracted oil. The generation of a persistent foam substantiated this observation upon rigorous agitation and gentle heating of the seed and oil extracts with distilled water.

3.7.3 Ferric Chloride Test

The manifestation of a discernible blue-green coloration after the ferric chloride test provided definitive evidence of phenolic compounds in both fenugreek seed and oil extracts.

3.7.4 Braymer's Test

The absence of green precipitates in response to Braymer's test effectively indicated the non-occurrence of tannins within both the fenugreek seed and oil extracts.

Table 3.8: *Phytochemical screening of seed and oil extracts in fenugreek.*

Sr #.	Screening Test	Screened Phytochemical	Inference	Result	
				Extract	Oil
1.	Wagner's Test	Alkaloids	Appearance of reddish brown color with Wagner's reagent	+++	+++
2.	Foam Test	Saponins	Formation of stable foam	+++	+++
3.	Ferric Chloride Test	Phenols	Indication of blue green color with ferric chloride	+++	+++
4.	Braymer's Test	Tannins	Formation of green precipitates	---	---
5.	Salkowski's Test	Terpenoids	Appearance of yellow color	---	---
6.	Bontrager's Test	Quinones	Occurrence of red color in alkaline phase	+++	+++
7.	Keller Killani's Test	Cardiac Glycosides	Formation of pink to blood red coloration	---	---
8.	Glycosides Test	Glycosides	Indication of pink color	+++	+++
9.	Alkaline Reagent Test	Flavonoids	Formation of yellow color which becomes colorless on addition of acid	+++	+++
10.	Precipitate Test	Phlobatannins	Appearance of red precipitates	---	---

3.7.5 Salkowski's Test

The non-appearance of yellow coloration in the Salkowski's Test indicated the absence of terpenoids in both the fenugreek seed and oil extracts.

3.7.6 Bontrager's Test

Identifying a red color in the alkaline phase of Bontrager's test provided conclusive affirmation of the presence of quinones in the derived tincture of fenugreek seed and oil.

3.7.7 Keller-Killian's Test

The lack of pink, red, or blood-red coloration in response to Keller-Killian's test excluded the presence of cardiac glycosides in the fenugreek seed and oil extracts.

3.7.8 Glycosides Test

The glycosides test yielded a pink coloration, serving as a clear indication of the presence of glycoside phytochemicals in the extracted fenugreek seed and oil.

3.7.9 Alkaline Reagent Test

The emergence of a fading yellow color transitioning to colorlessness upon acid introduction validated the presence of flavonoids. This analytical procedure employing an alkaline reagent was employed on fenugreek seed and oil extracts.

3.7.10 Precipitate Test

The absence of a red color precipitate definitively ascertained the absence of phlobatannin phytochemicals within the fenugreek seed and oil extracts.

3.8 Evaluation of Total Flavonoid Content

Flavonoid concentration in the fenugreek seed and oil extracts was quantified using the formula. The calculated concentrations were 285 mg/g (seed extract) and 225 mg/g (oil extract) in a solvent volume of 100 ml. Both extracts shared an equivalent dry weight of 20 g. The comparatively higher flavonoid concentration in the fenugreek seed extract (285 mg/g) than the oil extract (225 mg/g) implies that the seeds could serve as a richer source of these valuable phytochemicals. Moreover, these findings provide a foundation for exploring the potential health benefits of fenugreek extracts, where the variation in flavonoid concentrations might contribute to varying degrees of biological activity.

3.9 Evaluation of Total Phenolic Content

The determined phenolic content within the extracts derived from fenugreek seeds and oil yielded 335 mg/g and 195 mg/g, respectively, in a solvent volume of 100 ml. Both extracts were formulated using an identical dry weight of 20 g. These findings hold significant implications for the compositional richness of fenugreek extracts. Phenolic compounds, renowned for their diverse biological activities, encompass antioxidant, anti-inflammatory, and potential health-promoting attributes. The substantial difference in phenolic content between the fenugreek seed extract (335 mg/g) and the oil extract (195 mg/g) underscores the differential distribution of these bioactive compounds within the various parts of the fenugreek plant. Such variations in phenolic content could contribute to the functional properties attributed to the extracts.

3.10 Synthesis of Lipid Nanoparticles

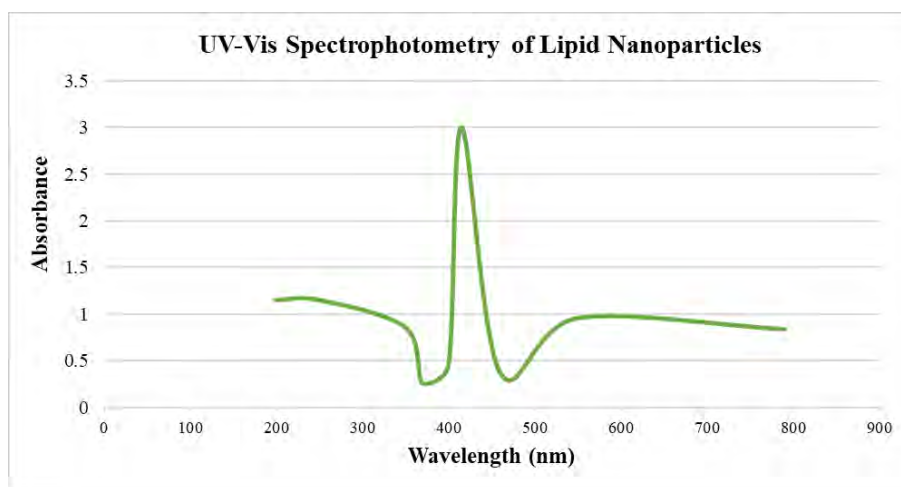


Figure 3.13: UV-visible spectroscopy for synthesized lipid nanoparticles showing maximum peak at 415 nm using oil extract of fenugreek seeds as precursor with methanolic seed extract at 1:1.

No palpable color alteration was noted throughout the lipid nanoparticle synthesis process. Nevertheless, using a UV-VIS spectrophotometer, the successful synthesis of lipid nanoparticles was validated by employing surface plasmon resonance analysis, specifically at a wavelength of 415 nm. This approach provided a reliable means to confirm the attainment of lipid nanoparticles with the anticipated properties.

3.11 Encapsulation of L-Arginine in Lipid Nanoparticles

Upon the introduction of L-arginine to the lipid nanoparticle formulation, a subtle alteration in coloration was perceptible, transitioning from a golden yellow shade to a lime yellow hue. However, the product exhibited a light greenish tint after desiccating the L-arginine encapsulated lipid nanoparticles. A variety of characterization techniques were employed to comprehensively ascertain the physiochemical attributes of the L-arginine encapsulated lipid nanoparticles. These methodologies allowed for an in-depth understanding of the nanoparticle's properties, which included but were not limited to, size distribution, morphology, surface chemistry, and encapsulation efficiency.

3.12 Characterization of Encapsulated Nanoparticles

3.12.1 UV-VIS Spectrophotometry

The UV-Vis spectroscopic analysis revealed a prominent light absorbance peak for the L-arginine encapsulated lipid nanoparticles at a specific wavelength of 521 nm, as depicted in Figure 3.14.

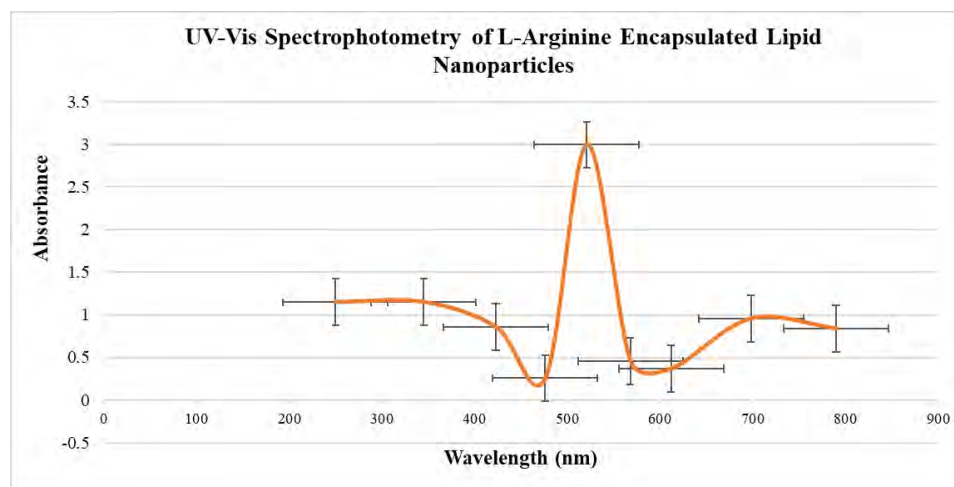


Figure 3.14: UV visible spectroscopy for synthesized L-arginine encapsulated lipid nanoparticles showing maximum absorbance at 521 nm.

Additionally, it was observed that this absorbance value was subject to variation based on the incubation duration, and prolonged incubation periods resulted in a detectable

elevation of absorbance at the designated wavelength. This relationship between absorbance and incubation time highlights the temporal influence on the optical properties of the L-arginine encapsulated lipid nanoparticles.

3.12.2 Scanning Electron Microscopy

The surface morphology and particle dimensions of the L-arginine encapsulated lipid nanoparticles were examined through scanning electron microscopy (SEM). An illustrative scanning electron micrograph depicted the nanoparticles possessing a spherical configuration. Moreover, employing image analysis software like Image J, the average particle size was quantified at approximately 100.2 nm (Figure 3.15). This microscopy-based investigation enabled a comprehensive understanding of the nanoparticles' physical attributes, precisely elucidating their morphology and size distribution.

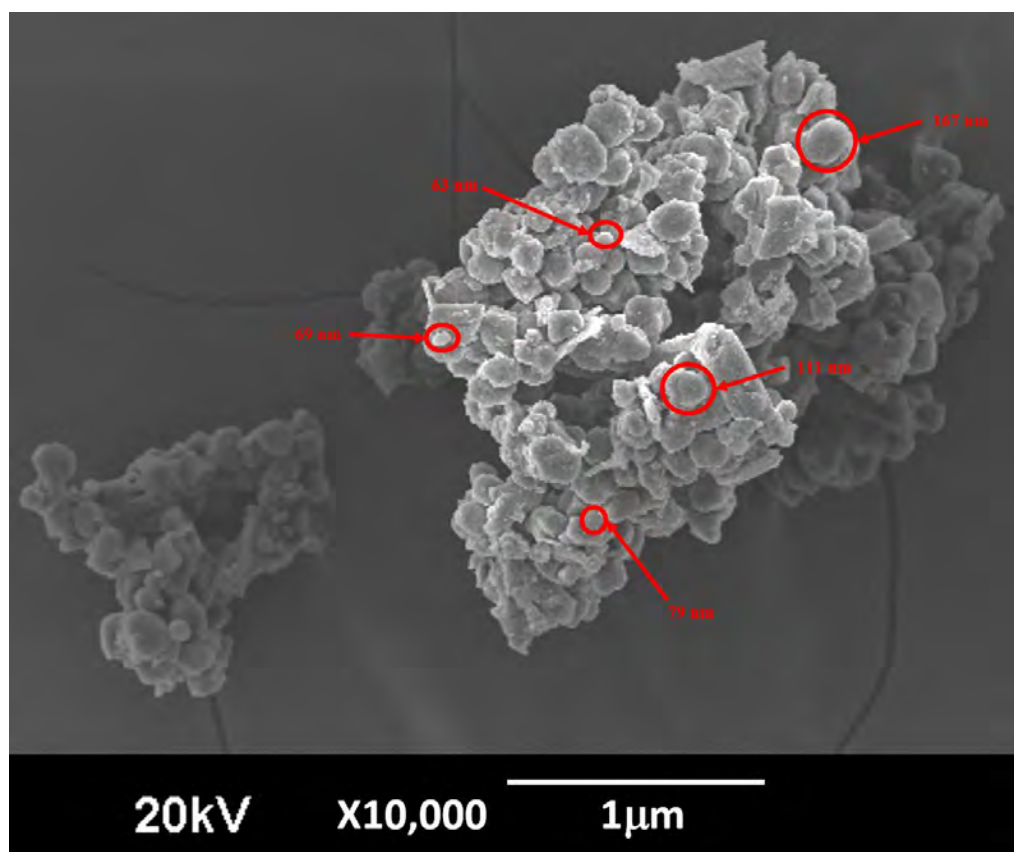


Figure 3.15: SEM micrograph of L-arginine encapsulated lipid nanoparticles synthesized by using seed and oil extract of fenugreek showing an average size of 100.2 nm at 10,000X and 1 micrometer known distance.

3.12.3 FTIR Analysis

The FTIR spectra revealed a spectrum of functional groups on the nanoparticle surface, contributing to its reduction and overall stability. An evident peak at 1007.72 cm^{-1} highlighted the presence of symmetrical and asymmetrical C–O vibrational stretching, affirming the participation of these bonds in the nanoparticle's constitution (Figure 3.16). In addition, the FTIR analysis exhibited a peak at 1636.46 cm^{-1} , indicative of C=C bonds present in the sample. These peaks offered an understanding of the distinct chemical composition of the fenugreek seed extract, further establishing its unique role in the nanoparticle synthesis process. The FTIR chart was read according to the reference tables provided by Sigma-Aldrich, available at: <https://www.sigmaaldrich.com/PK/en/technical-documents/technical-article/analytical-chemistry/photometry-and-reflectometry/ir-spectrum-table>.

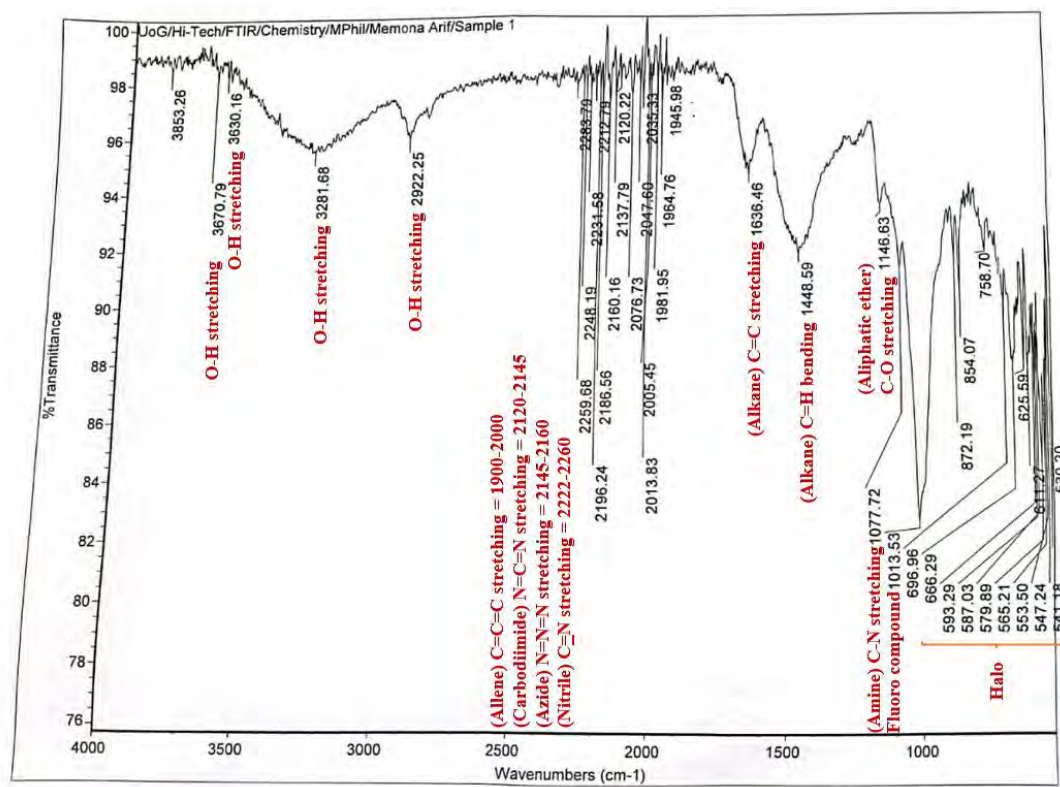


Figure 3.16: FTIR analysis of L-arginine encapsulated lipid nanoparticles.

The depiction of these functional groups, substantiated by FTIR analysis, assumes paramount importance as they act as capping and reducing agents. Originating from the

fenugreek seed extract, these functional groups collectively contribute to stabilizing and effectively reducing the L-arginine encapsulated lipid nanoparticles.

3.12.4 EDX Analysis

The EDX analysis (Figure 3.17) systematically identified and quantified the elemental constituents, revealing a composition predominantly carbon, oxygen, nitrogen, and hydrogen. The outcomes establish the nanoparticles' elemental composition, summarized in Table 3.9.

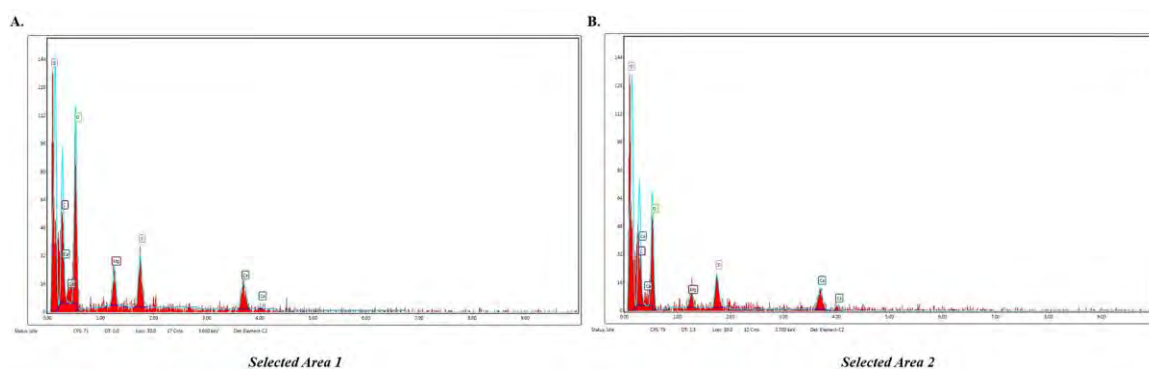


Figure 3.17: EDX analysis showing graphical representation of the elements present in L-arginine encapsulated lipid nanoparticles.

The elemental profiling through EDX analysis provides a critical understanding of the nanoparticles' constituent components, thereby contributing to a comprehensive understanding of their chemical makeup and potential functional attributes.

Table 3.9: Elemental Composition of L-arginine encapsulated lipid nanoparticles

Element	Selected Area 1		Selected Area 2	
	Weight (%)	Atomic (%)	Weight (%)	Atomic (%)
C K	30.64	40.56	33.45	44.42
O K	48.43	30.98	45.11	44.97
M K	4.94	10.42	3.92	2.57
Si K	6.58	18.04	6.28	3.57
CaK	9.4	3.75	11.23	4.47

3.12.5 Particle Size Distribution Analyzer

The results of the size distribution analysis indicate that the average size of the synthesized arginine-encapsulated lipid nanoparticles (NPs) is approximately 100 nm, as

illustrated in Figure 3.18. This hydrodynamic size encompasses the hydration layer on the NP surface, leading to a measurement typically larger than the dimensions obtained from scanning electron microscopy (SEM) images. Furthermore, it is noteworthy that the presence of phytochemicals within the seed extract could also influence the hydrodynamic size measurement. Nanoparticle sizes falling below 150 nm are suitable for cellular uptake, which indicates that our synthesized and encapsulated nanoparticles are fit for drug delivery.

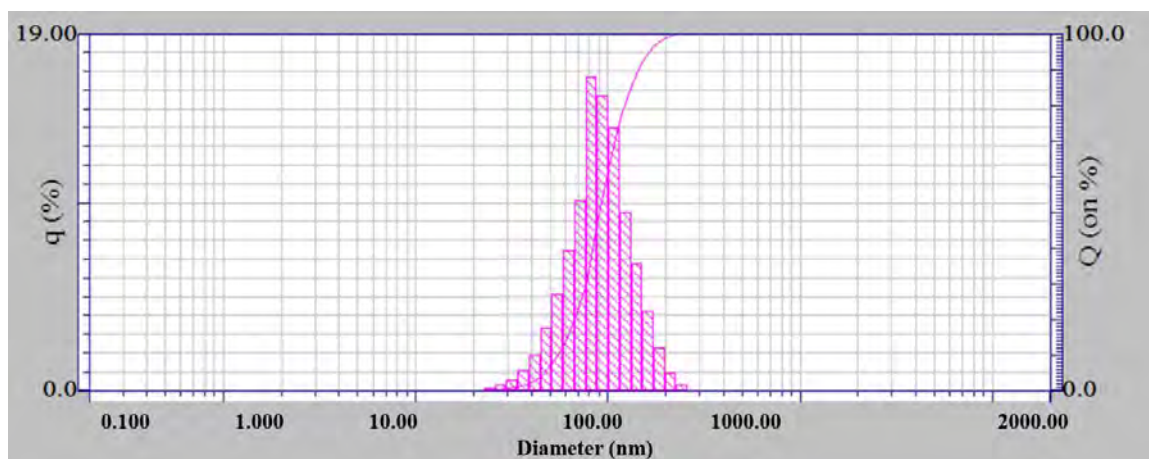


Figure 3.18: Size calculation of arginine-encapsulated lipid nanoparticles using PSD.

3.12.6 ζ -potential Analysis

The obtained ζ -potential value was recorded as -9.37 mV at a pH of 8.5, as depicted in Figure 3.19. Nanoparticles with zeta potentials ranging between -10 and +10 mV are generally classified as neutrally charged, whereas those with zeta potentials exceeding +30 mV or falling below -30 mV are considered strongly cationic and strongly anionic, respectively.

Given that most cellular membranes exhibit a negative charge, the zeta potential of nanoparticles can influence their ability to traverse these membranes, with cationic particles typically displaying a higher potential for cell wall disruption-associated toxicity. As a result, the observed zeta potential of our nanoparticles suggests an enhanced affinity for cellular membranes, as indicated by the findings.

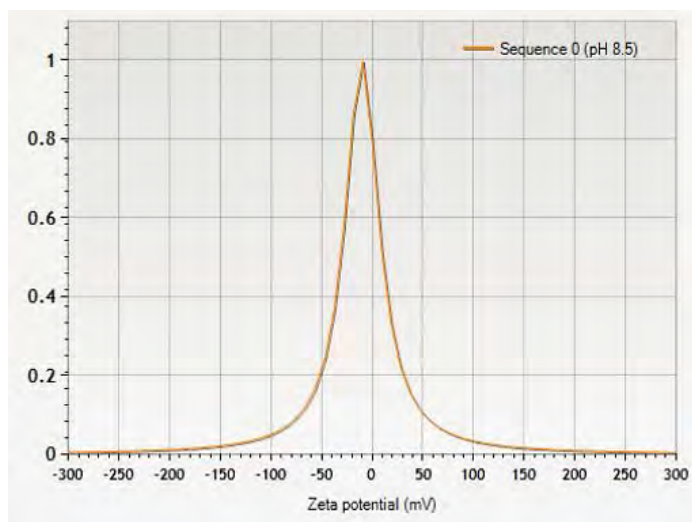


Figure 3.19: The calculated ζ -potential of the arginine-encapsulated lipid nanoparticles.

3.12.7 XRD Analysis

The X-ray Diffraction (XRD) analysis, illustrated in Figure 3.20, revealed distinctive humped peaks indicative of short-range ordering within the nanoparticles. Nonetheless, a subset of well-defined sharp peaks, notably at 44° (2theta), was also clear. This observation indicates the predominant amorphous character of the nanoparticles, punctuated by a subtle semblance of semi-crystalline attributes.

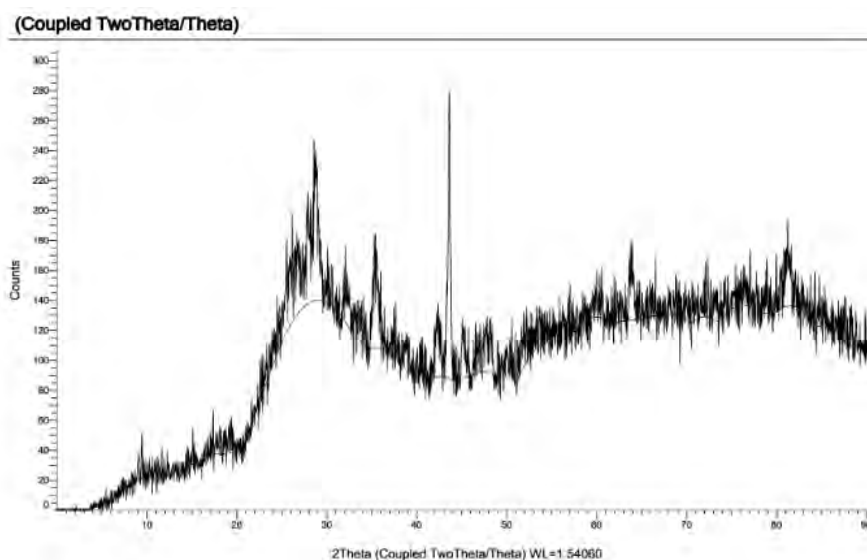


Figure 3.20: XRD graph of arginine-encapsulated lipid nanoparticles indicating their amorphous to semi-crystalline nature.

3.13 Biopotential Analysis of the Encapsulated Nanoparticles

3.13.1 Anti-Oxidant Activity

Compared with conventional antidiabetic medications, the lipid nanoparticles encapsulating L-arginine exhibited enunciated antioxidant characteristics upon interaction with the DPPH radical. This interaction was substantiated by the noticeable reduction in DPPH radical absorbance at 517 nm, indicative of effective radical scavenging activity. It signifies the nanoparticles' capability to counteract deleterious free radicals, a key attribute in mitigating the oxidative stress often inherent in diabetes.

The lipid nanoparticles encapsulating L-arginine displayed significant antioxidant potential at the 500 $\mu\text{g}/\text{mL}$ maximal concentration. Their antioxidative efficacy attained a remarkable magnitude of 84.44% and an IC_{50} value of 40.5. Notably, these values surpassed those observed for the control (62.84%: IC_{50} -231.27), fenugreek seed extract (59.73%: 208.98), and oil extract (61.03%: 196.6), as depicted in Figures 3.21 and 3.22. It highlighted the nanoparticles' proficiency in radical scavenging, a quality potentially attributed to their specific composition and the presence of L-arginine.

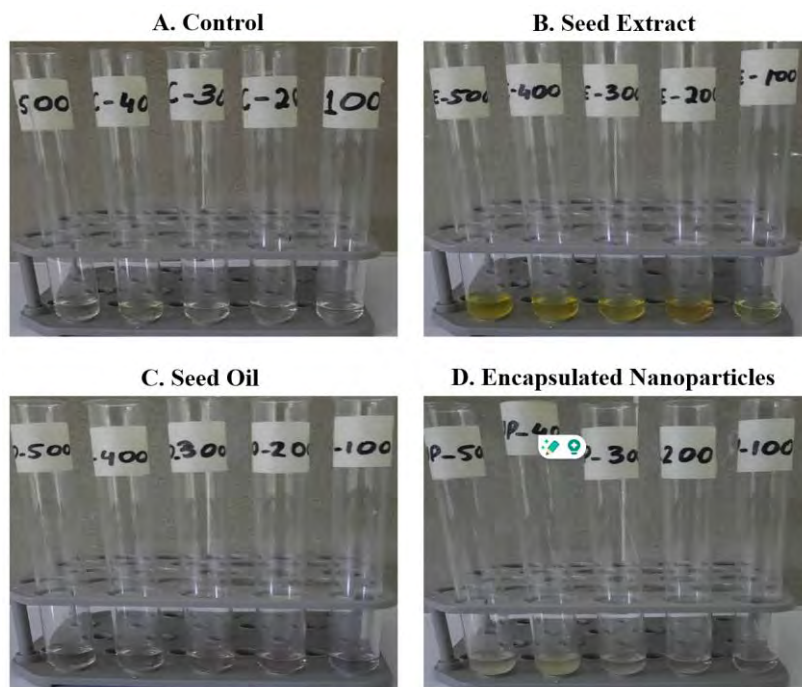


Figure 3.21: Experimental overview of anti-oxidant activity; A. Control; B. Seed Extract; C. Seed Oil, and D. Nanoparticles; all, at concentrations of 100 g/mL, 200 g/mL, 300 g/mL, 400 g/mL, and 500 g/mL.

In contrast, while conventional antidiabetic agents predominantly concentrate on modulating blood glucose levels and enhancing insulin sensitivity, the antioxidative attributes inherent to the lipid nanoparticles incorporating L-arginine offer additional potential advantages.

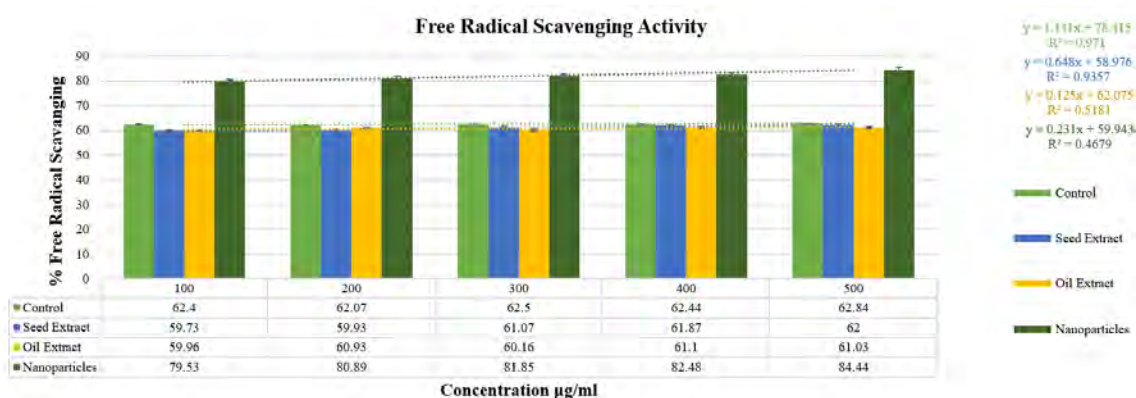


Figure 3.22: Percentage of free radical scavenging by the control, seed extract, oil extract, and L-arginine-encapsulated lipid nanoparticles at various concentrations.

Given that oxidative stress is a prominent contributor to the complications associated with diabetes, including cardiovascular ailments and nerve impairments, the nanoparticles' capacity to combat radicals could complement the effects of antidiabetic medications by addressing the complications linked to oxidative stress.

3.13.2 Anti-Inflammatory Potential

Albumin, a fundamental protein intricately involved in numerous physiological processes, assumes a key role in assessing the biological potential of nanoparticles, especially those used for drug delivery. In the context of diabetes, the denaturation of albumin ensues due to escalated oxidative stress, consequently contributing to the progression of diabetic complications. Through their demonstrated capacity to impede albumin denaturation, the lipid nanoparticles encapsulating L-arginine manifest their potential to ameliorate diabetic complications and uphold overall well-being.

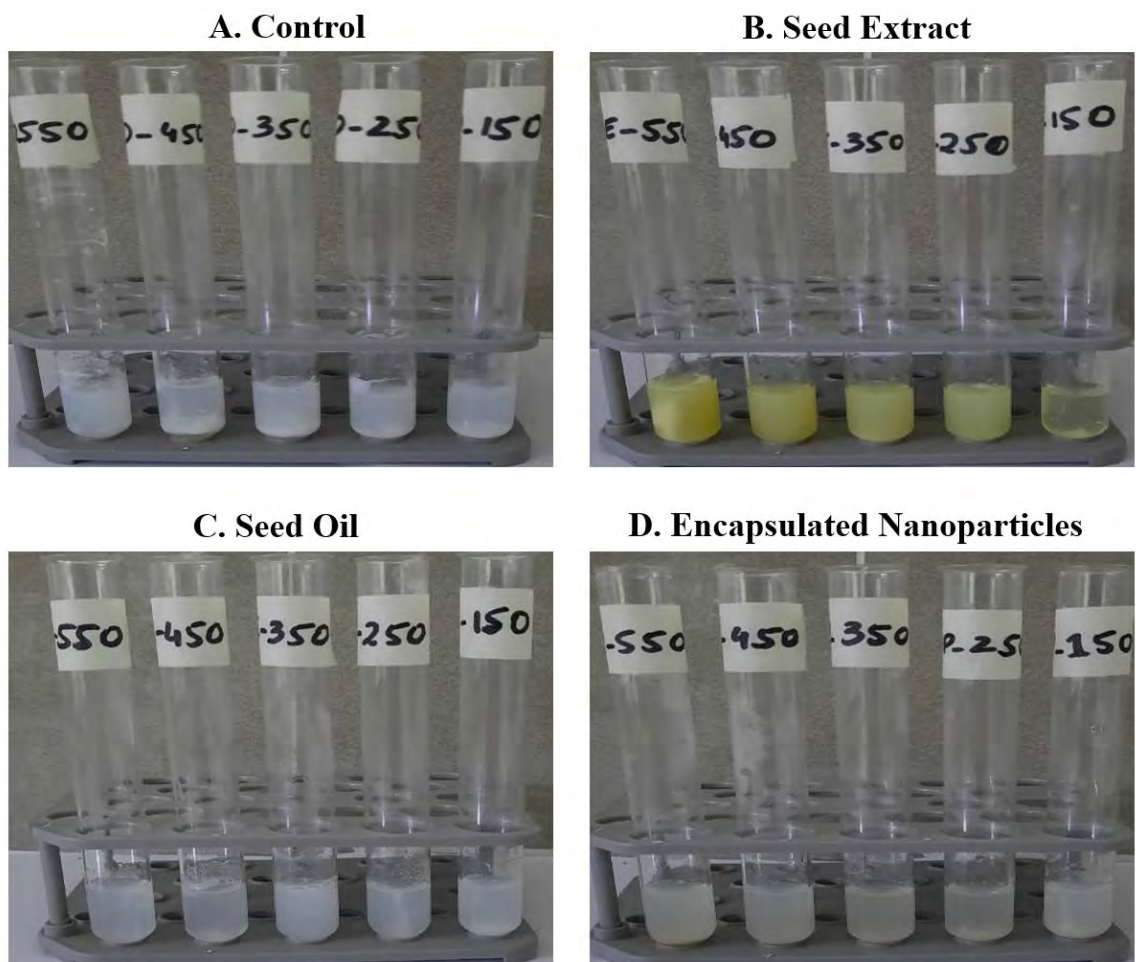


Figure 3.23: Experimental overview of anti-inflammatory activity; A. Control; B. Seed Extract; C. Seed Oil, and D. Nanoparticles; all, at concentrations of 150 g/mL, 250 g/mL, 350 g/mL, 450 g/mL, and 550 g/mL.

The investigation evaluated the proficiency of L-arginine encapsulated lipid nanoparticles in inhibiting albumin denaturation over varying concentrations (Figure 3.23). Notably, amidst these concentrations, a concentration of 550 $\mu\text{g/mL}$ exhibited an impressive 81.10% inhibition of albumin denaturation, in contrast to the control group (43.50%), seed extract (51.44%), and seed oil (31.63%), as depicted in Figure 3.24. It underlines the nanoparticles' remarkable efficacy in counteracting albumin protein denaturation, a consequence carrying consequential therapeutic implications.

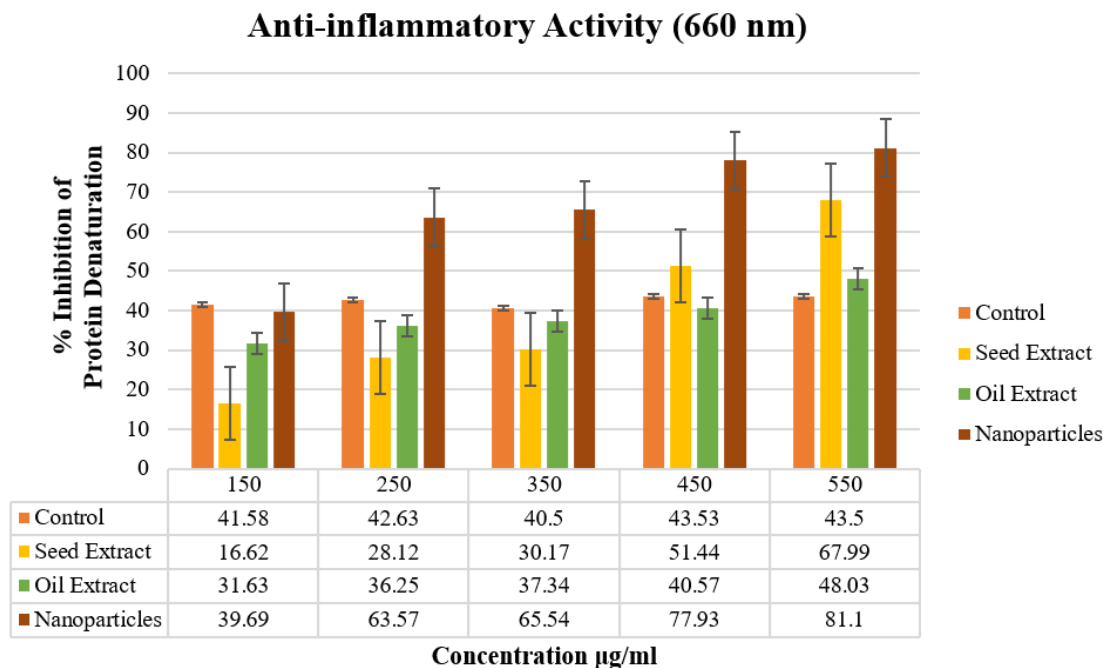


Figure 3.24: Percentage inhibition of albumin denaturation by the control, seed extract, oil extract, and L-arginine-encapsulated lipid nanoparticles at various concentrations.

3.13.3 Anti-Diabetic Activity

Alpha amylase, a key enzyme in carbohydrate breakdown, is critical in managing blood glucose levels. Inhibiting this enzyme stands as a fundamental strategy in this respect. The lipid nanoparticles encapsulating L-arginine, distinguished by their extraordinary potential to inhibit alpha-amylase, offer a promising avenue for regulating elevated postprandial blood glucose levels.

Remarkably, the observed inhibitory effect of the L-arginine encapsulated lipid nanoparticles exhibited a direct correlation with concentration (spanning from 200 $\mu\text{g/mL}$ to 1000 $\mu\text{g/mL}$), demonstrating a dose-dependent relationship, as shown in Figure 3.25. This dose-dependent behavior is integral to their role in combating diabetes, emphasizing the nanoparticles' consistent and progressive impact on curtailing alpha-amylase activity.

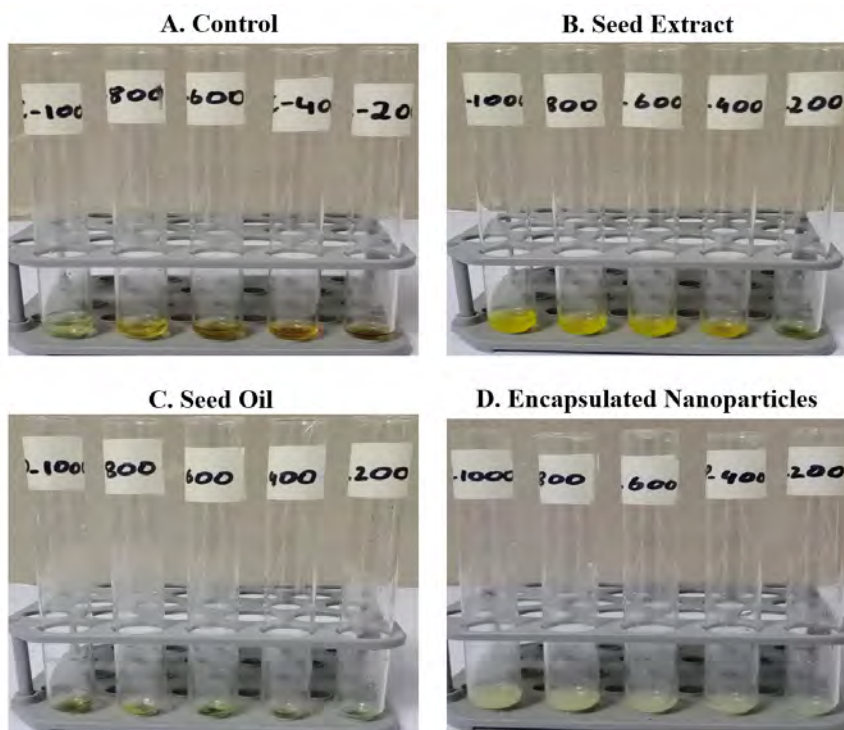


Figure 3.25: Experimental overview of anti-diabetic activity; A. Control; B. Seed Extract; C. Seed Oil, and D. Nanoparticles; all, at concentrations of 200 g/mL, 400 g/mL, 600 g/mL, 800 g/mL, and 1000 g/mL.

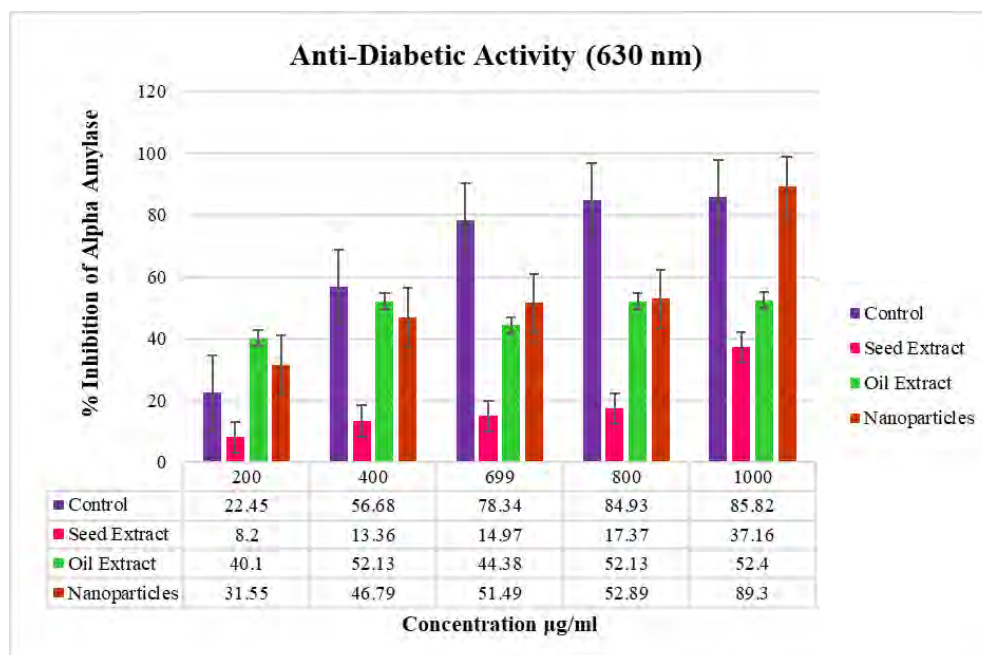


Figure 3.26: A graphic representation of the anti-diabetic effect demonstrates the percentage inhibition of the -amylase assay by the control, seed extract, oil extract, and L-arginine-encapsulated lipid nanoparticles at various concentrations.

Importantly, the alpha-amylase inhibition attributed to the L-arginine encapsulated lipid nanoparticles reached 89.30%, a significant finding when contrasted with metformin, a widely utilized antidiabetic medication. Metformin, at an equivalent dose (1000 $\mu\text{g/mL}$), achieved a maximum inhibition of 78.43%, as illustrated in Figure 3.26. This observation stresses the compelling potential of nanoparticles in terms of alpha-amylase inhibition, positioning them as a remarkable candidate in diabetes management strategies.

3.13.4 Hemolytic Activity

During the hemolytic testing, it was determined that the hemolytic activity of the L-arginine encapsulated lipid nanoparticles was contingent on their concentration. The considerable hemolysis percentage of 10.54% was particularly noteworthy, recorded at the highest concentration of 350 $\mu\text{g/mL}$ for the L-arginine encapsulated lipid nanoparticles (Figure 3.27). This value stands in stark contrast to the corresponding hemolysis percentages observed for the control (91.70%), fenugreek seed extract (39.17%), and fenugreek oil extract (46.08%), as depicted in Figure 3.28.

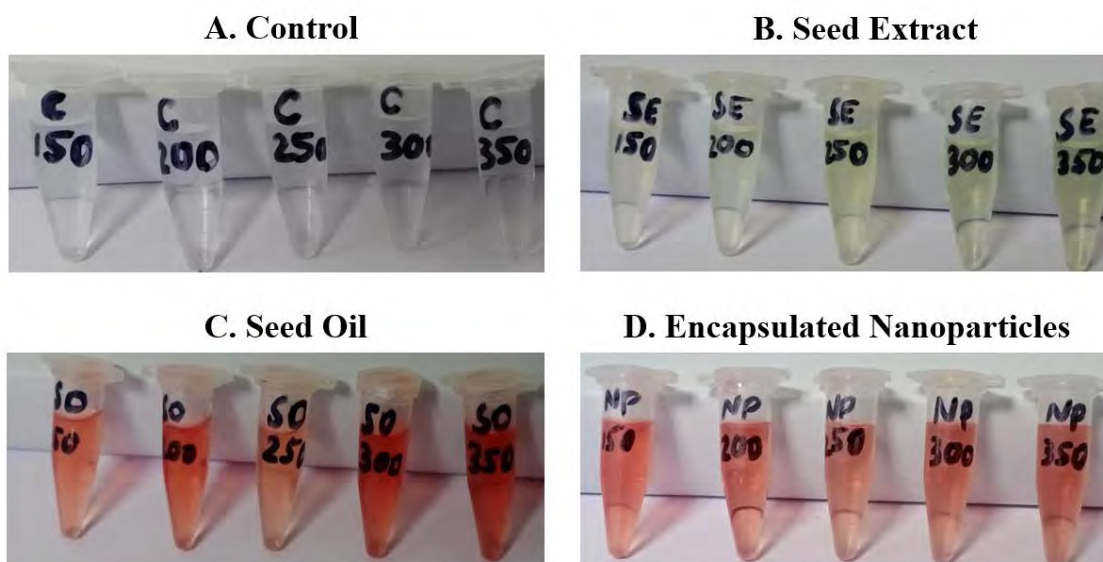


Figure 3.27: Experimental overview of hemolytic activity; A. Control; B. Seed Extract; C. Seed Oil, and D. Nanoparticles; all, at 150 g/mL, 200 g/mL, 250 g/mL, 300 g/mL, and 350 g/mL.

This outcome accentuates the extraordinary attributes of the L-arginine encapsulated lipid nanoparticles. The minimal hemolysis percentage at the highest concentration accentuates their commendable biocompatibility and non-toxic nature. The nanoparticles demonstrate a remarkable absence of detrimental effects on red blood cells, thus insinuating their potential safety for prospective utilization.

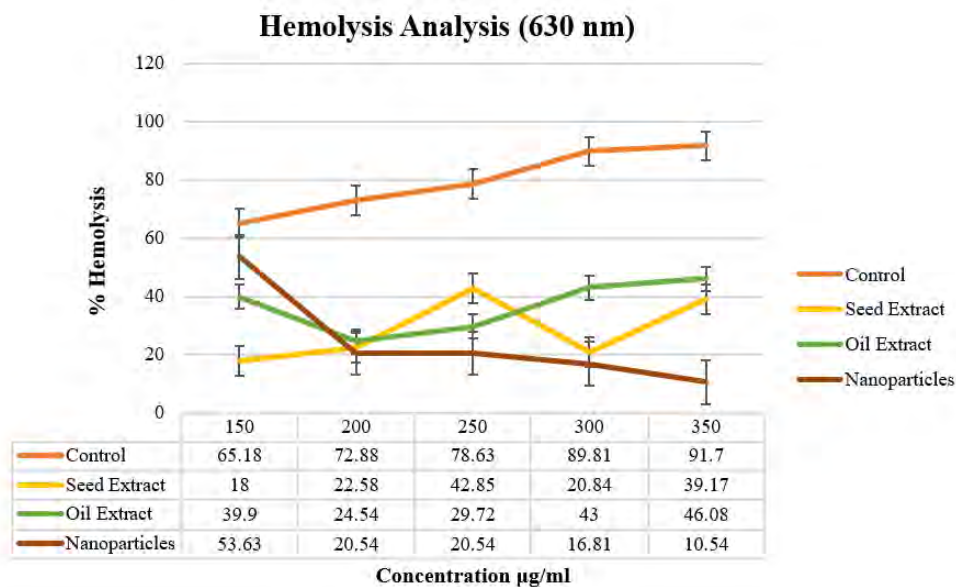


Figure 3.28: A graphic representation of the hemolysis effect showing RBCs destruction by the control, seed extract, oil extract, and L-arginine-encapsulated lipid nanoparticles at various concentrations.

3.13.5 Anti-Bacterial Activity

Exploring the antimicrobial attributes of L-arginine encapsulated lipid nanoparticles encompassed a comparative assessment with the antibiotic cefoxitin. Notably, at a concentration of 250 $\mu\text{g/mL}$, the nanoparticles exhibited noteworthy efficacy in curtailing microbial growth. Specifically, the L-arginine encapsulated lipid nanoparticles displayed substantial zones of inhibition, measuring 20 mm, as illustrated in Figure 3.29 (A) against *Vibrio cholera* and 22 mm (as depicted in Figure 3.29 (B)) against *Bacillus anthracis*. This remarkable inhibitory effect emphasizes the nanoparticles' inherent ability to impede the proliferation of these detrimental microorganisms.

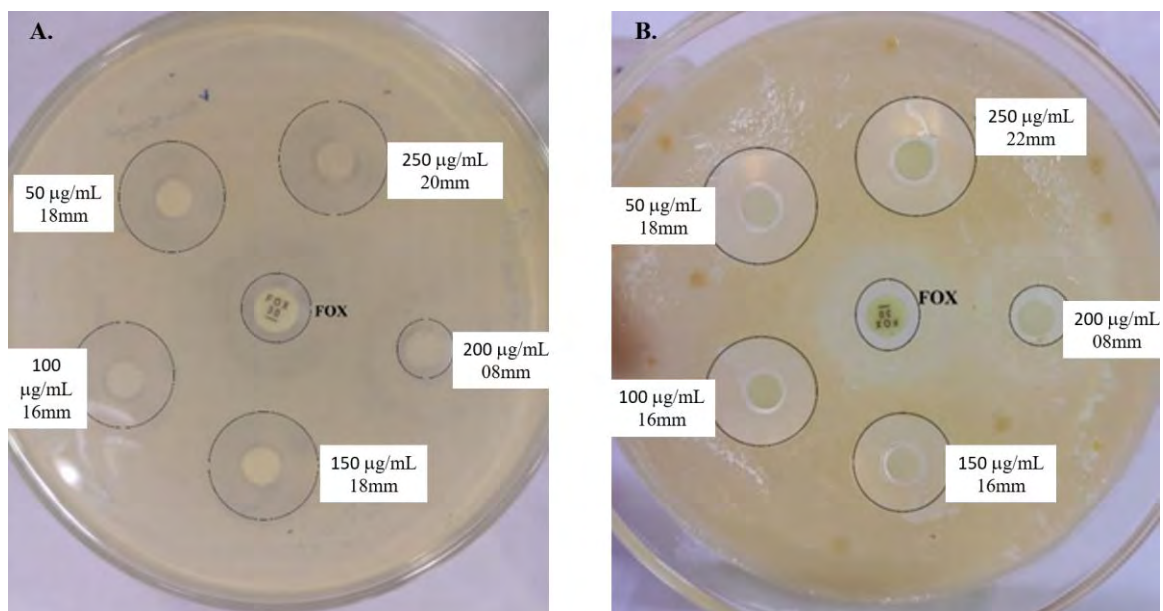


Figure 3.29: Inhibition zones of synthesized L-arginine encapsulated lipid nanoparticles and control antibacterial disc cefoxitin against specific bacteria (A) *Vibrio cholera* (B) *Bacillus anthracis*.

CHAPTER FOUR

DISCUSSION & CONCLUSION

DISCUSSION AND CONCLUSION

The widespread prevalence and intricate nature of Diabetes demands continuous research efforts to advance effective therapeutic strategies for improved patient outcomes (Tiwari, 2015). This investigation explored the potential roles of L-arginine and *Trigonella foenum-graecum* (Fenugreek) in diabetes management while also evaluating the efficacy of lipid nanocarriers for drug delivery in diabetes treatment. Additionally, we explored the emergent domain of network pharmacology and its implications in Diabetes research.

This chapter aims to establish the significance of our findings and a robust foundation for future studies. The limited utilization of fenugreek for therapeutic purposes, primarily in certain regions like North and South America and select Asian areas, raises questions about its potential benefits on a broader scale. Notably, the contrasting use of fenugreek in India and Pakistan, despite their geographic proximity, highlights the need for exploring cultural and healthcare factors influencing its adoption.

Further investigation could elucidate the reasons behind this disparity and pave the way for expanding fenugreek's medicinal applications. Our investigation identified two compounds, Daidzein (CMAUP Compound ID: NPC234560) and L-arginine (CMAUP Compound ID: NPC226453), as potential anti-diabetic agents. Upon detailed analysis, we finalized L-arginine as our target lead compound. Although L-arginine targets lesser genes than Daidzein, its targets play a more critical role in Diabetes, as summarized in Table 3.5.

For example, the complex role of nitrogen metabolism in the context of type 2 diabetes mellitus emphasizes its significance in the pathogenesis and progression of this metabolic disorder (Hameed et al., 2015). The interplay between nitrogen metabolism, insulin sensitivity, glucose homeostasis, and overall metabolic balance sheds light on potential mechanisms contributing to diabetes-related dysfunctions (Petersen & Shulman, 2018). Our research highlighting the critical role of L-arginine from fenugreek in nitrogen metabolism adds valuable to this puzzle and suggests potential therapeutic avenues.

Moreover, the relationship between lipophilicity and Topological Polar Surface Area (TPSA) in drug design brings to light the crucial interplay between these parameters and a drug's pharmacokinetics and bioavailability (Ahmad et al., 2023). The significance of lipophilicity in determining a drug's ability to traverse cellular membranes, along with

the relevance of TPSA in predicting its interactions with polar environments, emphasizes the need for a delicate balance between these attributes.

The balance between lipophilicity and TPSA is pivotal in designing drug candidates with desirable pharmacological properties. Our results highlighting L-arginine's ideal TPSA and lipophilicity values strengthen its candidacy as a potential drug (Ahmad et al., 2023). Also, using the Rule of Five, a widely accepted guideline in drug design, adds rigor to evaluating drug-like properties. The molecular weight, lipophilicity, hydrogen bond donors, and acceptors align with industry standards and aid in predicting oral absorption and bioavailability (Benet et al., 2016). Our analyses of L-arginine's scores against the Rule of Five and other parameters also affirm its suitability as a drug candidate. Addressing concerns about its size by utilizing lipid nanoparticles for drug delivery demonstrates a creative solution that leverages nanotechnology to overcome potential limitations. This approach showcases the adaptability of L-arginine as a potential therapeutic agent.

We utilized the Molecular Operating Environment (MOE) software to investigate molecular interactions between core gene targets and Fenugreek's active compounds and finalize our lead compound. Among the array of parameters assessed, the S score emerged as the cornerstone of our docking analysis, effectively gauging the quality of molecular docking solutions (Vilar et al., 2008). This metric quantifies the alignment between predicted and experimental binding sites, with higher S scores indicative of a superior match.

The energy scores generated from the docking analysis revealed intriguing information about the binding potential of the compounds. L-arginine exhibited robust interactions across multiple poses and all three compounds, forming numerous hydrogen bonds (Figures 3.8-3.10). Hydrogen bonds, as critical determinants of molecular interactions, play a fundamental role in mediating binding affinity and specificity (Chen et al., 2016). Our emphasis on L-arginine stems from its profound and consistent hydrogen bonding interactions, which signify strong molecular associations and potential therapeutic efficacy, validating our choice based on these critical molecular interactions.

Our findings align with other studies in the field. For instance, in a study exploring antidiabetic peptides derived from hypoglycemic polypeptide-P of *M. charantia*, top-

performing peptides were shortlisted based on S-scores and binding affinities (Arif et al., 2021). Similarly, a study on drug repurposing for α -glucosidase inhibition used FDA-approved drugs and identified promising molecular mechanisms (Saeed et al., 2023). Like findings in the mentioned studies, L-arginine's ability to establish significant hydrogen bonding interactions reinforces its potential as a drug target. The parallel outcomes across diverse studies lend further credence to L-arginine's viability as a candidate for therapeutic intervention in diabetes management.

Our study focused specifically on fenugreek seeds due to their prominence in various therapeutic applications. Both the leaves and seeds of *T. foenum-graecum* have been widely utilized in extracts and powders for therapeutic purposes, supported by numerous animal and human trials that have highlighted their hypoglycemic, hypolipidemic, and hypocholesterolemic effects (Visuvanathan et al., 2022; Wani & Kumar, 2018). This approach aligns with the findings of preliminary investigations, further substantiating the potential of fenugreek seeds as a valuable resource for therapeutic applications.

The determination of Total Flavonoid Content (TFC) within our fenugreek extracts indicated a higher concentration in the seed extract (285 mg/g) compared to the oil extract (225 mg/g). This disparity implies that fenugreek seeds are a richer source of these valuable phytochemicals. Our results resonate with previous studies by Akbari et al. (2019) and Al-Timimi (2019), emphasizing the pivotal role of fenugreek seeds in addressing inflammation, cancer, and diabetes. Similarly, our Total Phenolic Content (TPC) findings parallel these observations, with fenugreek seed extracts yielding 335 mg/g, compared to 195 mg/g from oil extracts. This consistency with prior research highlights a well-established trend where seed extracts exhibit higher TPC and TFC levels than oil extracts.

This disparity in content can be attributed to various factors. The extraction process for seed extracts involves solvents like methanol or ethanol, which possess high solubility for phenolic compounds and flavonoids. It allows for effectively extracting and preserving a larger quantity of these compounds from the seeds, contributing to higher TPC and TFC levels (Phuyal et al., 2020). Concentration processes used for seed extracts, such as evaporation or freeze-drying, further enhance phenolic and flavonoid content while

reducing the extract volume (Zulkifli et al., 2020). Additionally, the broader range of compounds found in seed extracts, including phenolics and flavonoids, compared to the lipid-rich composition of seed oil extracts, explains the observed higher TPC and TFC levels in seed extracts (Saeed et al., 2012).

The UV-Vis spectroscopic analysis identified distinct light absorbance peaks for the simple lipid nanoparticles at 415 nm and the L-arginine encapsulated lipid nanoparticles at 521 nm. Interestingly, no existing literature could be found either supporting or negating these specific peaks, stressing the novelty of our approach in synthesizing L-arginine encapsulated lipid nanoparticles. This unique spectral signature prompts further investigation into the underlying mechanisms governing these absorbance peaks.

Our scanning electron microscopy (SEM) results indicated an average size of 100.2 nm for our L-arginine encapsulated lipid nanoparticles, aligning well with the size range reported by Rawat et al. (2011). Comparable studies by Parvez et al. (2020) illustrated solid lipid nanoparticles encapsulated with Amphotericin B and Paromomycin, exhibiting a size of 140.2 ± 10.15 nm. Nanoparticle size is a critical determinant of their interactions within biological systems. Literature suggests that nanoparticles falling within the size range of 10 to 60 nm (Sabourian et al., 2020), irrespective of their surface charge or composition, are generally conducive to cellular uptake.

Moreover, nanoparticles below 200 nm exhibit enhanced passive transport into red blood cells (RBCs) (Hoshyar et al., 2016). Importantly, nanoparticles approximately 100 nm in size have demonstrated more than a threefold increase in arterial uptake compared to larger counterparts (Prabha et al., 2014). Thus, based on current research, nanoparticles sized between 60 to 200 nm are poised for favorable uptake by living systems. However, the interplay of composition, surface charge, and target cells or tissues can influence nanoparticle behavior and efficacy.

Therefore, a comprehensive evaluation of nanoparticles in the context of specific applications and requirements is recommended. Zeta-potential analysis revealed that the synthesized nanoparticles possess a neutral charge. However, nanoparticles with neutral zeta potential might not be optimal for drug delivery applications. The zeta potential of

nanoparticles substantially influences their stability and interactions with biological components. High zeta potential values, indicating elevated surface charge, contribute to nanoparticle stability and deter aggregation (Clogston & Patri, 2010).

Conversely, neutral zeta potential values may lead to reduced stability and heightened aggregation susceptibility (Honary & Zahir, 2013), as seen in our SEM micrograph. Surface modification strategies, such as targeting ligands or using protective coatings, are often employed to enhance nanoparticle stability and optimize drug delivery (Honary & Zahir, 2013). Therefore, our near-future plans include surface modifications to augment zeta potential and enhance the stability and suitability of our nanoparticles for drug delivery applications.

Our X-ray diffraction (XRD) analyses conclusively confirm the amorphous nature of our synthesized nanoparticles. The exploration of amorphous nanoparticles in the context of pharmaceuticals is an area yet to be extensively explored. Still, it is widely recognized that amorphous pharmaceutical formulations offer distinct advantages over their crystalline counterparts, particularly in dissolution and subsequent bioavailability properties (Valenti et al., 2021). This intriguing attribute of amorphous nanoparticles holds the potential to impact drug delivery strategies significantly.

The amorphous state in pharmaceuticals enhances drug dissolution rates, improving bioavailability. Significantly, the amorphous structure promotes increased surface area and reduced diffusion distances, enabling more efficient dissolution in biological fluids. These characteristics are particularly relevant for poorly water-soluble drugs, as they can significantly enhance drug solubility and effective membrane permeability (Andrews et al., 2023). This improvement in oral absorption can play a pivotal role in enhancing the therapeutic efficacy of such drugs.

The evidence from Andrews et al. (2023) further strengthens the idea that amorphous nanoparticles can facilitate oral absorption of poorly water-soluble drugs. By leveraging the enhanced solubility and permeability characteristics of amorphous nanoparticles, our synthesized nanoparticles hold promise in overcoming the challenges associated with poorly soluble drugs.

These comprehensive characterization analyses, coupled with the extraordinary biological potential evaluations, accentuate the promising role of our synthesized L-arginine-encapsulated lipid nanoparticles as a potential anti-diabetic strategy. Remarkably, their antioxidative efficacy displayed an exceptional magnitude, recording an impressive 84.44% inhibition and an IC₅₀ value of 40.5. These values notably surpassed those of the control (62.84%: IC₅₀-231.27), fenugreek seed extract (59.73%: 208.98), and oil extract (61.03%: 196.6).

Equally significant, the L-arginine encapsulated lipid nanoparticles exhibited a striking 81.10% inhibition of albumin denaturation at a concentration of 550 µg/mL, distinctly surpassing the control (43.50%), seed extract (51.44%), and seed oil (31.63%). Moreover, the alpha-amylase inhibition achieved by these nanoparticles reached an impressive 89.30%, outperforming metformin, a widely employed antidiabetic medication, which recorded a maximum inhibition of 78.43% at an equivalent dose (1000 µg/mL).

Most importantly, the substantial hemolysis percentage of 10.54% at the highest concentration of 350 µg/mL for L-arginine encapsulated lipid nanoparticles merits attention, particularly when contrasted with the corresponding hemolysis percentages observed for the control (91.70%), fenugreek seed extract (39.17%), and fenugreek oil extract (46.08%). These findings collectively highlight the anti-diabetic potential of our L-arginine encapsulated lipid nanoparticles, substantiating their viability as a promising avenue for advancing therapeutic interventions in diabetes management.

4.1 Concluding Remarks

Our research endeavors have illuminated a multifaceted perspective on the potential therapeutic utility of fenugreek and L-arginine in diabetes management. We have explored the novel pharmacological potential of L-arginine-encapsulated lipid nanoparticles through detailed analyses encompassing molecular interactions, drug-likeness parameters, and encapsulated-nanoparticle synthesis. The elaborate web of nitrogen metabolism emerges as a critical player in the pathogenesis of type 2 diabetes mellitus, showcasing the intricate connections between metabolic dysregulation, inflammation, oxidative stress, and lipid metabolism. Our investigations have revealed L-arginine's pivotal role within this

framework, affirming its promise as a potential therapeutic target. On the other hand, our tailored drug design approach employs lipophilicity and Topological Polar Surface Area (TPSA), along with many other pharmacokinetic factors, as guiding principles in identifying L-arginine as a drug candidate with ideal properties.

Moreover, the synthesis of L-arginine encapsulated lipid nanoparticles presents a benchmark avenue, with amorphous nanoparticles potentially enhancing drug solubility and membrane permeability. These nanoparticles exhibit impressive anti-diabetic potential, showcasing notable improvements in antioxidative efficacy, albumin denaturation inhibition, alpha-amylase inhibition, and even hemolysis percentage compared to traditional treatments. These findings highlight the immense promise of L-arginine and fenugreek, both individually and synergistically, in revolutionizing diabetes management. Our research opens new horizons for therapeutic innovation, offering novel strategies to combat this complex metabolic disorder and ultimately improving the quality of life for those affected.

4.2 Future Prospects of this Study

The prospects of this study hold exciting opportunities for advancing our understanding of fenugreek and L-arginine's potential in diabetes management and translating these findings into substantial therapeutic strategies.

4.2.1 Optimization of Nanoparticles

Building upon our synthesized L-arginine encapsulated lipid nanoparticles, future research can focus on optimizing their characteristics. Enhancing the zeta potential, for instance, can significantly improve their stability and efficacy as drug-delivery vehicles. Modifying the surface charge through innovative approaches could support their potential for targeted drug delivery and controlled release.

4.2.2 Cell-line and In vivo Assays

To further substantiate our in vitro assessments, cell-line assays can provide insights into nanoparticle interactions with living cells. In vivo assays, using animal models,

would provide a closer approximation of their effects within a complex biological system. Such assays could contribute to a more comprehensive understanding of the nanoparticles' potential therapeutic impact.

4.2.3 Formulation Development

The synthesized encapsulated nanoparticles exhibit remarkable anti-diabetic potential. Researchers can leverage this finding to explore the creation of oral or other suitable formulations. By encapsulating other anti-diabetic agents with complementary mechanisms of action, novel combination therapies can be developed to enhance treatment outcomes and minimize adverse effects.

4.2.4 Clinical Trials

The next step on the translational journey involves small-scale clinical trials. Validating the anti-diabetic potential of our synthesized nanoparticles in humans would provide critical evidence of their efficacy and safety. If proven successful, larger-scale clinical trials can follow, paving the way for potential regulatory approvals and eventual incorporation into clinical practice.

CHAPTER FIVE

REFERENCES

REFERENCES

Aamir, A. H., Ul-Haq, Z., Mahar, S. A., Qureshi, F. M., Ahmad, I., Jawa, A., Sheikh, A., Raza, A., Fazid, S., Jadoon, Z., Ishtiaq, O., Safdar, N., Afridi, H., & Heald, A. H. (2019). Diabetes Prevalence Survey of Pakistan (DPS-PAK): prevalence of type 2 diabetes mellitus and prediabetes using HbA1c: a population-based survey from Pakistan. *BMJ Open*, 9(2), e025300. <https://doi.org/10.1136/bmjopen-2018-025300>

Adnan, Md., Jeon, B.-B., Chowdhury, Md. H. U., Oh, K.-K., Das, T., Chy, Md. N. U., & Cho, D.-H. (2022). Network Pharmacology Study to Reveal the Potentiality of a Methanol Extract of *Caesalpinia sappan* L. Wood against Type-2 Diabetes Mellitus. *Life*, 12(2), 277. <https://doi.org/10.3390/life12020277>

Agüero, L., Zaldivar-Silva, D., Peña, L., & Dias, M. L. (2017). Alginate microparticles as oral colon drug delivery device: A review. *Carbohydrate Polymers*, 168, 32–43. <https://doi.org/10.1016/j.carbpol.2017.03.033>

Ahmad, I., Kuznetsov, A. E., Pirzada, A. S., Alsharif, K. F., Daglia, M., & Khan, H. (2023). Computational pharmacology and computational chemistry of 4-hydroxyisoleucine: Physicochemical, pharmacokinetic, and DFT-based approaches. *Frontiers in Chemistry*, 11. <https://doi.org/10.3389/fchem.2023.1145974>

Akbari, S., Abdurahman, N. H., Yunus, R. M., Alara, O. R., & Abayomi, O. O. (2019). Extraction, characterization and antioxidant activity of fenugreek (*Trigonella Foenum Graecum*) seed oil. *Materials Science for Energy Technologies*, 2(2), 349–355. <https://doi.org/10.1016/j.mset.2018.12.001>

Al-Timimi, L. A. N. (2019). Antibacterial and Anticancer Activities of Fenugreek Seed Extract. *Asian Pacific Journal of Cancer Prevention*, 20(12), 3771–3776. <https://doi.org/10.31557/apjcp.2019.20.12.3771>

Ali, L. M. A., Shaker, S. A., Piñol, R., Millán, Á., Hanafy, M. Y., Helmy, M. M., Kamel, M. A., & Mahmoud, S. A. (2020). Effect of superparamagnetic iron oxide nanoparticles on glucose homeostasis on type 2 diabetes experimental model. *Life Sciences*, 245, 117361–117361. <https://doi.org/10.1016/j.lfs.2020.117361>

American Diabetes Association. (2022, July 28). Statistics About Diabetes | ADA. Diabetes.org. <https://diabetes.org/about-us/statistics/about-diabetes#:~:text=Diabetes%20in%20youth>

Andrews, G. P., Qian, K., Jacobs, E., Jones, D. S., & Tian, Y. (2023). High drug loading nanosized amorphous solid dispersion (NASD) with enhanced in vitro solubility and permeability: Benchmarking conventional ASD. *International Journal of Pharmaceutics*, 632, 122551. <https://doi.org/10.1016/j.ijpharm.2022.122551>

Angel Rose Rajan, Rajan, A., John, A., & Philip, D. (2019). Green synthesis of CeO₂ nanostructures by using *Morus nigra* fruit extract and its antidiabetic activity. *Nucleation and Atmospheric Aerosols*. <https://doi.org/10.1063/1.5100693>

Araujo, T. R., Freitas, I. N., Vettorazzi, J. F., Batista, T. M., Santos-Silva, J. C., Bonfleur, M. L., Balbo, S. L., Boschero, A. C., Carneiro, E. M., & Ribeiro, R. A. (2017). Benefits of L-alanine or L-arginine supplementation against adiposity and glucose intolerance in monosodium glutamate-induced obesity. *European Journal of Nutrition*, 56(6), 2069–2080. <https://doi.org/10.1007/s00394-016-1245-6>

Arif, R., Ahmad, S., Mustafa, G., Mahrosh, H. S., Ali, M., Tahir ul Qamar, M., & Dar, H. R. (2021). Molecular Docking and Simulation Studies of Antidiabetic Agents Devised from Hypoglycemic Polypeptide-P of *Momordica charantia*. *BioMed Research International*, 2021, e5561129. <https://doi.org/10.1155/2021/5561129>

Avalos-Soriano, A., De la Cruz-Cordero, R., Rosado, J., & Garcia-Gasca, T. (2016). 4-Hydroxyisoleucine from Fenugreek (*Trigonella foenum-graecum*): Effects on Insulin Resistance Associated with Obesity. *Molecules*, 21(11), 1596. <https://doi.org/10.3390/molecules21111596>

Ayyoub, S., Al-Trad, B., Aljabali, A. A. A., Alshaer, W., Zoubi, A., Omari, S., Fayyad, D., & Tambuwala, M. M. (2022). Biosynthesis of gold nanoparticles using leaf extract of *Dittrichia viscosa* and *in vivo* assessment of its anti-diabetic efficacy. *Drug Delivery and Translational Research*, 12(12), 2993–2999. <https://doi.org/10.1007/s13346-022-01163-0>

- Azeem, S., Khan, U., & Liaquat, A. (2022). The increasing rate of diabetes in Pakistan: A silent killer. *Annals of Medicine and Surgery*, 79, 103901. <https://doi.org/10.1016/j.amsu.2022.103901>
- Bagyalakshmi, J., & Haritha, H. (2017). Green Synthesis and Characterization of Silver Nanoparticles Using *Pterocarpus marsupium* and Assessment of its In vitro Antidiabetic Activity. *American Journal of Advanced Drug Delivery*, 5(3). <https://doi.org/10.21767/2321-547x.1000019>
- Balouiri, M., Sadiki, M., & Ibsouda, S. K. (2016). Methods for in Vitro Evaluating Antimicrobial activity: a Review. *Journal of Pharmaceutical Analysis*, 6(2), 71–79. <https://doi.org/10.1016/j.jpha.2015.11.005>
- Barnett, A. (2006). DPP-4 inhibitors and their potential role in the management of type 2 diabetes. *International Journal of Clinical Practice*, 60(11), 1454–1470. <https://doi.org/10.1111/j.1742-1241.2006.01178.x>
- Basit, A., Fawwad, A., Qureshi, H., & Shera, A. S. (2018). Prevalence of diabetes, pre-diabetes and associated risk factors: second National Diabetes Survey of Pakistan (NDSP), 2016–2017. *BMJ Open*, 8(8), e020961. <https://doi.org/10.1136/bmjopen-2017-020961>
- Bateman, A., Martin, M.-J., Orchard, S., Magrane, M., Ahmad, S., Alpi, E., Bowler-Barnett, E. H., Britto, R., Bye-A-Jee, H., Cukura, A., Denny, P., Dogan, T., Ebenezer, T., Fan, J., Garmiri, P., da Costa Gonzales, L. J., Hatton-Ellis, E., Hussein, A., Ignatchenko, A., & Insana, G. (2022). UniProt: the Universal Protein Knowledgebase in 2023. *Nucleic Acids Research*, 51(D1). <https://doi.org/10.1093/nar/gkac1052>
- Batool, S., Javed, M. R., Aslam, S., Noor, F., Javed, H. M. F., Seemab, R., Rehman, A., Aslam, M. F., Paray, B. A., & Gulnaz, A. (2022). Network Pharmacology and Bioinformatics Approach Reveals the Multi-Target Pharmacological Mechanism of *Fumaria indica* in the Treatment of Liver Cancer. *Pharmaceuticals*, 15(6), 654. <https://doi.org/10.3390/ph15060654>
- Bellou, V., Belbasis, L., Tzoulaki, I., & Evangelou, E. (2018). Risk factors for type 2 diabetes mellitus: An exposure-wide umbrella review of meta-analyses. *PLOS ONE*, 13(3), e0194127. <https://doi.org/10.1371/journal.pone.0194127>

- Benet, L. Z., Hosey, C. M., Ursu, O., & Oprea, T. I. (2016). BDDCS, the Rule of 5 and drugability. *Advanced Drug Delivery Reviews*, 101, 89–98. <https://doi.org/10.1016/j.addr.2016.05.007>
- Berman, H. M. (2000). The Protein Data Bank. *Nucleic Acids Research*, 28(1), 235–242. <https://doi.org/10.1093/nar/28.1.235>
- Bhatti, J. S., Sehrawat, A., Mishra, J., Sidhu, I. S., Navik, U., Khullar, N., Kumar, S., Bhatti, G. K., & Reddy, P. H. (2022). Oxidative stress in the pathophysiology of type 2 diabetes and related complications: Current therapeutics strategies and future perspectives. *Free Radical Biology and Medicine*, 184, 114–134. <https://doi.org/10.1016/j.freeradbiomed.2022.03.019>
- Bi, Y., Wang, T., Xu, M., Xu, Y., Li, M., Lu, J., Zhu, X., & Ning, G. (2012). Advanced research on risk factors of type 2 diabetes. *Diabetes/Metabolism Research and Reviews*, 28(s2), 32–39. <https://doi.org/10.1002/dmrr.2352>
- Bisht, A. S., Tewari, D. P., Kumar, S., & Chandra, S. (2023). Network pharmacology, molecular docking, and molecular dynamics simulation to elucidate the mechanism of anti-aging action of *Tinospora cordifolia*. *Molecular Diversity*. <https://doi.org/10.1007/s11030-023-10684-w>
- Bommer, C., Sagalova, V., Heesemann, E., Manne-Goehler, J., Atun, R., Bärnighausen, T., Davies, J., & Vollmer, S. (2018). Global Economic Burden of Diabetes in Adults: Projections From 2015 to 2030. *Diabetes Care*, 41(5), 963–970. <https://doi.org/10.2337/dc17-1962>
- Böttger, R., Pauli, G., Chao, P.-H., AL Fayez, N., Hohenwarter, L., & Li, S.-D. (2020). Lipid-based nanoparticle technologies for liver targeting. *Advanced Drug Delivery Reviews*, 154-155, 79–101. <https://doi.org/10.1016/j.addr.2020.06.017>
- Boushra, M., Tous, S., Fetih, G., Xue, H.-Y., Tran, N. T., & Wong, H. L. (2016). Methocel-Lipid Hybrid Nanocarrier for Efficient Oral Insulin Delivery. *Journal of Pharmaceutical Sciences*, 105(5), 1733–1740. <https://doi.org/10.1016/j.xphs.2016.02.018>
- Bruno, C. D., Harmatz, J. S., Duan, S. X., Zhang, Q., Chow, C. R., & Greenblatt, D. J. (2021). Effect of lipophilicity on drug distribution and elimination: Influence of

obesity. *British Journal of Clinical Pharmacology*, 87(8).

<https://doi.org/10.1111/bcp.14735>

Carvalho, D. S., Diniz, M. M., Haidar, A. A., Cavanal, M. de F., da Silva Alves, E., Carpinelli, A. R., Gil, F. Z., & Hirata, A. E. (2016). L-Arginine supplementation improves insulin sensitivity and beta cell function in the offspring of diabetic rats through AKT and PDX-1 activation. *European Journal of Pharmacology*, 791, 780–787.

<https://doi.org/10.1016/j.ejphar.2016.10.001>

Centers for Disease Control and Prevention. (2022, March 11). What Is Type 1 Diabetes? Centers for Disease Control and Prevention.

[https://www.cdc.gov/diabetes/basics/what-is-type-1-](https://www.cdc.gov/diabetes/basics/what-is-type-1-diabetes.html#:~:text=Type%20%20diabetes%20was%20once)

[diabetes.html#:~:text=Type%20%20diabetes%20was%20once](https://www.cdc.gov/diabetes/basics/what-is-type-1-diabetes.html#:~:text=Type%20%20diabetes%20was%20once)

Chaudhury, A., Duvoor, C., Reddy Dendi, V. S., Kraleti, S., Chada, A., Ravilla, R., Marco, A., Shekhawat, N. S., Montales, M. T., Kuriakose, K., Sasapu, A., Beebe, A., Patil, N., Musham, C. K., Lohani, G. P., & Mirza, W. (2017). Clinical Review of Antidiabetic Drugs: Implications for Type 2 Diabetes Mellitus Management. *Frontiers in Endocrinology*, 8(6). <https://doi.org/10.3389/fendo.2017.00006>

Chen, D., Oezguen, N., Urvil, P., Ferguson, C., Dann, S. M., & Savidge, T. C. (2016). Regulation of protein-ligand binding affinity by hydrogen bond pairing. *Science Advances*, 2(3). <https://doi.org/10.1126/sciadv.1501240>

Chen, Y.-M., Li, H., Chiu, Y.-S., Huang, C.-C., & Chen, W.-C. (2020). Supplementation of L-Arginine, L-Glutamine, Vitamin C, Vitamin E, Folic Acid, and Green Tea Extract Enhances Serum Nitric Oxide Content and Antifatigue Activity in Mice. *Evidence-Based Complementary and Alternative Medicine*, 2020, 1–10.

<https://doi.org/10.1155/2020/8312647>

Chenthamara, D., Subramaniam, S., Ramakrishnan, S. G., Krishnaswamy, S., Essa, M. M., Lin, F.-H., & Qoronfleh, M. W. (2019). Therapeutic efficacy of nanoparticles and routes of administration. *Biomaterials Research*, 23(1).

<https://doi.org/10.1186/s40824-019-0166-x>

Cheung, W. (2009). The management of gestational diabetes. *Vascular Health and Risk Management*, 153. <https://doi.org/10.2147/vhrm.s3405>

Cho, J., Horikawa, Y., Enya, M., Takeda, J., Imai, Y., Imai, Y., Handa, H., & Imai, T. (2020). L-Arginine prevents cereblon-mediated ubiquitination of glucokinase and stimulates glucose-6-phosphate production in pancreatic β -cells. *Communications Biology*, 3(1). <https://doi.org/10.1038/s42003-020-01226-3>

Clemmensen, C., Madsen, A. N., Smajilovic, S., Holst, B., & Bräuner-Osborne, H. (2011). L-Arginine improves multiple physiological parameters in mice exposed to diet-induced metabolic disturbances. *Amino Acids*, 43(3), 1265–1275. <https://doi.org/10.1007/s00726-011-1199-1>

Clogston, J. D., & Patri, A. K. (2010). Zeta Potential Measurement. *Methods in Molecular Biology*, 63–70. https://doi.org/10.1007/978-1-60327-198-1_6

Colberg, S. R., Sigal, R. J., Fernhall, B., Regensteiner, J. G., Blissmer, B. J., Rubin, R. R., Chasan-Taber, L., Albright, A. L., & Braun, B. (2010). Exercise and Type 2 Diabetes: The American College of Sports Medicine and the American Diabetes Association: joint position statement. *Diabetes Care*, 33(12), e147–e167. <https://doi.org/10.2337/dc10-9990>

Cooke, D. W., & Plotnick, L. (2008). Type 1 Diabetes Mellitus in Pediatrics. *Pediatrics in Review*, 29(11), 374–385. <https://doi.org/10.1542/pir.29-11-374>

Costa, C. P., Moreira, J. N., Sousa Lobo, J. M., & Silva, A. C. (2021). Intranasal delivery of nanostructured lipid carriers, solid lipid nanoparticles and nanoemulsions: A current overview of *in vivo* studies. *Acta Pharmaceutica Sinica B*, 11(4), 925–940. <https://doi.org/10.1016/j.apsb.2021.02.012>

Daina, A., Michielin, O., & Zoete, V. (2017). SwissADME: a Free web Tool to Evaluate pharmacokinetics, drug-likeness and Medicinal Chemistry Friendliness of Small Molecules. *Scientific Reports*, 7(1). <https://doi.org/10.1038/srep42717>

De, R., Mahata, M. K., & Kim, K. (2022). Structure-Based Varieties of Polymeric Nanocarriers and Influences of Their Physicochemical Properties on Drug Delivery Profiles. *Advanced Science*, 9(10), 2105373. <https://doi.org/10.1002/advs.202105373>

Dennison, R. A., Fox, R. A., Ward, R. J., Griffin, S. J., & Usher-Smith, J. A. (2019). Women's views on screening for Type 2 diabetes after gestational diabetes: a

- systematic review, qualitative synthesis and recommendations for increasing uptake. *Diabetic Medicine*, 37(1), 29–43. <https://doi.org/10.1111/dme.14081>
- DiMeglio, L. A., Evans-Molina, C., & Oram, R. A. (2018). Type 1 Diabetes. *The Lancet*, 391(10138), 2449–2462. [https://doi.org/10.1016/s0140-6736\(18\)31320-5](https://doi.org/10.1016/s0140-6736(18)31320-5)
- Dirir, A. M., Daou, M., Yousef, A. F., & Yousef, L. F. (2021). A review of alpha-glucosidase inhibitors from plants as potential candidates for the treatment of type-2 diabetes. *Phytochemistry Reviews*. <https://doi.org/10.1007/s11101-021-09773-1>
- England, L. J., Dietz, P. M., Njoroge, T., Callaghan, W. M., Bruce, C., Buus, R. M., & Williamson, D. F. (2009). Preventing type 2 diabetes: public health implications for women with a history of gestational diabetes mellitus. *American Journal of Obstetrics and Gynecology*, 200(4), 365.e1–365.e8. <https://doi.org/10.1016/j.ajog.2008.06.031>
- Ermondi, G., Vallaro, M., Goetz, G., Shalaeva, M., & Caron, G. (2020). Updating the portfolio of physicochemical descriptors related to permeability in the beyond the rule of 5 chemical space. *European Journal of Pharmaceutical Sciences*, 146, 105274. <https://doi.org/10.1016/j.ejps.2020.105274>
- Ettliger, R., Lächelt, U., Gref, R., Horcajada, P., Lammers, T., Serre, C., Couvreur, P., Morris, R. E., & Wuttke, S. (2022). Toxicity of metal–organic framework nanoparticles: from essential analyses to potential applications. *Chemical Society Reviews*, 51(2), 464–484. <https://doi.org/10.1039/d1cs00918d>
- Farkhani, S. M., Valizadeh, A., Karami, H., Mohammadi, S., Sohrabi, N., & Badrzadeh, F. (2014). Cell penetrating peptides: Efficient vectors for delivery of nanoparticles, nanocarriers, therapeutic and diagnostic molecules. *Peptides*, 57, 78–94. <https://doi.org/10.1016/j.peptides.2014.04.015>
- Fatima, N., Rehman, A., Ashfaq, U. A., Saleem, M. H., Okla, M. K., Al-Hashimi, A., AbdElgawad, H., & Aslam, S. (2022). Integrating Network Pharmacology and Molecular Docking Approaches to Decipher the Multi-Target Pharmacological Mechanism of *Abrus precatorius* L. Acting on Diabetes. *Pharmaceuticals*, 15(4), 414–414. <https://doi.org/10.3390/ph15040414>

Feldman, E. L., Callaghan, B. C., Pop-Busui, R., Zochodne, D. W., Wright, D. E., Bennett, D. L., Bril, V., Russell, J. W., & Viswanathan, V. (2019). Diabetic neuropathy. *Nature Reviews Disease Primers*, 5(1). <https://doi.org/10.1038/s41572-019-0092-1>

Fletcher, B., Gulanick, M., & Lamendola, C. (2002). Risk Factors for Type 2 Diabetes Mellitus. *Journal of Cardiovascular Nursing*, 16(2), 17–23. https://journals.lww.com/jcnjournal/Abstract/2002/01000/Risk_Factors_for_Type_2_Diabetes_Mellitus.3.aspx

Fletcher, J. (2023, January 12). Diabetes fatigue: Causes, management, and when to see a doctor. *Www.medicalnewstoday.com*. <https://www.medicalnewstoday.com/articles/323398>

Fonte, P., Nogueira, T., Gehm, C., Ferreira, D., & Sarmiento, B. (2011). Chitosan-coated solid lipid nanoparticles enhance the oral absorption of insulin. *Drug Delivery and Translational Research*, 1(4), 299–308. <https://doi.org/10.1007/s13346-011-0023-5>

Forzano, I., Avvisato, R., Varzideh, F., Jankauskas, S. S., Cioppa, A., Mone, P., Salemme, L., Kansakar, U., Tesorio, T., Trimarco, V., & Santulli, G. (2023). L-Arginine in diabetes: clinical and preclinical evidence. *Cardiovascular Diabetology*, 22(1). <https://doi.org/10.1186/s12933-023-01827-2>

Gaddam, A., Galla, C., Thummiseti, S., Marikanty, R. K., Palanisamy, U. D., & Rao, P. V. (2015). Role of Fenugreek in the prevention of type 2 diabetes mellitus in prediabetes. *Journal of Diabetes & Metabolic Disorders*, 14(1). <https://doi.org/10.1186/s40200-015-0208-4>

Galaviz, K. I., Narayan, K. M. V., Lobelo, F., & Weber, M. B. (2018). Lifestyle and the Prevention of Type 2 Diabetes: A Status Report. *American Journal of Lifestyle Medicine*, 12(1), 4–20. <https://doi.org/10.1177/1559827615619159>

Galicia-Garcia, U., Benito-Vicente, A., Jebari, S., Larrea-Sebal, A., Siddiqi, H., Uribe, K. B., Ostolaza, H., & Martín, C. (2020). Pathophysiology of type 2 diabetes mellitus. *International Journal of Molecular Sciences*, 21(17), 1–34. <https://doi.org/10.3390/ijms21176275>

- Giannarelli, R., Aragona, M., Coppelli, A., & Del Prato, S. (2003). Reducing insulin resistance with metformin: the evidence today. *Diabetes & Metabolism*, 29(4), 6S28–6S35. [https://doi.org/10.1016/s1262-3636\(03\)72785-2](https://doi.org/10.1016/s1262-3636(03)72785-2)
- Goff, H. D., Repin, N., Fabek, H., El Khoury, D., & Gidley, M. J. (2018). Dietary fibre for glycaemia control: Towards a mechanistic understanding. *Bioactive Carbohydrates and Dietary Fibre*, 14, 39–53. <https://doi.org/10.1016/j.bcdf.2017.07.005>
- Goyal, S., Gupta, N., & Chatterjee, S. (2016). Investigating Therapeutic Potential of *Trigonella foenum-graecum* L. as Our Defense Mechanism against Several Human Diseases. *Journal of Toxicology*, 2016, 1–10. <https://doi.org/10.1155/2016/1250387>
- Gregory, A. (2023, June 22). More than 1.3bn adults will have diabetes by 2050, study predicts. *The Guardian*. <https://www.theguardian.com/society/2023/jun/22/more-than-13bn-adults-will-have-diabetes-by-2050-study-predicts>
- Hameed, I., Masoodi, S. R., Mir, S. A., Nabi, M., Ghazanfar, K., & Ganai, B. A. (2015). Type 2 diabetes mellitus: From a metabolic disorder to an inflammatory condition. *World Journal of Diabetes*, 6(4), 598. <https://doi.org/10.4239/wjd.v6.i4.598>
- Hassan, O. (2022, May 15). Prevalence of Diabetes in Pakistan | MMI. Memon Medical Institute Hospital. <https://mmi.edu.pk/blog/prevalence-of-diabetes-in-pakistan/>
- He, T., Wang, M., Kong, J., Wang, Q., Tian, Y., Li, C., Wang, Q., Liu, C., & Huang, J. (2022). Integrating network pharmacology and non-targeted metabolomics to explore the common mechanism of Coptis Categorized Formula improving T2DM zebrafish. *Journal of Ethnopharmacology*, 284, 114784–114784. <https://doi.org/10.1016/j.jep.2021.114784>
- Honary, S., & Zahir, F. (2013). Effect of Zeta Potential on the Properties of Nano-Drug Delivery Systems - A Review (Part 2). *Tropical Journal of Pharmaceutical Research*, 12(2). <https://doi.org/10.4314/tjpr.v12i2.20>
- Hoshyar, N., Gray, S., Han, H., & Bao, G. (2016). The effect of nanoparticle size on *in vivo* pharmacokinetics and cellular interaction. *Nanomedicine*, 11(6), 673–692. <https://doi.org/10.2217/nmm.16.5>
- Hosseini, S. A., Hamzavi, K., Safarzadeh, H., & Salehi, O. (2020). Interactive effect of swimming training and fenugreek (*Trigonella foenum graecum* L.) extract on

glycemic indices and lipid profile in diabetic rats. *Archives of Physiology*, 1–5.

<https://doi.org/10.1080/13813455.2020.1826529>

Hu, Y., Liu, S., Liu, W., Zhang, Z., Liu, Y., Li, S., Sun, D., Zhang, G., & Fang, J. (2022). Potential Molecular Mechanism of Yishen Capsule in the Treatment of Diabetic Nephropathy Based on Network Pharmacology and Molecular Docking. *Diabetes, Metabolic Syndrome and Obesity: Targets and Therapy*, Volume 15, 943–962.

<https://doi.org/10.2147/dms0.s350062>

Huang, J., Li, Y., Orza, A., Lu, Q., Guo, P., Wang, L., Yang, L., & Mao, H. (2016). Magnetic Nanoparticle Facilitated Drug Delivery for Cancer Therapy with Targeted and Image-Guided Approaches. *Advanced Functional Materials*, 26(22), 3818–3836. <https://doi.org/10.1002/adfm.201504185>

Huang, Y., Wang, X., Yan, C., Li, C., Zhang, L., Zhang, L., Liang, E., Liu, T., & Mao, J. (2022). Effect of metformin on nonalcoholic fatty liver based on meta-analysis and network pharmacology. *Medicine*, 101(43), e31437.

<https://doi.org/10.1097/md.00000000000031437>

Hussain, T., Tan, B., Murtaza, G., Liu, G., Rahu, N., Saleem Kalhoro, M., Hussain Kalhoro, D., Adebawale, T. O., Usman Mazhar, M., Rehman, Z. ur, Martínez, Y., Akber Khan, S., & Yin, Y. (2020). Flavonoids and type 2 diabetes: Evidence of efficacy in clinical and animal studies and delivery strategies to enhance their therapeutic efficacy. *Pharmacological Research*, 152, 104629.

<https://doi.org/10.1016/j.phrs.2020.104629>

Incalza, M. A., D’Oria, R., Natalicchio, A., Perrini, S., Laviola, L., & Giorgino, F. (2018). Oxidative stress and reactive oxygen species in endothelial dysfunction associated with cardiovascular and metabolic diseases. *Vascular Pharmacology*, 100, 1–19. <https://doi.org/10.1016/j.vph.2017.05.005>

International Diabetes Federation. (2021). *IDF Diabetes Atlas 10th edition 2021*. [Diabetesatlas.org](https://diabetesatlas.org/). <https://diabetesatlas.org/>

Jamshaid, P. D. T. (2023). Diabetes Mellitus – The Epidemic of 21 Century. *Esculapio Journal of SIMS*, 19(01), 1–2. <https://esculapio.pk/journal/index.php/journal-files/article/view/272>

- Janaszak-Jasiecka, A., Płoska, A., Wierońska, J. M., Dobrucki, L. W., & Kalinowski, L. (2023). Endothelial dysfunction due to eNOS uncoupling: molecular mechanisms as potential therapeutic targets. *PubMed Central*, 28(1).
<https://doi.org/10.1186/s11658-023-00423-2>
- Ježek, P., Holendová, B., Jabůrek, M., Tauber, J., Dlasková, A., & Plecítá-Hlavatá, L. (2021). The Pancreatic β -Cell: The Perfect Redox System. *Antioxidants*, 10(2), 197. <https://doi.org/10.3390/antiox10020197>
- Jiang, G., Sun, C., Wang, X., Mei, J., Li, C., Zhan, H., Liao, Y., Zhu, Y., & Mao, J. (2022). Hepatoprotective mechanism of *Silybum marianum* on nonalcoholic fatty liver disease based on network pharmacology and experimental verification. *Bioengineered*, 13(3), 5216–5235. <https://doi.org/10.1080/21655979.2022.2037374>
- Kamoun, E. A., Loutfy, S. A., Hussein, Y., & Kenawy, E.-R. S. (2021). Recent advances in PVA-polysaccharide based hydrogels and electrospun nanofibers in biomedical applications: A review. *International Journal of Biological Macromolecules*, 187, 755–768. <https://doi.org/10.1016/j.ijbiomac.2021.08.002>
- Kanehisa Laboratories. (2023). KEGG PATHWAY: Type II diabetes mellitus - Homo sapiens (human). www.genome.jp. <https://www.genome.jp/pathway/hsa04930>
- Kesharwani, P., Gorain, B., Low, S. Y., Tan, S. A., Ling, E. C. S., Lim, Y. K., Chin, C. M., Lee, P. Y., Lee, C. M., Ooi, C. H., Choudhury, H., & Pandey, M. (2018). Nanotechnology based approaches for anti-diabetic drugs delivery. *Diabetes Research and Clinical Practice*, 136, 52–77. <https://doi.org/10.1016/j.diabres.2017.11.018>
- Khan, R. S., Bril, F., Cusi, K., & Newsome, P. N. (2019). Modulation of Insulin Resistance in Nonalcoholic Fatty Liver Disease. *Hepatology*.
<https://doi.org/10.1002/hep.30429>
- Khan, S. (2022, March). What is driving Pakistan’s alarming diabetes surge? | DW | 03.01.2022. DW.COM. <https://www.dw.com/en/what-is-driving-pakistans-alarming-diabetes-surge/a-60318409>
- Khosa, A., Reddi, S., & Saha, R. N. (2018). Nanostructured lipid carriers for site-specific drug delivery. *Biomedicine & Pharmacotherapy*, 103, 598–613.
<https://doi.org/10.1016/j.biopha.2018.04.055>

Kiss, R., Szabó, K., Gesztelyi, R., Somodi, S., Kovács, P., Szabó, Z., Németh, J., Priksz, D., Kurucz, A., Juhász, B., & Szilvássy, Z. (2018). Insulin-Sensitizer Effects of Fenugreek Seeds in Parallel with Changes in Plasma MCH Levels in Healthy Volunteers. *International Journal of Molecular Sciences*, 19(3), 771.

<https://doi.org/10.3390/ijms19030771>

Kong, W.-J., Zhang, H., Song, D.-Q., Xue, R., Zhao, W., Wei, J., Wang, Y.-M., Shan, N., Zhou, Z.-X., Yang, P., You, X.-F., Li, Z.-R., Si, S.-Y., Zhao, L.-X., Pan, H.-N., & Jiang, J.-D. (2009). Berberine reduces insulin resistance through protein kinase C–dependent up-regulation of insulin receptor expression. *Metabolism - Clinical and Experimental*, 58(1), 109–119. <https://doi.org/10.1016/j.metabol.2008.08.013>

Kuang, Y., Chai, Y., Su, H., Lo, J.-Y., Qiao, X., & Ye, M. (2022). A network pharmacology-based strategy to explore the pharmacological mechanisms of *Antrodia camphorata* and antcin K for treating type II diabetes mellitus. *Phytomedicine*, 96, 153851. <https://doi.org/10.1016/j.phymed.2021.153851>

Kumar, A., Bharti, S. K., & Kumar, A. (2017). Therapeutic molecules against type 2 diabetes: What we have and what are we expecting? *Pharmacological Reports*, 69(5), 959–970. <https://doi.org/10.1016/j.pharep.2017.04.003>

Kuzuya, T., Nakagawa, S., Satoh, J., Kanazawa, Y., Iwamoto, Y., Kobayashi, M., Nanjo, K., Sasaki, A., Seino, Y., Ito, C., Shima, K., Nonaka, K., & Kadowaki, T. (2002). Report of the Committee on the classification and diagnostic criteria of diabetes mellitus. *Diabetes Research and Clinical Practice*, 55(1), 65–85. [https://doi.org/10.1016/s0168-8227\(01\)00365-5](https://doi.org/10.1016/s0168-8227(01)00365-5)

Laiteerapong, N., & Huang, E. S. (2018). Diabetes in Older Adults (C. C. Cowie, S. S. Casagrande, A. Menke, M. A. Cissell, M. S. Eberhardt, J. B. Meigs, E. W. Gregg, W. C. Knowler, E. Barrett-Connor, D. J. Becker, F. L. Brancati, E. J. Boyko, W. H. Herman, B. V. Howard, K. M. V. Narayan, M. Rewers, & J. E. Fradkin, Eds.). PubMed; National Institute of Diabetes and Digestive and Kidney Diseases (US). <https://www.ncbi.nlm.nih.gov/books/NBK567980/>

Latres, E., Finan, D. A., Greenstein, J. L., Kowalski, A., & Kieffer, T. J. (2019). Navigating Two Roads to Glucose Normalization in Diabetes: Automated Insulin

Delivery Devices and Cell Therapy. *Cell Metabolism*, 29(3), 545–563.

<https://doi.org/10.1016/j.cmet.2019.02.007>

Law, K. P., & Zhang, H. (2017). The pathogenesis and pathophysiology of gestational diabetes mellitus: Deductions from a three-part longitudinal metabolomics study in China. *Clinica Chimica Acta; International Journal of Clinical Chemistry*, 468, 60–70. <https://doi.org/10.1016/j.cca.2017.02.008>

Li, H., Zhao, L., Zhang, B., Jiang, Y., Wang, X., Guo, Y., Liu, H., Li, S., & Tong, X. (2014). A Network Pharmacology Approach to Determine Active Compounds and Action Mechanisms of Ge-Gen-Qin-Lian Decoction for Treatment of Type 2 Diabetes. *Evidence-Based Complementary and Alternative Medicine*, 2014, 1–12. <https://doi.org/10.1155/2014/495840>

Li, S., Shan, X., Wang, Y., Chen, Q., Sun, J., He, Z., Sun, B., & Luo, C. (2020). Dimeric prodrug-based nanomedicines for cancer therapy. *Journal of Controlled Release*, 326, 510–522. <https://doi.org/10.1016/j.jconrel.2020.07.036>

Li, X., Wei, S., Niu, S., Ma, X., Li, H., Jing, M., & Zhao, Y. (2022). Network pharmacology prediction and molecular docking-based strategy to explore the potential mechanism of Huanglian Jiedu Decoction against sepsis. *Computers in Biology and Medicine*, 144, 105389. <https://doi.org/10.1016/j.compbiomed.2022.105389>

Lin, Z., Tong, Y., Li, N., Zhu, Z., & Li, J. (2020). Network pharmacology-based study of the mechanisms of action of anti-diabetic triterpenoids from *Cyclocarya paliurus*. *RSC Advances*, 10(61), 37168–37181. <https://doi.org/10.1039/d0ra06846b>

Loureiro, G., & Martel, F. (2019). The effect of dietary polyphenols on intestinal absorption of glucose and fructose: Relation with obesity and type 2 diabetes. *Food Reviews International*, 35(4), 390–406. <https://doi.org/10.1080/87559129.2019.1573432>

Ma, X., & Williams, R. O. (2017). Polymeric nanomedicines for poorly soluble drugs in oral delivery systems: an update. *Journal of Pharmaceutical Investigation*, 48(1), 61–75. <https://doi.org/10.1007/s40005-017-0372-2>

Makrilakis, K. (2019). The Role of DPP-4 Inhibitors in the Treatment Algorithm of Type 2 Diabetes Mellitus: When to Select, What to Expect. *International Journal of*

Environmental Research and Public Health, 16(15), 2720.

<https://doi.org/10.3390/ijerph16152720>

Malaikozhundan, B., Vinodhini, J., Kalanjiam, M. A. R., Vinotha, V., Palanisamy, S., Vijayakumar, S., Vaseeharan, B., & Mariyappan, A. (2020). High synergistic antibacterial, antibiofilm, antidiabetic and antimetabolic activity of *Withania somnifera* leaf extract-assisted zinc oxide nanoparticle. *Bioprocess and Biosystems Engineering*, 43(9), 1533–1547. <https://doi.org/10.1007/s00449-020-02346-0>

Mallik, S., Sharangi, A. B., & Sarkar, T. (2020). Phytochemicals of Coriander, Cumin, Fenugreek, Fennel and Black Cumin: A Preliminary Study. *National Academy Science Letters*. <https://doi.org/10.1007/s40009-020-00884-5>

Martiz, R. M., Patil, S. M., Abdulaziz, M., Babalghith, A., Al-Areefi, M., Al-Ghorbani, M., Mallappa Kumar, J., Prasad, A., Mysore Nagalingaswamy, N. P., & Ramu, R. (2022). Defining the Role of Isoeugenol from *Ocimum tenuiflorum* against Diabetes Mellitus-Linked Alzheimer's Disease through Network Pharmacology and Computational Methods. *Molecules*, 27(8), 2398.

<https://doi.org/10.3390/molecules27082398>

McNeil-Watson, F. (2013). Electrophoretic Light Scattering. *Encyclopedia of Biophysics*, 648–654. https://doi.org/10.1007/978-3-642-16712-6_288

Milewska, S., Niemirowicz-Laskowska, K., Siemiaszko, G., Nowicki, P., Wilczewska, A. Z., & Car, H. (2021). Current Trends and Challenges in Pharmacoeconomic Aspects of Nanocarriers as Drug Delivery Systems for Cancer Treatment. *International Journal of Nanomedicine*, 16, 6593–6644.

<https://doi.org/10.2147/IJN.S323831>

Milkovic, B., Hadzi-Djokic, J., Dzamic, Z., & Pejcic, T. (2007). The significance of TPSA, free to total PSA ratio and PSA density in prostate carcinoma diagnostics. *Acta Chirurgica Iugoslavica*, 54(4), 105–107. <https://doi.org/10.2298/aci0704105m>

Mishra, D. K., Shandilya, R., & Mishra, P. K. (2018). Lipid based nanocarriers: a translational perspective. *Nanomedicine: Nanotechnology, Biology and Medicine*, 14(7), 2023–2050. <https://doi.org/10.1016/j.nano.2018.05.021>

Mohammadi-Samani, S., & Ghasemiyeh, P. (2018). Solid lipid nanoparticles and nanostructured lipid carriers as novel drug delivery systems: applications, advantages and disadvantages. *Research in Pharmaceutical Sciences*, 13(4), 288.

<https://doi.org/10.4103/1735-5362.235156>

Mukhtar, Y., Galalain, A., & Yunusa, U. (2020). A MODERN OVERVIEW ON DIABETES MELLITUS: A CHRONIC ENDOCRINE DISORDER. *European Journal of Biology*, 5(2), 1–14. <https://doi.org/10.47672/ejb.409>

Mura, P. (2020). Advantages of the combined use of cyclodextrins and nanocarriers in drug delivery: A review. *International Journal of Pharmaceutics*, 579, 119181. <https://doi.org/10.1016/j.ijpharm.2020.119181>

Nagulapalli Venkata, K. C., Swaroop, A., Bagchi, D., & Bishayee, A. (2017). A small plant with big benefits: Fenugreek (*Trigonella foenum-graecum*Linn.) for disease prevention and health promotion. *Molecular Nutrition & Food Research*, 61(6), 1600950. <https://doi.org/10.1002/mnfr.201600950>

Narmani, A., Rezvani, M., Farhood, B., Darkhor, P., Mohammadnejad, J., Amini, B., Refahi, S., & Abdi Goushbolagh, N. (2019). Folic acid functionalized nanoparticles as pharmaceutical carriers in drug delivery systems. *Drug Development Research*, 80(4), 404–424. <https://doi.org/10.1002/ddr.21545>

Naveed, M., Makhdoom, S. I., Rehman, S. ur, Aziz, T., Bashir, F., Ali, U., Alharbi, M., Alshammari, A., & Alasmari, A. F. (2023). Biosynthesis and Mathematical Interpretation of Zero-Valent Iron NPs Using *Nigella sativa* Seed Tincture for Indemnification of Carcinogenic Metals Present in Industrial Effluents. *Molecules*, 28(8), 3299. <https://doi.org/10.3390/molecules28083299>

Nigam, S., Bishop, J. O., Hayat, H., Quadri, T., Hayat, H., & Wang, P. (2022). Nanotechnology in Immunotherapy for Type 1 Diabetes: Promising Innovations and Future Advances. *Pharmaceutics*, 14(3), 644. <https://doi.org/10.3390/pharmaceutics14030644>

Nikolaeva, M., & Johnstone, M. T. (2023). Nitric Oxide, Its Role in Diabetes Mellitus and Methods to Improve Endothelial Function. Springer EBooks, 159–200. https://doi.org/10.1007/978-3-031-13177-6_7

Nogales, C., Mamdouh, Z. M., List, M., Kiel, C., Casas, A. I., & Schmidt, H. H. H. W. (2022). Network pharmacology: curing causal mechanisms instead of treating symptoms. *Trends in Pharmacological Sciences*, 43(2), 136–150.

<https://doi.org/10.1016/j.tips.2021.11.004>

Noor, F., Tahir ul Qamar, M., Ashfaq, U. A., Albutti, A., Alwashmi, A. S. S., & Aljasir, M. A. (2022). Network Pharmacology Approach for Medicinal Plants: Review and Assessment. *Pharmaceuticals*, 15(5), 572. <https://doi.org/10.3390/ph15050572>

Odorico, J., Markmann, J., Melton, D., Greenstein, J., Hwa, A., Nostro, C., Reznia, A., Oberholzer, J., Pipeleers, D., Yang, L., Cowan, C., Huangfu, D., Egli, D., Ben-David, U., Vallier, L., Grey, S. T., Tang, Q., Roep, B., Ricordi, C., & Naji, A. (2018). Report of the Key Opinion Leaders Meeting on Stem Cell-derived Beta Cells. *Transplantation*, 102(8), 1223–1229. <https://doi.org/10.1097/TP.0000000000002217>

Oliveros, J. C. (2015). Venny. An interactive tool for comparing lists with Venn's diagrams. *Bioinfogp.cnb.csic.es*. <https://bioinfogp.cnb.csic.es/tools/venny/index.html>

Osman, N., Devnarain, N., Omolo, C. A., Fasiku, V., Jaglal, Y., & Govender, T. (2022). Surface modification of nano-drug delivery systems for enhancing antibiotic delivery and activity. *Wiley Interdisciplinary Reviews. Nanomedicine and Nanobiotechnology*, 14(1), e1758. <https://doi.org/10.1002/wnan.1758>

Palanuvej, C. (2009). In Vitro Glucose Entrapment and Alpha-Glucosidase Inhibition of Mucilaginous Substances from Selected Thai Medicinal Plants. *Scientia Pharmaceutica*, 77. <https://doi.org/10.3797/scipharm.0907-17>

Parati, G., Goncalves, A., Soergel, D., Bruno, R. M., Caiani, E. G., Gerdts, E., Mahfoud, F., Mantovani, L., McManus, R. J., Santalucia, P., & Kahan, T. (2022). New Perspectives for Hypertension Management: Progress in Methodological and Technological Developments. *European Journal of Preventive Cardiology*. <https://doi.org/10.1093/eurjpc/zwac203>

Parvez, S., Yadagiri, G., Gedda, M. R., Singh, A., Singh, O. P., Verma, A., Sundar, S., & Mudavath, S. L. (2020). Modified solid lipid nanoparticles encapsulated with Amphotericin B and Paromomycin: an effective oral combination against

experimental murine visceral leishmaniasis. *Scientific Reports*, 10(1).

<https://doi.org/10.1038/s41598-020-69276-5>

Patel, P., Raval, M., Airao, V., Bhatt, V., & Shah, P. (2021). Silibinin loaded inhalable solid lipid nanoparticles for lung targeting. *Journal of Microencapsulation*, 39(1), 1–24. <https://doi.org/10.1080/02652048.2021.2002448>

Perkins, B. A., Sherr, J. L., & Mathieu, C. (2021). Type 1 diabetes glycemic management: Insulin therapy, glucose monitoring, and automation. *Science*, 373(6554), 522–527. <https://doi.org/10.1126/science.abg4502>

Pernicova, I., & Korbonits, M. (2014). Metformin—mode of action and clinical implications for diabetes and cancer. *Nature Reviews Endocrinology*, 10(3), 143–156. <https://doi.org/10.1038/nrendo.2013.256>

Petersen, M. C., & Shulman, G. I. (2018). Mechanisms of insulin action and insulin resistance. *Physiological Reviews*, 98(4), 2133–2223. <https://doi.org/10.1152/physrev.00063.2017>

Phuyal, N., Jha, P. K., Raturi, P. P., & Rajbhandary, S. (2020, March 16). Total Phenolic, Flavonoid Contents, and Antioxidant Activities of Fruit, Seed, and Bark Extracts of *Zanthoxylum armatum* DC. *The Scientific World Journal*. <https://www.hindawi.com/journals/tswj/2020/8780704/>

Pickup, J. C. (2018). Is insulin pump therapy effective in Type 1 diabetes? *Diabetic Medicine*, 36(3), 269–278. <https://doi.org/10.1111/dme.13793>

Pollastri, M. P. (2010). Overview on the Rule of Five. *Current Protocols in Pharmacology*, 49(1). <https://doi.org/10.1002/0471141755.ph0912s49>

Poudwal, S., Misra, A., & Shende, P. (2021). Role of lipid nanocarriers for enhancing oral absorption and bioavailability of insulin and GLP-1 receptor agonists. *Journal of Drug Targeting*, 29(8), 834–847. <https://doi.org/10.1080/1061186x.2021.1894434>

Powers, M. A., Bardsley, J. K., Cypress, M., Funnell, M. M., Harms, D., Hess-Fischl, A., Hooks, B., Isaacs, D., Mandel, E. D., Maryniuk, M. D., Norton, A., Rinker, J., Siminerio, L. M., & Uelman, S. (2020). Diabetes Self-management Education and Support in Adults With Type 2 Diabetes: A Consensus Report of the American Diabetes

Association, the Association of Diabetes Care & Education Specialists, the Academy of Nutrition and Dietetics, the American Academy of Family Physicians, the American Academy of PAs, the American Association of Nurse Practitioners, and the American Pharmacists Association. *The Diabetes Educator*, 46(4), 014572172093095.

<https://doi.org/10.1177/0145721720930959>

Prabha, S., Arya, G., Chandra, R., Ahmed, B., & Nimesh, S. (2014). Effect of size on biological properties of nanoparticles employed in gene delivery. *Artificial Cells, Nanomedicine, and Biotechnology*, 44(1), 83–91.

<https://doi.org/10.3109/21691401.2014.913054>

Rahman, Md. M., Dhar, P., Sumaia, N., Anika, F., Ahmed, L., Islam, R., Sultana, N., Cavalu, S., Pop, O., & Rauf, A. (2022). Exploring the plant-derived bioactive substances as antidiabetic agent: An extensive review. *Biomedicine and Pharmacotherapy*, 152, 113217–113217. <https://doi.org/10.1016/j.biopha.2022.113217>

Rawat, M. K., Jain, A., & Singh, S. (2011). Studies on Binary Lipid Matrix Based Solid Lipid Nanoparticles of Repaglinide: *in Vitro* and *in vivo* Evaluation. *Journal of Pharmaceutical Sciences*, 100(6), 2366–2378. <https://doi.org/10.1002/jps.22435>

Rowley, W. R., Bezold, C., Arikian, Y., Byrne, E., & Krohe, S. (2017). Diabetes 2030: Insights from Yesterday, Today, and Future Trends. *Population Health Management*, 20(1), 6–12. <https://doi.org/10.1089/pop.2015.0181>

Sabourian, P., Yazdani, G., Ashraf, S. S., Frounchi, M., Mashayekhan, S., Kiani, S., & Kakkar, A. (2020). Effect of Physico-Chemical Properties of Nanoparticles on Their Intracellular Uptake. *International Journal of Molecular Sciences*, 21(21), 8019. <https://doi.org/10.3390/ijms21218019>

Saeed, N., Khan, M. R., & Shabbir, M. (2012). Antioxidant activity, total phenolic and total flavonoid contents of whole plant extracts *Torilis leptophylla* L. *BMC Complementary and Alternative Medicine*, 12(1). <https://doi.org/10.1186/1472-6882-12-221>

Saeed, R., Temurlu, S., Abourajab, A., Karsili, P., Dinleyici, M., Al-Khateeb, B., & Icil, H. (2023). Drug Repurposing of FDA Compounds against α -Glucosidase for the Treatment of Type 2 Diabetes: Insights from Molecular Docking and Molecular

Dynamics Simulations. *Pharmaceuticals*, 16(4), 555–555.

<https://doi.org/10.3390/ph16040555>

Saeedi, P., Petersohn, I., Salpea, P., Malanda, B., Karuranga, S., Unwin, N., Colagiuri, S., Guariguata, L., Motala, A. A., Ogurtsova, K., Shaw, J. E., Bright, D., & Williams, R. (2019). Global and Regional Diabetes Prevalence Estimates for 2019 and Projections for 2030 and 2045: Results from the International Diabetes Federation Diabetes Atlas, 9th Edition. *Diabetes Research and Clinical Practice*, 157(157), 107843.

<https://doi.org/10.1016/j.diabres.2019.107843>

Sauvaire, Y., Petit, P., Broca, C., Manteghetti, M., Baissac, Y., Fernandez-Alvarez, J., Gross, R., Roye, M., Leconte, A., Gomis, R., & Ribes, G. (1998). 4-Hydroxyisoleucine: A Novel Amino Acid Potentiator of Insulin Secretion. *Diabetes*, 47(2), 206–210. <https://doi.org/10.2337/diab.47.2.206>

Semwal, D. K., Kumar, A., Aswal, S., Chauhan, A., & Semwal, R. B. (2020). Protective and therapeutic effects of natural products against diabetes mellitus via regenerating pancreatic β -cells and restoring their dysfunction. *Phytotherapy Research*, 35(3), 1218–1229. <https://doi.org/10.1002/ptr.6885>

Shannon, P. (2003). Cytoscape: A Software Environment for Integrated Models of Biomolecular Interaction Networks. *Genome Research*, 13(11), 2498–2504.

<https://doi.org/10.1101/gr.1239303>

Shao, T., Yuan, P., Zhu, L., Xu, H., Li, X., He, S., Li, P., Wang, G., & Chen, K. (2019). Carbon Nanoparticles Inhibit α -Glucosidase Activity and Induce a Hypoglycemic Effect in Diabetic Mice. *Molecules*, 24(18), 3257.

<https://doi.org/10.3390/molecules24183257>

Sherrell, Z. (2022, August 31). What is the rate of diabetes by country? [www.medicalnewstoday.com](https://www.medicalnewstoday.com/articles/diabetes-rates-by-country). <https://www.medicalnewstoday.com/articles/diabetes-rates-by-country>

Shrivastava, S., Shrivastava, P., & Ramasamy, J. (2013). Role of self-care in Management of Diabetes Mellitus. *Journal of Diabetes & Metabolic Disorders*, 12(1), 14.

<https://doi.org/10.1186/2251-6581-12-14>

- Singh, A. P., Biswas, A., Shukla, A., & Maiti, P. (2019). Targeted therapy in chronic diseases using nanomaterial-based drug delivery vehicles. *Signal Transduction and Targeted Therapy*, 4(1). <https://doi.org/10.1038/s41392-019-0068-3>
- Singh, S., Kushwah, V., Agrawal, A. K., & Jain, S. (2018). Insulin- and quercetin-loaded liquid crystalline nanoparticles: implications on oral bioavailability, antidiabetic and antioxidant efficacy. *Nanomedicine*, 13(5), 521–537. <https://doi.org/10.2217/nmm-2017-0278>
- Singleton, V. L., Orthofer, R., & Lamuela-Raventós, R. M. (1999, January 1). Analysis of total phenols and other oxidation substrates and antioxidants by means of folin-ciocalteu reagent. *ScienceDirect*; Academic Press. <https://www.sciencedirect.com/science/article/abs/pii/S0076687999990171>
- Srinivasa, U. M., & Naidu, M. M. (2021, January 1). Chapter 6 - Fenugreek (*Trigonella foenum-graecum* L.) seed: promising source of nutraceutical (A. Rahman, Ed.). *ScienceDirect*; Elsevier. <https://www.sciencedirect.com/science/article/abs/pii/B9780323910958000143>
- Stelzer, G., Rosen, N., Plaschkes, I., Zimmerman, S., Twik, M., Fishilevich, S., Stein, T. I., Nudel, R., Lieder, I., Mazor, Y., Kaplan, S., Dahary, D., Warshawsky, D., Guan-Golan, Y., Kohn, A., Rappaport, N., Safran, M., & Lancet, D. (2016). The GeneCards Suite: From Gene Data Mining to Disease Genome Sequence Analyses. *Current Protocols in Bioinformatics*, 54(1), 1.30.1–1.30.33. <https://doi.org/10.1002/cpbi.5>
- Stetefeld, J., McKenna, S. A., & Patel, T. R. (2016). Dynamic light scattering: a practical guide and applications in biomedical sciences. *Biophysical Reviews*, 8(4), 409–427. <https://doi.org/10.1007/s12551-016-0218-6>
- Suhail, M., Rosenholm, J. M., Minhas, M. U., Badshah, S. F., Naeem, A., Khan, K. U., & Fahad, M. (2019). Nanogels as drug-delivery systems: a comprehensive overview. *Therapeutic Delivery*, 10(11), 697–717. <https://doi.org/10.4155/tde-2019-0010>
- Sun, L., Yang, Z., Zhao, W., Qin, C., Bai, H., Wang, S., Yang, L., Bi, C., Shi, Y., & Liu, Y.-Q. (2022). Integrated lipidomics, transcriptomics and network pharmacology analysis to reveal the mechanisms of Danggui Buxue Decoction in the treatment of

diabetic nephropathy in type 2 diabetes mellitus. *Journal of Ethnopharmacology*, 283, 114699–114699. <https://doi.org/10.1016/j.jep.2021.114699>

Sur, S., Rathore, A., Dave, V., Reddy, K. R., Chouhan, R. S., & Sadhu, V. (2019). Recent developments in functionalized polymer nanoparticles for efficient drug delivery system. *Nano-Structures & Nano-Objects*, 20, 100397. <https://doi.org/10.1016/j.nanoso.2019.100397>

Szklarczyk, D., Kirsch, R., Koutrouli, M., Nastou, K., Mehryary, F., Hachilif, R., Gable, A. L., Fang, T., Doncheva, N., Pyysalo, S., Bork, P., Jensen, L., & von Mering, C. (2022). The STRING database in 2023: protein–protein association networks and functional enrichment analyses for any sequenced genome of interest. *Nucleic Acids Research*, 51(D1), D638–D646. <https://doi.org/10.1093/nar/gkac1000>

Tahrani, A. A., Barnett, A. H., & Bailey, C. J. (2016). Pharmacology and therapeutic implications of current drugs for type 2 diabetes mellitus. *Nature Reviews Endocrinology*, 12(10), 566–592. <https://doi.org/10.1038/nrendo.2016.86>

Tariq, A., Sadia, S., Fan, Y., Ali, S., Amber, R., Mussarat, S., Ahmad, M., Murad, W., Zafar, M., & Adnan, M. (2020). Herbal medicines used to treat diabetes in Southern regions of Pakistan and their pharmacological evidence. *Journal of Herbal Medicine*, 21, 100323. <https://doi.org/10.1016/j.hermed.2019.100323>

Tiwari, P. (2015). Recent Trends in Therapeutic Approaches for Diabetes Management: A Comprehensive Update. *Journal of Diabetes Research*, 2015, 1–11. <https://doi.org/10.1155/2015/340838>

Tran, T. H., Ramasamy, T., Truong, D. H., Shin, B. S., Choi, H.-G., Yong, C. S., & Kim, J. O. (2014). Development of Vorinostat-Loaded Solid Lipid Nanoparticles to Enhance Pharmacokinetics and Efficacy against Multidrug-Resistant Cancer Cells. *Pharmaceutical Research*, 31(8), 1978–1988. <https://doi.org/10.1007/s11095-014-1300-z>

Uemura, T., Hirai, S., Mizoguchi, N., Goto, T., Lee, J.-Y., Taketani, K., Nakano, Y., Shono, J., Hoshino, S., Tsuge, N., Narukami, T., Takahashi, N., & Kawada, T. (2010). Diosgenin present in fenugreek improves glucose metabolism by promoting adipocyte differentiation and inhibiting inflammation in adipose tissues. *Molecular Nutrition & Food Research*, 54(11), 1596–1608. <https://doi.org/10.1002/mnfr.200900609>

- Ungaro, F., Angelo, I. d' , Miro, A., Immacolata, M., & Quaglia, F. (2012). Engineered PLGA nano- and micro-carriers for pulmonary delivery: challenges and promises. *Journal of Pharmacy and Pharmacology*, 64(9), 1217–1235. <https://doi.org/10.1111/j.2042-7158.2012.01486.x>
- Vairavamurthy, J., Cheskin, L. J., Kraitchman, D. L., Arepally, A., & Weiss, C. R. (2017). Current and cutting-edge interventions for the treatment of obese patients. *European Journal of Radiology*, 93, 134–142. <https://doi.org/10.1016/j.ejrad.2017.05.019>
- Valenti, S., Barrio, M., Negrier, P., Romanini, M., Macovez, R., & Tamarit, J.-L. (2021). Comparative Physical Study of Three Pharmaceutically Active Benzodiazepine Derivatives: Crystalline versus Amorphous State and Crystallization Tendency. *Molecular Pharmaceutics*, 18(4), 1819–1832. <https://doi.org/10.1021/acs.molpharmaceut.1c00081>
- Verma, N., Usman, K., Patel, N., Jain, A., Dhakre, S., Swaroop, A., Bagchi, M., Kumar, P., Preuss, H. G., & Bagchi, D. (2016). A multicenter clinical study to determine the efficacy of a novel fenugreek seed (*Trigonella foenum-graecum*) extract (Fenfuro™) in patients with type 2 diabetes. *Food & Nutrition Research*, 60(1), 32382. <https://doi.org/10.3402/fnr.v60.32382>
- Vilar, S., Cozza, G., & Moro, S. (2008). Medicinal Chemistry and the Molecular Operating Environment (MOE): Application of QSAR and Molecular Docking to Drug Discovery. *Current Topics in Medicinal Chemistry*, 8(18), 1555–1572. <https://doi.org/10.2174/156802608786786624>
- Visuvanathan, T., Than, L. T. L., Stanslas, J., Chew, S. Y., & Vellasamy, S. (2022). Revisiting *Trigonella foenum-graecum* L.: Pharmacology and Therapeutic Potentialities. *Plants*, 11(11), 1450. <https://doi.org/10.3390/plants11111450>
- Wang, T., Jiang, X., Ruan, Y., Li, L., & Chu, L. (2022). The mechanism of action of the combination of *Astragalus membranaceus* and *Ligusticum chuanxiong* in the treatment of ischemic stroke based on network pharmacology and molecular docking. *Medicine*, 101(28), e29593–e29593. <https://doi.org/10.1097/md.00000000000029593>

- Wani, S. A., & Kumar, P. (2018). Fenugreek: A review on its nutraceutical properties and utilization in various food products. *Journal of the Saudi Society of Agricultural Sciences*, 17(2), 97–106. <https://doi.org/10.1016/j.jssas.2016.01.007>
- WHO. (2021, June 9). Obesity and Overweight. World Health Organization. <https://www.who.int/news-room/fact-sheets/detail/obesity-and-overweight>
- World Health Organization. (2023, April 5). Diabetes. World Health Organisation; WHO. <https://www.who.int/news-room/fact-sheets/detail/diabetes>
- Xiong, G., Wu, Z., Yi, J., Fu, L., Yang, Z., Hsieh, C., Yin, M., Zeng, X., Wu, C., Lu, A., Chen, X., Hou, T., & Cao, D. (2021). ADMETlab 2.0: an integrated online platform for accurate and comprehensive predictions of ADMET properties. *Nucleic Acids Research*, 49(W1), W5–W14. <https://doi.org/10.1093/nar/gkab255>
- Xu, X., Zhang, W., Huang, C., Li, Y., Yu, H., Wang, Y., Duan, J., & Ling, Y. (2012). A Novel Chemometric Method for the Prediction of Human Oral Bioavailability. *International Journal of Molecular Sciences*, 13(6), 6964–6982. <https://doi.org/10.3390/ijms13066964>
- Yaribeygi, H., Katsiki, N., Butler, A. E., & Sahebkar, A. (2019). Effects of antidiabetic drugs on NLRP3 inflammasome activity, with a focus on diabetic kidneys. *Drug Discovery Today*, 24(1), 256–262. <https://doi.org/10.1016/j.drudis.2018.08.005>
- Yuan, Z., Pan, Y., Leng, T., Chen, Y., Zhang, H., Ma, J., & Ma, X. (2022). Progress and Prospects of Research Ideas and Methods in the Network Pharmacology of Traditional Chinese Medicine. *Journal of Pharmacy and Pharmaceutical Sciences*, 25, 218–226. <https://doi.org/10.18433/jpps32911>
- Zeng, X., Zhang, P., Wang, Y., Qin, C., Chen, S., He, W., Tao, L., Tan, Y., Gao, D., Wang, B., Chen, Z., Chen, W., Jiang, Y. Y., & Chen, Y. Z. (2019). CMAUP: a database of collective molecular activities of useful plants. *Nucleic Acids Research*, 47(D1), D1118–D1127. <https://doi.org/10.1093/nar/gky965>
- Zhang, A., Sun, H., Yang, B., & Wang, X. (2012). Predicting new molecular targets for rhein using network pharmacology. *BMC Systems Biology*, 6(1), 20. <https://doi.org/10.1186/1752-0509-6-20>

- Zhang, L., Han, L., Ma, J., Wu, T., Wei, Y., Zhao, L., & Tong, X. (2022). Exploring the synergistic and complementary effects of berberine and paeoniflorin in the treatment of type 2 diabetes mellitus by network pharmacology. *European Journal of Pharmacology*, 919, 174769. <https://doi.org/10.1016/j.ejphar.2022.174769>
- Zhang, X., Shedden, K., & Rosania, G. R. (2006). A Cell-Based Molecular Transport Simulator for Pharmacokinetic Prediction and Cheminformatic Exploration. *Molecular Pharmaceutics*, 3(6), 704–716. <https://doi.org/10.1021/mp060046k>
- Zhang, X., Wang, X., Wang, M., Hu, B., Tang, W., Wu, Y., Gu, J., Ni, T., & Li, Q. (2022). The global burden of type 2 diabetes attributable to high body mass index in 204 countries and territories, 1990–2019: An analysis of the Global Burden of Disease Study. *Frontiers in Public Health*, 10. <https://doi.org/10.3389/fpubh.2022.966093>
- Zhang, X.-X., Eden, H. S., & Chen, X. (2012). Peptides in cancer nanomedicine: Drug carriers, targeting ligands and protease substrates. *Journal of Controlled Release*, 159(1), 2–13. <https://doi.org/10.1016/j.jconrel.2011.10.023>
- Zhang, Y., Mao, X., Guo, Q., Lin, N., & Li, S. (2016). Network Pharmacology-based Approaches Capture Essence of Chinese Herbal Medicines. *Chinese Herbal Medicines*, 8(2), 107–116. [https://doi.org/10.1016/s1674-6384\(16\)60018-7](https://doi.org/10.1016/s1674-6384(16)60018-7)
- Zheng, J., Cheng, J., Zheng, S., Feng, Q., & Xiao, X. (2018). Curcumin, A Polyphenolic Curcuminoid With Its Protective Effects and Molecular Mechanisms in Diabetes and Diabetic Cardiomyopathy. *Frontiers in Pharmacology*, 9. <https://doi.org/10.3389/fphar.2018.00472>
- Zhou, M., Ren, G., Zhang, B., Fu-li, M., Fan, J., & Qiu, Z. (2022). Screening and identification of a novel antidiabetic peptide from collagen hydrolysates of Chinese giant salamander skin: network pharmacology, inhibition kinetics and protection of IR-HepG2 cells. *Food & Function*, 13(6), 3329–3342. <https://doi.org/10.1039/d1fo03527d>
- Zięba, A., Stępnicki, P., Matusiuk, D., & Kaczor, A. A. (2022). What are the challenges with multi-targeted drug design for complex diseases? *Expert Opinion on Drug Discovery*, 17(7), 673–683. <https://doi.org/10.1080/17460441.2022.2072827>
- Zulkifli, S. A., Abd Gani, S. S., Zaidan, U. H., & Halmi, M. I. E. (2020). Optimization of Total Phenolic and Flavonoid Contents of Defatted Pitaya (*Hylocereus*

polyrhizus) Seed Extract and Its Antioxidant Properties. *Molecules*, 25(4), 787.
<https://doi.org/10.3390/molecules25040787>

TEST - 1

ORIGINALITY REPORT

15%

SIMILARITY INDEX

11%

INTERNET SOURCES

11%

PUBLICATIONS

4%

STUDENT PAPERS

PRIMARY SOURCES

1	www.mdpi.com Internet Source	2%
2	Submitted to Higher Education Commission Pakistan Student Paper	2%
3	Ayesha Saleem, Muhammad Afzal, Muhammad Naveed, Syeda Izma Makhdoom et al. "HPLC, FTIR and GC-MS Analyses of Thymus vulgaris Phytochemicals Executing In Vitro and In Vivo Biological Activities and Effects on COX-1, COX-2 and Gastric Cancer Genes Computationally", Molecules, 2022 Publication	1%
4	www.ncbi.nlm.nih.gov Internet Source	1%
5	mdpi-res.com Internet Source	<1%
6	www.frontiersin.org Internet Source	<1%
7	link.springer.com	